Universidade de Aveiro
2012

Departamento de Electrónica, Telecomunicações e Informática (DETI)

Tiago Miguel da Paz Santos Mendes

Redes Ópticas Passivas de Operação Estendida

Stacked Passive Optical Network

Universidade de Aveiro
2012

Departamento de Electrónica, Telecomunicações e Informática (DETI)

Tiago Miguel da Paz Santos Mendes

Redes Ópticas Passivas de Operação Estendida

Dissertação apresentada à Universidade de Aveiro para cumprimento dos requisitos necessários à obtenção do grau de Mestre em Engenharia Electrónica e Telecomunicações, realizada sob a orientação científica do Dr. António Teixeira e Dr. Mário Lima, ambos do Departamento de Electrónica, Telecomunicações e Informática e do Instituto de Telecomunicações da Universidade de Aveiro.

Dedico este trabalho aos meus Pais á minha irmã e a todos os meus amigos e familiares que me acompanharam e inspiraram no meu percurso.

O júri / The jury

Presidente / President

Prof. Doutor José Rodrigues Ferreira da Rocha
Professor Catedrático da Universidade de Aveiro

vogais / examiners committee

Prof. Doutor António Luís Jesus Teixeira
Professor Associado da Universidade de Aveiro (Orientador)

Prof. Doutor Mário José Neves de Lima
Professor Auxiliar da Universidade de Aveiro (Co-Orientador)

Prof. Doutora Maria do Carmo Raposo de Medeiros
Professora Associada da Universidade do Coimbra

Agradecimentos

Agradeço ao meu orientador, Doutor António Teixeira pelos conhecimentos transmitidos e por me fazer acreditar que era possível o que vezes sem conta não pareceu ser; ao meu co-orientador Doutor Mário Lima que me fez escolher o ramo de ótica e pela prontidão com que sempre me ajudou.

Ao Eng. Ali Shapari, Eng. João Prata, Eng. Cláudia Mendonça, Eng. Paulo Monteiro e Eng Carlos Oliveira por toda a ajuda durante as infindáveis horas de laboratório e por terem tornado a ambientação ao mesmo menos custosa.

Agradeço à cergal crew, Manel, Cavaleiro, Bixas, Kant, Mauro e Jónatas por todos os momentos bem passados e pela amizade de muitos anos; ao Hugo, Andreia, Palhursas, Nuno e Gonçalo por todos os momentos passados no nosso ano de Erasmus, pela viagem da minha vida e por me terem aturado e ajudado a crescer.

Um agradecimento especial à Sofia por ter sido namorada, amiga, uma das maiores fontes de coragem e inspiração que tive e por me ter tornado uma pessoa melhor.

Finalmente, quero agradecer à minha família, Mãe, Pai e Mana e também aos meus Avós, Primos e Tios, pois tudo o que sou hoje devo-o a vocês e ao excelente trabalho que fizeram na minha educação.

Ao meu Avô Américo um especial agradecimento pelos valores com que pautou a sua vida e pelo sacrifício que fez por nós.

A todos, o meu sincero, Muito Obrigado!.

palavras-chave

Redes Óticas Passivas, GPON, EPON, stacking, Conversão de Comprimento de Onda, Modulação Cruzada do Ganho, Modulação Cruzada da Fase, Rotação Cruzada de Polarização.

Resumo

A crescente procura por serviços de banda larga, e diversificação de conteúdos e serviços disponibilizados pela rede tem contribuído fortemente para o que se designa "*last mile bottleneck".* Como solução surgiram as redes óticas de acesso passivas, que oferecem elevada largura de banda e uma relação preço por número de clientes servidos muito competitiva.

Ao longo deste documento são estudadas as redes passivas de acesso que atualmente têm maior taxa de implementação, EPON e GPON e é proposto um cenário de convivência entre as duas utilizando a mesma fibra de distribuição. Para implementação do cenário proposto, foi estudada e avaliada separadamente a convivência no sentido ONU-OLT e OLT-ONU. Na comunicação ONU-OLT a viabilidade estatística da convivência foi comprovada através de simulação e seguidamente corroboração experimental. Na comunicação OLT-ONU diversos mecanismos de conversão de comprimento de onda exclusivamente óticos como modulação de ganho e fase cruzada, e rotação cruzada de polarização, foram avaliados por simulação e comprovados em laboratório.

Keywords Passive Optical Networks, GPON, EPON, stacking, Wavelength Conversion, Cross Gain Modulation (XGM), Cross Phase Modulation (XPM), Cross Polarization Rotation (XPR).

Abstract The increasing demand for broadband services and the diversification of content and services provided by the network has strongly contributed for the so-called "last mile bottleneck". As a solution, the passive optical networks (PON) emerged, offering high bandwidth and a very competitive cost per number of customers served.

Throughout this document are studied the passive access networks that currently experience higher deployment rates, EPON and GPON and a coexistence scenario over the same distribution fiber is proposed. To implement the proposed scenario and due to incompatibility between the two referred standards, upstream and downstream communication directions were studied and evaluated separately. For upstream communication the statistical viability of the network was assessed using simulation and experimental corroboration. In the downstream communication several mechanisms for all-optical wavelength conversion such as cross gain and phase modulation, and also cross polarization rotation were evaluated and tested.

Contents

List of Figures

List of Tables

List Of Acronyms

A	**ADSL**	Asymmetric Digital Subscriber Line
	AON	Active Optical Networks
	AO-WC	All optical Wavelength converter
	APD	Avalanche Photodiode
	ASE	Amplified Spontaneous Emission
	ATM	Asynchronous Transfer Mode
B	**BER**	Bit Error Rate
	BPON	Broadband Passive Optical Networks
	BW	Bandwidth
C	**CATV**	Cable Television
	CW	Continuous wave
	CWDM	Coarse Wavelength Division Multiplexing
D	**DBA**	Dynamic Bandwidth Allocation
	DWDM	Dense Wavelength Division Multiplexing
E	**EDFA**	Erbium-Doped Fiber Amplifier
	EOP	Eye Opening Penalty
	EPON	Ethernet Passive Optical Network
	ER	Extinction Ratio
F	**FEC**	Forward Error Correction
	FDM	Frequency Division Multiplex
	FSAN	Full Service Access Network
	FTTB	Fiber-to-the-Building
	FTTC	Fiber-to-the-Curb
	FTTCab	Fiber-to-the-Curb
	FTTH	Fiber-to-the-Home
	FWM	Four Wave Mixing
G	**GEM**	GPON Encapsulation Method
	GFP	Generic Framing Procedure
	GPON	Gigabit Passive Optical Network

I	**IEEE**	Institute of Electrical and Electronics Engineers
	IP	Internet Protocol
	ITU	International Telecommunication Union
	ITU-T	Telecommunication Standardization Sector
L	**LLC**	Logical Link Control
M		
	MAC	Medium Access Control
	MDI	Medium Dependent Interface
	MP2P	Multi Point to Point
	MZI	Mach-Zehnder Interferometer
	MZI-SOA	Mach-Zehnder Interferometer with Semiconductor Optical Amplifiers
	MZM	Mach-Zehnder Modulator
N	**NF**	Noise Figure
	NG-HDTV	New Generation High Definition Television
	NPR	Non-Linear Polarization Rotation
	NRZ	Non-Return-to-Zero
O	**OBPF**	Optical Band Pass Filter
	ODN	Optical Distribution Network
	OEO-WC	Optical-Electric-Optical Wavelength Converter
	OF	Optical Filter
	OLT	Optical Line Termination
	ONT	Optical Network Termination
	ONU	Optical Network Unit
	OSA	Optical Spectrum Analyzer
	OSNR	Optical Signal to Noise Ratio
P	**P2P**	Point to Point
	PBS	Polarization Beam Splitter
	PC	Polarization Controler
	PCBd	Physical Control Block downstream
	PER	Packet Error Rate
	PHY	Physical Layer
	PIN	Photodiode
	PLOu	Physical Layer Overhead Upstream
	PM	Phase Modulator
	PMD	Physical Medium Dependent

	PON	Passive Optical Network
	Port-ID	Port identifier
	PRBS	Pseudo-Random Bit Sequence
	PS	Phase shift
Q	**Q-Factor**	Quality Factor
R	**RTT**	Round Trip Time
S	**SBA**	Static Bandwidth Allocation
	SOA	Semiconductor Optical Amplifier
T	**TC**	Transmission Convergence
	T-Cont	Transmission Container
	TDM	Time Division Multiplexing
	TDMA	Time Division Multiple Access
	TE	Transversal Electric
	TM	Transversal Magnetic
U	**UNI**	User Network Interface
V	**VDSL**	Very-high-bit-rate Digital Subscriber Line
	V	Volts
	VOA	Variable Optical Attenuator
W	**WC**	Wavelength Conversion
	WDM	Dense Wavelength Division Multiplexing
X	**XGM**	Cross Gain Modulation
	XPM	Cross Phase Modulation
	XPR	Cross Polarization Rotation

1. Introduction

1.1. Context and motivation

Telecommunications industry had always been pushed by both, human geniality and consumers' demands. After the achievement of high purity fibers that enabled the light propagation with low losses over high distances, nowadays are the consumers' demands that keep pushing the evolution in optical networks. Today the evolution in optical networks is especially focused in the access networks due to the bottleneck experienced.

The steady increasing bandwidth demand is a consequence of the up and coming high bandwidth services such as next generation high definition television (NG-HDTV), 3D TV, video on demand, online games and cloud services. Figure 1.1 presents the different services and the bandwidth request of each one of them, both in downstream and upstream traffic.

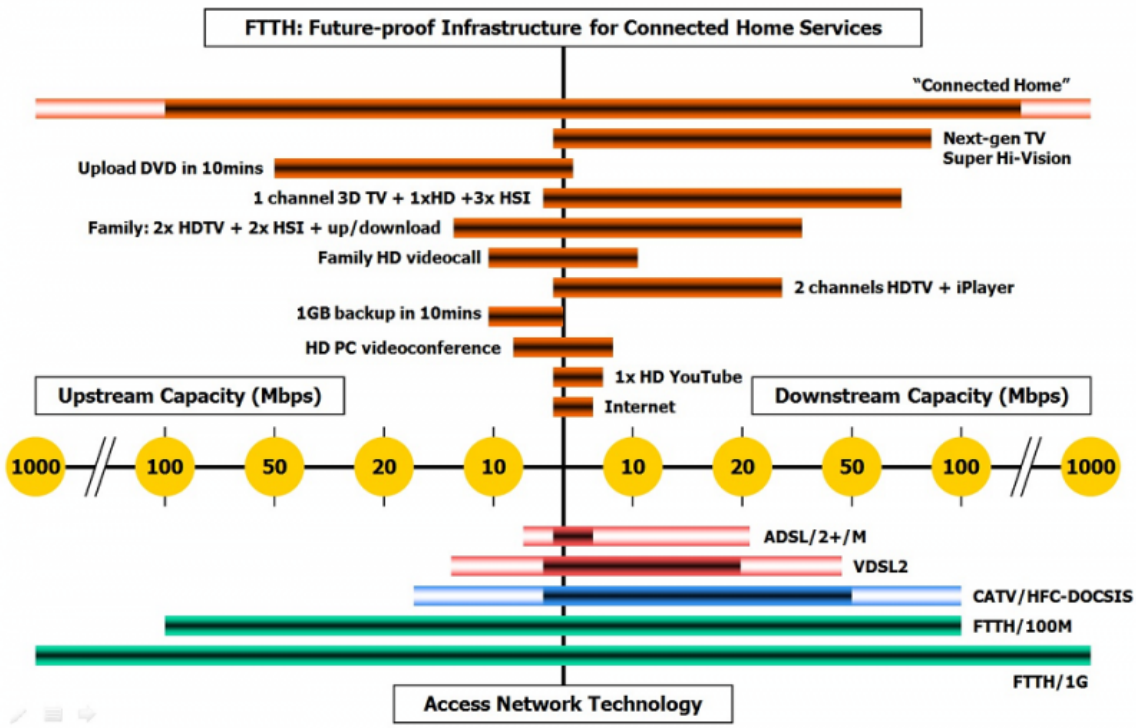

Figure 1.1 Access network capacity and applications bandwidth demands **[FTTH Council, 2012]**

As it is presented in Figure 1.1 the bandwidth offered by the copper based access technologies such as Asymmetric Digital Subscriber Line (ADSL), Very-high-bit-rate Digital Subscriber Line (VDSL) and Cable Television (CATV) is frankly insufficient and presents short lifetime. Passive optical networks (PON) arise as the replacement for the old copper based technologies mentioned and present a future-proof infrastructure capable of coping with the increasing bandwidth demand.

Nowadays, the most prominent PONs are: Gigabit PON (GPON), created by the International Telecommunication Union (ITU), and Ethernet PON (EPON) created by the Institute of Electrical and Electronics Engineers (IEEE). Both share the same basic principles such as point-to-multipoint architecture and upstream/downstream transmission principles but, due to the different institutions that support them, the coexistence between both standards was not taken in mind. Adding to the fact that no straight communication between standards is possible, both standards use the same wavelength plan for upstream and downstream communication, making the coexistence over the same fiber span difficult to happen without prohibitive packet losses.

In this dissertation we evaluate the coexistence scenario of both PON standards referred previously, according to the different specifications for the upstream and downstream traffic transmissions.

1.2. Objectives and Structure

For the sake of simplicity it is important to clearly identify the problem presented in this dissertation, as well as the steps followed from the problem presentation to the final solution achieved.

In a Fiber-to-the-home PON (FTTH-PON) scenario, the physical link costs are of the most importance, thus any possibility of a shared medium between more subscribers, or even subscribers from different PON access topologies can imply major savings for the communications service providers.

The Stacked-PON scenario can be presented as a regular PON scenario composed by two different access topologies (EPON and GPON) over the same fiber span between the optical splitter location and Optical Line Termination (OLT) premises. The key factor to this scenario is the wavelength allocation plan used by these two systems that overlap each other, not allowing a straightforward implementation.

PON systems relies on different communication procedures for upstream (time division multiple access) and downstream directions (broadcast), with this in mind, are

presented different approaches for the upstream and downstream stacked-PON coexistence.

This dissertation is organized in five chapters with the main goal of presenting and evaluating the stacked PON system. The main objectives are:

- Identification of the principal constraints to the implementation of an EPON/GPON Stacked scenario.
- Proposal and specification of a valid Stacked-PON environment accordingly to the upstream and downstream constraints.
- Study of the upstream coexistence between EPON and GPON systems over a shared medium.
- Study of all optical wavelength conversion techniques to use in downlink communication direction.

To cope with these objectives, the dissertations structure is the following:

Chapter **one** presents the context, motivation, structure and objectives, as well as the main contributions of this dissertation.

Chapter **two** starts with a general overview of the current passive optical networks, their architecture, functionalities and wavelength plan. Both EPON and GPON systems are also presented in terms of the respective system sub-layers, bandwidth assignment and upstream/downstream frame format. Finally, the stacked PON scenario is presented, as it is the main focus of study in this dissertation.

Chapter **three** presents the theoretical basics for all optical wavelength conversion, as a solution for the downstream communication inoperability of the Stacked PON scenario. The wavelength conversion techniques presented are: cross phase modulation (XPM), cross gain modulation (XGM) and cross polarization rotation (XPR). The wavelength conversion techniques presented were also evaluated using laboratorial setups.

In Chapter **four** we evaluate the upstream coexistence scenario. In this study the different traffic and bandwidth allocation mechanisms are assessed and upstream coexistence without wavelength conversion is proven feasible.

Chapter **five** presents the summary of the work and the main conclusions. Proposals for future work are also presented.

1.3. Contributions

The main contributions of this dissertation can be summarized as follows:

- Proposal and specification of an EPON and GPON stacked environment.
- Simulation and experimental validation of EPON and GPON upstream communication over a shared medium.
- Study of XGM, XPM and XPR wavelength conversion techniques to use in stacked PON downlink.

Additionally to the already mentioned contributions:

- A paper was published in the “X Symposium on Enabling Optical Networks and Sensors 2012” with the name: Tiago Mendes et al, ”PON upstream Coexistence study”;
- An article was accepted for publishing at the DETI-UA magazine named: Tiago Mendes et al, “PON Upstream traffic coexistence in a Stacked-PON environment”

2. Stacked Passive Optical Network

2.1. Introduction

Data networks can be divided into the following sub-networks Core, Metro and Access, and they differ specially in the reach, traffic transported and protocols utilized. In the access networks also called “last mile” (or first mile as is referred in IEEE standards), various access technologies could be implemented, depending if the medium chosen is copper link, radio waves or in the case of PON networks, an optical link. Independently if the medium is copper, cable or optical fiber, both electrical networks and optical networks are built with switching and routing equipment. Depending on the place in the network where the switching and routing functions are performed, they can be classified as passive or active.

In active optical networks (AON) the above functions are performed between the OLT and the Optical Network Unit (ONU), and the equipment utilized requires external power supply. On the other hand, passive networks use only passive elements between the OLT and the ONU, thus are not required any external power supplies. This fact allows significant power savings and reduces the maintenance required. [Leonid G. Kazovsky, 2011]

The OLTs used for passive optical networks have active transmitters. The ONUs can also have active transmitters or reuse the received power to transmit the data. The previous specifications allowed the PON systems to overcome active systems in the access network, as far as the operational costs associated are much lower [PON, 2008].

PONs are intended to solve the access networks bandwidth bottleneck by offering a cost-effective, flexible, and high bandwidth solution for access networks.

2.2. Passive Optical Networks (PON) Standards

The existing PON topologies were developed by two different organizations and the standards presented correspond to two different approaches based on the requirements of the upper protocols supported such as Ethernet, Asynchronous Transfer

Mode (ATM) , Generic Framing Procedure (GFP) etc..

The first relevant PON standard named Broadband Passive Optical Network (BPON) (G.983.x 1998) is an ITU-T standard and it was developed by a consortium of network operators and equipment vendors which cooperated together in the Full Service Access Network (FSAN) group. The other organization that developed PON standards was the EFM, Ethernet in the First Mile, the standard presented is known as “Ethernet Passive Optical Network” (EPON) [802.3ah 200] and is an IEEE standard. Figure 2.1 presents the evolution of PON standards and the respective bandwidth offered.

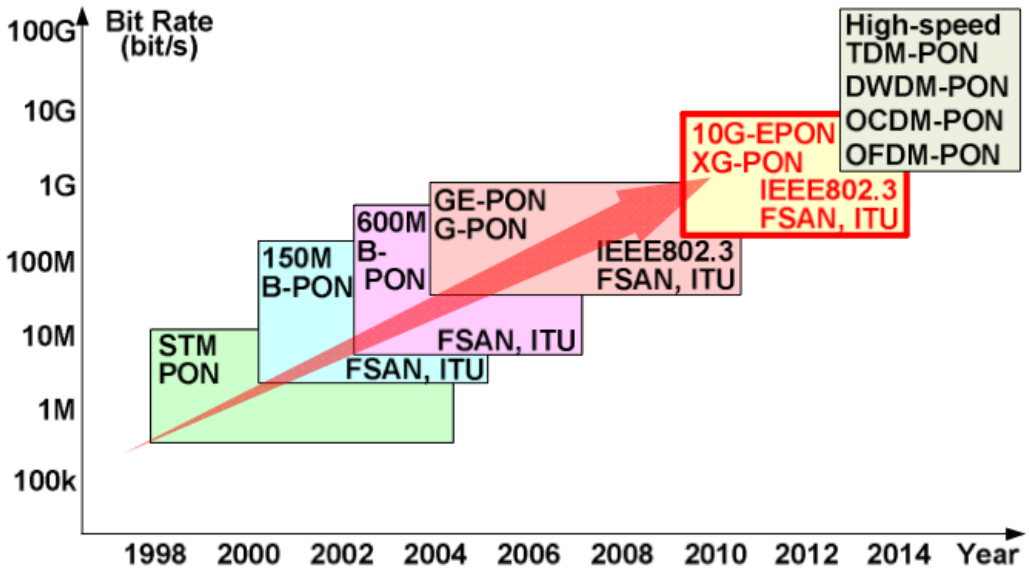

Figure 2.1 Progress of PON systems **[Masaki Noda, 2010]**

When the FSAN and ITU proposed the BPON, the transport data protocol chosen was the Asynchronous Transfer Mode. But with the success of the Internet, it did not take long before ATM based BPON systems proved out to be very inefficient dealing with the large, variable-sized IP frames that composes the majority of traffic through the access network. This created the opportunity for the development of the pure Ethernet based PON. Unlike ATM, the Ethernet is a data only oriented protocol, and has proven over the time to be the ideal protocol for transporting the IP packets that composes the bulk of the transported data.

Shortly after the EFM started working on the EPON standard, the FSAN group concentrated efforts to also create a Gigabit-capable PON, that could cope better with the changes toward the Ethernet and IP based network and its fast-growing bandwidth demand. The standard proposed was named “Gigabit-capable Passive Optical Network” (GPON) (G.984.x 2003).

Both EPON and GPON draw heavily from the BPON standard, when it comes to general concepts such as PON sub-layers functionalities, optical distribution network (ODN), and wavelength plan. Although both protocols basically support the same communication protocols, how they are encapsulated and how the overhead is introduced present the most visible differences between GPON and EPON.

EPON networks use a straightforward implementation of the Ethernet datagram. This arises as a great advantage because most networks on both sides of the PON (the customer and the service providers) use Ethernet protocol, thus unnecessary format conversions are not performed.

EPON achieved great penetration on the Asian market, especially Japan, South Korea and China. As for GPON, North America and Europe have become the main markets, nonetheless recent studies point to an increasing penetration of GPON in the Asian market (Figure 2.2) [Idate, 2009].

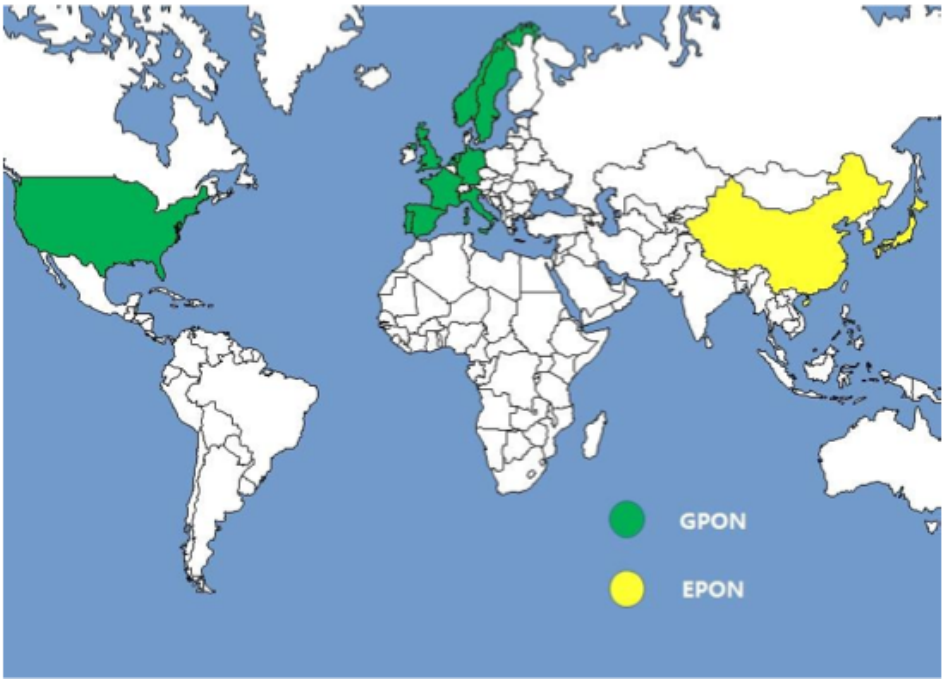

Figure 2.2 EPON and GPON deployment **[Mendonça, 2010]**

In the next years, and driven by the steady increasing users bandwidth demand, ITU and IEEE are going to keep up the pace, upgrading the previously referred standards to 10-GPON and 10G-EPON which provide an increased downstream and upstream speed as it can be noticed in Figure 2.1 [Leonid G. Kazovsky, 2011].

2.2.1. PON Architecture

The most important aspects in the PONs architectures are their simplicity and low power consumption [Leonid G. Kazovsky, 2011]. There are three main elements that compose the network, each one performing specific network functions. Figure 2.3 presents the elements that compose the PONs and the schematic architecture.

ONU- receives the broadcasted signal that comes from the OLT and selects the data that is intend to it.

Sends the upstream data in the time slot that was assigned to it.

Requests the upstream bandwidth according to its needs.

OLT- Sends the Broadcast signal to all the subsidiary ONUs as well as video broadcast if used.

Assigns the upstream bandwidth to the ONUs following a DBA algorithm.

Controls and synchronizes the exchange of the data in the PON.

Performs the Operation Administration and Maintenance (OAM) functions in the ODN.

Coupler/splitter - is the interface between the common single fiber that comes from the OLT and the fibers that connect to each of the ONUs served by that OLT.

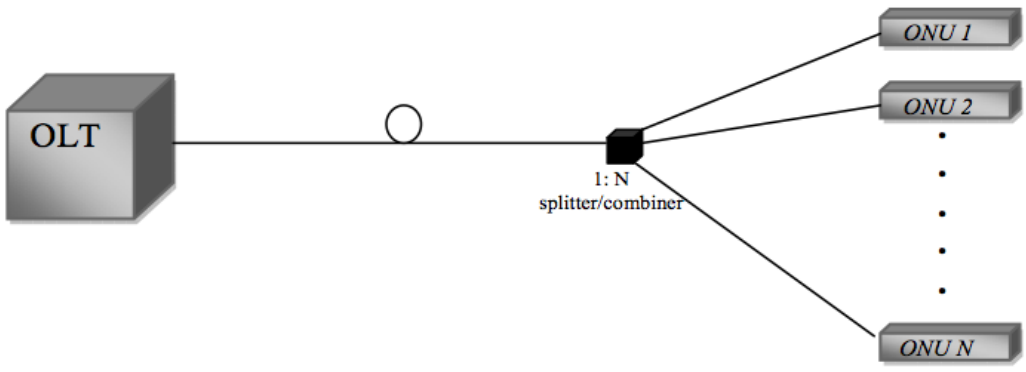

Figure 2.3 EPON Architecture **[A. M. Ragheb, 2010]**

The optical transmission in the ODN occurs in two ways. Downstream direction for

data travelling from the OLT to the ONUs and Upstream direction for data traveling from ONUs to the OLT. Transmission in downstream and upstream directions can take place on the same fiber due to different wavelength assignment and multiplexing mechanisms or on separate fibers.

In some PONs, a video signal is also broadcasted using the 1550-1560 nm wavelength range [Leonid G. Kazovsky, 2011]

2.2.2. Topology

Passive optical networks were designed to be as cost effective as possible, thus at the physical level the topology chosen was Point-to-Multipoint (P2MP) instead of Point-to-Point (P2P) allowing major savings in fiber cables between the OLT and the ONUs.

Passive Optical networks can also be categorized according to the type of architecture and reach of the optical path between the OLT and the ONU. Regarding the type of architecture the PONs can be classified depending on if the network arrangement is a ring, bus or in the case approached in this dissertation, tree shape.

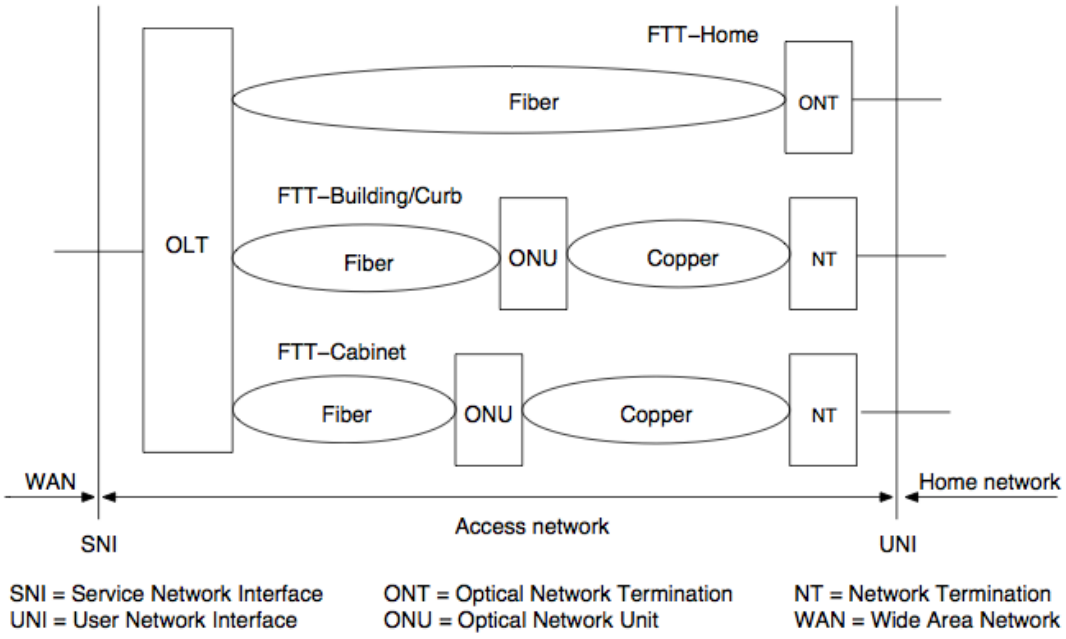

Figure 2.4 Optical Network Architecture **[ITU-T G.984.1, 2008]**

Figure 2.4 presents all the different Fiber-to-the-X (FTTX) possible configurations. The interface between the Metro an Access network is called Service Node Interface (SNI). In the opposite side, the interface between the Access network and the User side is the User Network Interface (UNI). The ODN is the physical link between SNI and UNI.

If the fiber runs from SNI to the UNI the topology is called FTTH and at the UNI the equipment is called ONT. If the fiber does not reach the user side at the UNI, different topologies are possible according to the place where the signals are converted from optical to electrical by an ONU.

In the FTTCab/FTTCurb/FTTB topologies the distance between ONU and NT is bridged by copper cables imposing limitations on the offered bandwidth. The differences between the FTTB, FTTC, FTTCab and FTTH network options, are mainly due the different services supported, so in the Recommendation [ITU-T G.984.3, 2008] as well as in this dissertation they are treated as the same.

2.2.3. Downstream and Upstream Transmission

EPON and GPON are Time Division Multiplexing (TDM) systems because all the users share the same optical fiber between OLT and the splitter in the time domain. In the downstream direction the data packets are broadcast to all ONUs in a continuous mode (Figure 2.5). Even if there is no data to send, the OLT sends periodically idle frames to maintain the synchronization with all ONUs. [Kramer, 2004]

In the upstream direction, all the users share the same optical link using a Time Division Multiple Access (TDMA) scheme (Figure 2.5). The use of TDMA allows packet collisions to be avoided as the OLT coordinates the upstream transmission and assigns different time slots to each of the subsidiary ONUs. Each ONU transmits data in bursts, and between bursts from different ONUs there are guard times to avoid the interference from different sources. It must be noticed that in the upstream direction, even if there is no data to be transmitted, idle frames are sent to maintain synchronization. These idle frames are sent as an answer to the synchronization frames sent by the OLT. [Kramer, 2004] [Leonid G. Kazovsky, 2011]

Due to the different ways of transmitting data in upstream and downstream direction the receivers and transmitters must have different specifications. For example, the OLT receiver must have a wide range of input power acceptance, and the transmitter high power output. The ONU receiver in the other way must be as sensitive as possible and the transmitter must allow fast turn on/off times. [Lam, 2007]

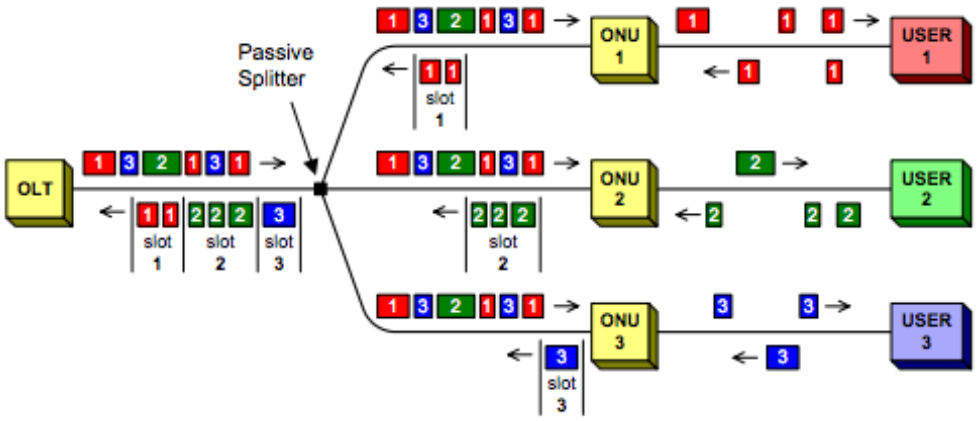

Figure 2.5 PON TDMA scheme **[Kramer, 2004]**

2.2.4. PON Layer Functionalities

Both the EPON and GPON recommendations are focused on the functionalities of the first two levels of the Open System Interconnection (OSI) (Figure 2.6). This differentiation by levels allows communication systems to be developed in a modular way. One of the major advantages for the hardware and software developers are the limitation of the interoperability concerns between all the levels to only two levels, one above and one bellow. The functionalities of the first two levels are well described by the standards and are presented bellow.

• Layer 1 - Physical layer, defines the physical specifications between the device and the transmission medium such as optical power, connectors, cable types and more.

• Layer 2- Data link layer, performs the data transfer between network devices, handle the physical level errors, encapsulates and de-capsules packets. Also provides the necessary flow control and frame synchronization.

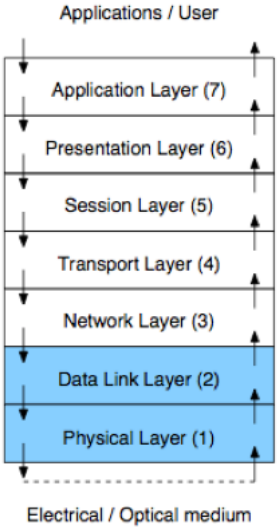

Figure 2.6 OSI model **[Boomsma, 2006]**

2.2.5. PON Packet Format and Encapsulation

The main difference between EPON and GPON systems is in the type of packet or frame transmission they support. As it was previously referred the majority of Internet traffic is Ethernet, and thus this is also true in the access networks.

Ethernet PON is a direct extension of the IEEE 802.3 Ethernet LAN standard to fiber optic access networks, which includes a Multi Point Control Protocol (MPCP) to allow the Multi Point to Point (MP2P) topology. On the other hand GPON inherits some of the ATM specifications from the BPON standard. However, GPON further adopts the GPON encapsulation method (GEM), which enables any packet type to be encapsulated in GEM frames and also adds packet fragmentation and packet reassembly. Taking in consideration the encapsulation method, GPON is more flexible than EPON because it can support a mix of Ethernet and TDM services, but on the other hand adds more complexity to the PON end devices.

2.3. Gigabit Passive Optical Network (GPON)

The GPON recommendation G.984.3 [ITU-T G.984.3, 2008] has defined a protocol stack, which divides the GPON functionalities into several layers as presented in Figure 2.7. Each layer has specific functions that can be viewed as a block, which contains different sub-layers and protocol adapters.

In the initial version of the ITU-T G.984.3 recommendation both GEM and ATM modes were supported but due to the network traffic evolution, ATM mode has proven not to be of great interest for future deployments in GPON systems [ITU-T G.984.3, 2008]. Thus, in this chapter the GPON encapsulation method (GEM) will be presented as the sole data transport scheme used in GPON transmission convergence layer.

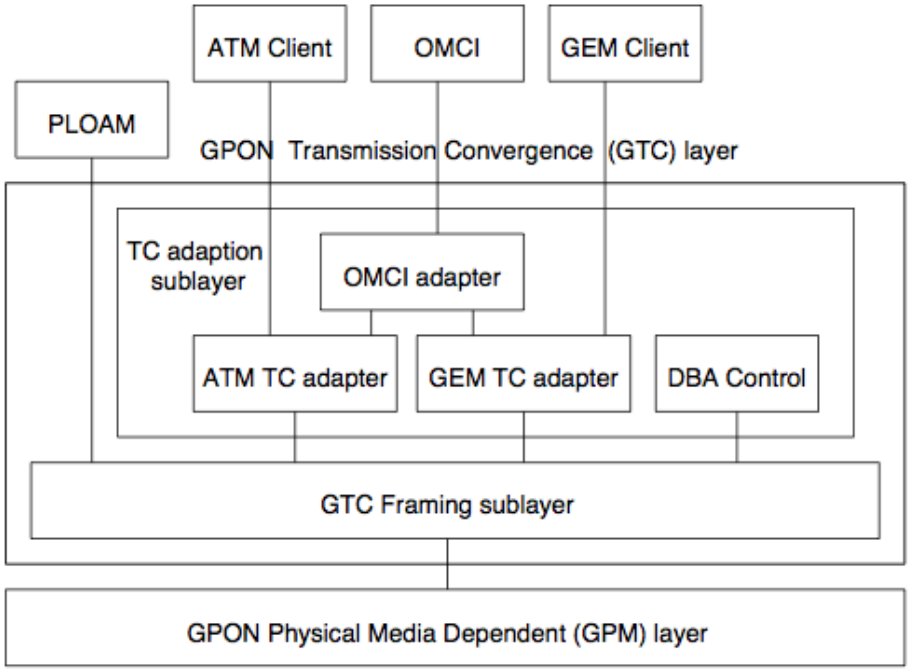

PLOAM = Physical Layer Operations, Adminitration and Maintenance
ATM = Asynchronous Transfer Mode
OMCI = ONU Management adn Control Channel
GEM = GPON Encapsulation Method
DBA = Dynamic Bandwidth Assignment
GTC = GPON Transmission Convergence
GPM = GPON Physical Media (Dependent)

Figure 2.7 GPON stack protocol **[ITU-T G.984.3, 2008]**

2.3.1. GPON Physical Media Dependent (GPM) Layer

The GPM Layer is the lowest layer in the GPON protocol stack. This layer is the interface between the GTC layer and the optical fiber medium or ODN. In this layer the conversion from electrical to optical signals and vice versa is performed, and the functions executed are similar to the ones in the physical layer in the OSI model.

The transmission line rates specified by ITU-T standard G.984.2 [TU-T G.984.2, 2003], are presented in Table 2.1.

Table 2:1 GPON Upstream and Downstream rates **[ITU-T G.984.3, 2008]**

Transmission Direction	Nominal Binary Velocity
Upstream	155.52 Mbit/s
	622.08 Mbit/s
	1244.16 Mbit/s
	2488.32 Mbit/s
Downstream	1244.16 Mbit/s
	2488.32 Mbit/s

In the remaining GPON recommendations [ITU-T G.984.1, 2008] [ITU-T G.984.2, 2003] [ITU-T G.984.3, 2008] are established the modulation techniques to be used, the maximum logical reach between OLT and ONU, the differential logical reach between the ONUs connected to the same OLT, the maximum number of ONUs and the maximum path loss allowed. All these requirements are presented in Table 2:2.

Table 2:2 GPON System specifications **[ITU-T G.984.3, 2008]**

Standard	ITU-T
Rate	2.488Gbits/1.244Gbits
Split Ratio	1:64 at PHY ~1:128 (TC layer : logical splits)
Data encapsulation mode	GEM
Broadband efficiency	92%
Line encoding	NRZ
Power budget	Class A (5-10 dB) /Class B (10-25B) /Class C (15-30 dB)
Ranging	Equalized logical reach by adjusting EqD
DBA	Standard format
TDM support	CESoP/ Native
ONT interconnectivity	OMCI
FEC	Reed-Solomon (255,239)
Logical reach (Maximum logical reach)	60km
Differential logical reach (Maximum logical range)	<20km (due to ranging window)
Maximum signal transfer delay	1.5ms
Maximum channel insertion loss	A: 20 dB, B: 25 dB, B+: 28dB, C: 30 dB
Fragmentation	Yes

The maximum logical reach between an OLT and an ONU is limited to 60 km due to hardware specifications. The difference in reach between different ONUs connected to the same OLT are defined as a differential logical reach and must not exceed 20km due to the maximum ranging window.

The split ratio is limited by the Physical layer to 1:64, but for future use the Transmission Convergence (TC) layer supports up to the double amount of ONUs, that is 1:128. The split ratio is limited by the link budget, and the limit in the optical power transmitted by the OLT.

The wavelength windows for GPON are from 1260 nm to 1360 nm for upstream direction, from 1480 nm to 1500 nm for downstream direction, and also assigns a wavelength range for video overlay, from 1550 nm to 1560 nm, as presented in Figure 2.8.

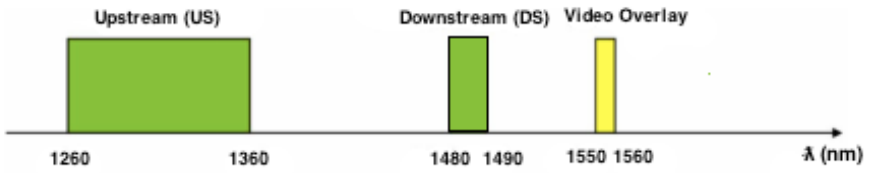

Figure 2.8 GPON wavelength allocation

2.3.2. GPON Transmission Convergence (GTC) Layer

The GPON Transmission Convergence (GTC) layer is the layer above the GPM and has similar functions to the Media Access Control (MAC) that belongs to Data Link layer of the OSI model. This layer is responsible for multiplexing data streams, as well as creating frame headers and maintain internal routing. It is also at the MAC layer that the data is divided into different Transmission Containers (T-CONT) allowing multiple users to share the medium [ITU-T G.984.4, 2008].

Inside the GTC layer there are two sub-layers named Transmission Convergence sub-layer (TC) and GTC Framing (GTC) sub-layer. The Framing sub-layer constructs GPON frames from data and extracts frames into individual data packages. The TC adaption sub-layer provides the upper adaptation to services such as GPON Encapsulation Method (GEM) and Dynamic Bandwidth Assignment (DBA).

The interactions between these two layers can be viewed in greater detail by consulting the Control and Management plane (C/M) and User data plane (U-plane) in the ITU-T G.984.4 Recommendation.

2.3.3. Transmission Containers

T-CONTs perform the management of upstream bandwidth allocation enabling Quality of Service (QoS) implementation in GPON.

Inside an ONU there are five T-CONT types, each one used for different types of traffic.

- T-CONT 1 guarantees fixed bandwidth allocation for real time applications.
- T-CONT 2 guarantees assured bandwidth allocation for non real time applications.
- T-CONT 3 comprises minimum guaranteed bandwidth and additional non-guaranteed.
- T-CONT 4 is best effort.
- T-CONT 5 comprises all service categories and is used for all traffic profiles. [ITU-T G.984.3, 2008]

By knowing the content of the different T-CONTs in all the ONUS, the OLT can allocate different time slot sizes for upstream transmission to the subsidiary ONUs respecting the QoS specifications. [ITU-T G.984.3, 2008]

2.3.4. GPON BWmap

As it was previously presented, one of the GTC layer functionalities is the medium access control, which is controlled by the OLT and makes use of the physical control block (PCBd) of the downstream frame. [TU-T G.984.3, 2008]

The PCBd is used to transmit the upstream bandwidth map (BWmap) (Figure 2.9), in which the OLT uses pointers to indicate the time slot when each ONU may begin and end its upstream transmission. In this way, only one ONU can access the medium at any time, eliminating frame superposition. [Leonid G. Kazovsky, 2011]

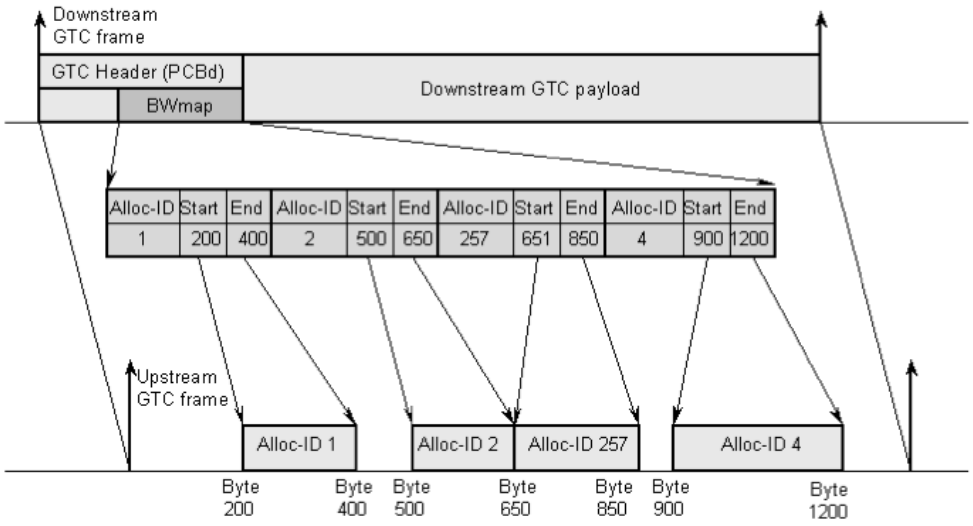

Figure 2.9 GPON BWmap **[ITU-T G.984.3, 2008]**

2.3.5. Dynamic Bandwidth Allocation

Dynamic bandwidth allocation (DBA) is a methodology, controlled by the OLT, used to avoid data collision and share the bandwidth resources fairly to the ONUs in the upstream direction. DBA allows fast bandwidth allocation based on current ONU and network traffic requirements. [Leonid G. Kazovsky, 2011]

The major benefits of DBA are increasing the number of subscribers in the PON, due to more efficient bandwidth use, enhancement of services that require variable rates, and the possibility of allocating substantially bigger rates than the ones that can be allocated in a static way.

The DBA method can be further divided into two categories, depending on the ONU buffer occupancy inference mechanism: Status reporting (SR) DBA, presented in Figure 2.10, is based on the explicit buffer (T-Conts) occupancy reports that are solicited by the OLT, and submitted by the ONUs in response. Traffic monitoring (TM) DBA is based on the OLTs observation of the idle GEM frame pattern and its comparison with the corresponding bandwidth maps. In TM DBA, the OLT continuously allocates a small amount of extra bandwidth to each ONU. If the ONU has no traffic to send, it transmits idle frames during its excess allocation. In the next cycle the OLT reduces the bandwidth allocated to that ONU. If on the other hand the OLT observes that a given ONU is not sending idle frames, it increases the bandwidth allocation to that ONU. In GPON both of these methods shall be supported as well as the possibility of a combination of both. [Leonid G. Kazovsky, 2011], [ITU-T G.984.3, 2008]

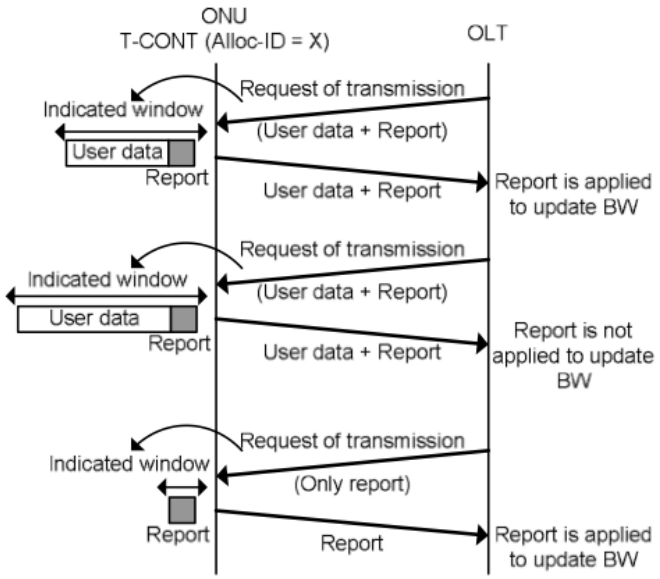

Figure 2.10- SR-DBA Process **[ITU-T G.984.2, 2003]**

2.3.6. GTC Layer Framing

Figure 2.11 shows the GTC frame structure for downstream and upstream directions. The downstream GTC frame consists of the physical control block downstream (PCBd) and the GTC payload section where the data is encapsulated. The upstream GTC frame contains multiple transmission bursts, each one with the upstream physical layer overhead (PLOu) and the allocation interval. Both upstream and downstream frames are 125 μs long.

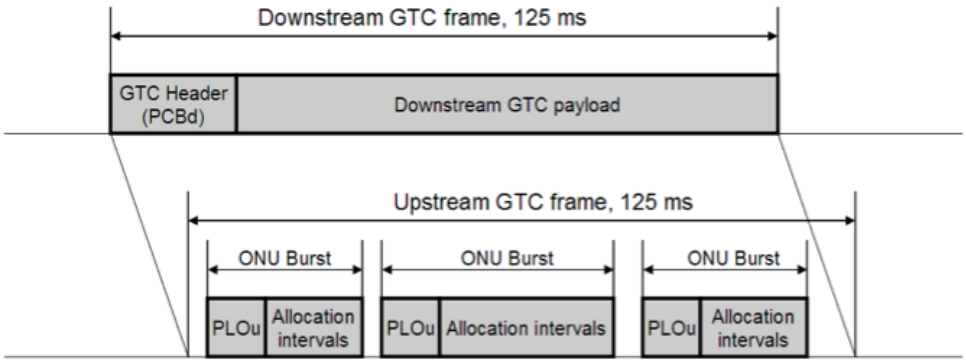

Figure 2.11 GTC Layer Framing **[ITU-T G.984.3, 2008]**

2.3.7. Downstream GTC frame structure

The Downstream GTC frame structure contains two principal fields, the PCBd and the payload that contains GEM frames. The PCBd is further divided into seven fields, which are presented in Table 2.3, and performs the control and synchronization functionalities for the downstream communication. GEM frames are presented in more detail in section 2.3.10.

As the downstream traffic is broadcasted, all the ONUs receive the same information but only unpack the payload according to the Port-ID assigned to the ONU.

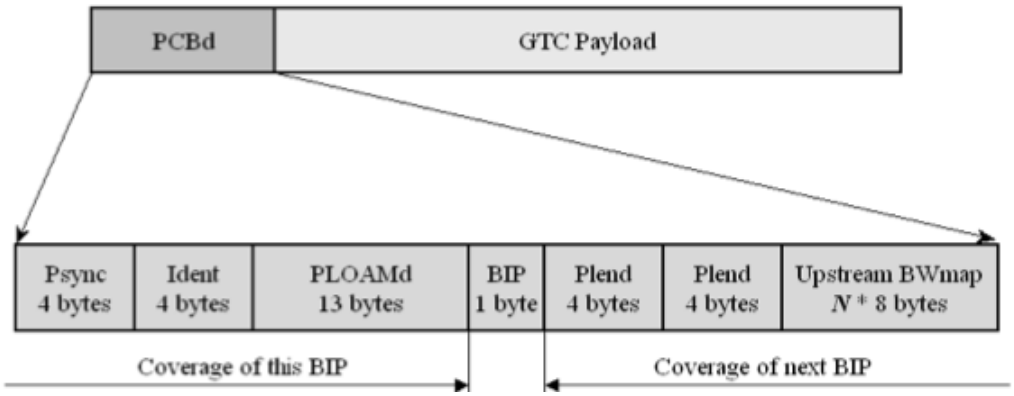

Figure 2.12 GTC physical control block (PCBd) **[TU-T G.984.3, 2008]**

The different fields in the PCBd are presented in Figure 2.12 and resumed in Table 2.3.

Table 2:3 GPON Downstream frame **[ITU-T G.984.3, 2008]**

Field Name	Functionality
PSync	Used for synchronization of the PCBd
Ident	Indicates larger framing structures, to provide error tolerance, including super frame counter and FEC
PLOAMd	Transmits the operation and management message from OLT to ONU
BIP	Used for bit-interleaved parity
Plend	Specifies the Bandwidth and is sent twice for error robustness
US BW Map	Indicates the upstream bandwidth allocation map

2.3.8. Upstream GTC frame structure

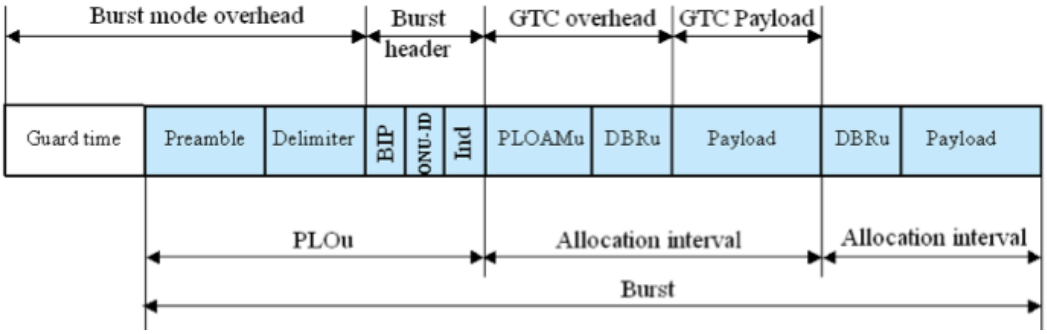

Figure 2.13 Upstream GTC frame structure **(ITU-T G.984.3, 2008)**

As can be seen in Figure 2.13 the upstream GTC frame consists of several bursts, each one containing a PLOu and one or more allocation intervals. The PLOu is mandatory and is composed by the Preamble, Delimiter, BIP, ONU-ID and Ind. Table 2.4 presents the different upstream frame fields as well as the respective functionalities.

The GPON payload is composed of GEM frames, which are explained in detail in the 2.3.10 section.

Table 2:4 GPON Upstream frame **[ITU-T G.984.3, 2008]**

Field Name	Function
PLOu	Signals the beginning of the transmission with ONU and connectivity specifications.
PLOAMu	Transmits the operation and management message from ONU to OLT
DBRu	Reports the upstream Dynamic bandwidth and the traffic status of the T-CONTs
Payload	Transmits the upstream payload, using GEM frames

2.3.9. Forward Error Correction

Forward Error Correction (FEC) is a mathematical processing technique that allows the link budget to be increased in 3 to 4 dBs [ITU-T G.984.3, 2008]. The data is encoded introducing a small amount of redundancy to allow the decoder to detect and correct transmission errors. With this improvement longer distances between OLT and ONUs and higher splitting ratios can be achieved.

The system used for the FEC encoding in GPON systems is the Reed-Solomon (255,239) which means the code word has 255 bytes, where 239 bytes are data and 16 are overhead parity bytes placed in the end of every codeword, as it is presented in Figure 2.14. An important feature of FEC is the fact that the original data is preserved allowing devices that not support FEC to be connected to devices that do. [ITU-T G.975, 1996]

In this dissertation, FEC assumes special importance for the upstream communication coexistence scenario proposed, therefore a deeper study on upstream FEC has been made.

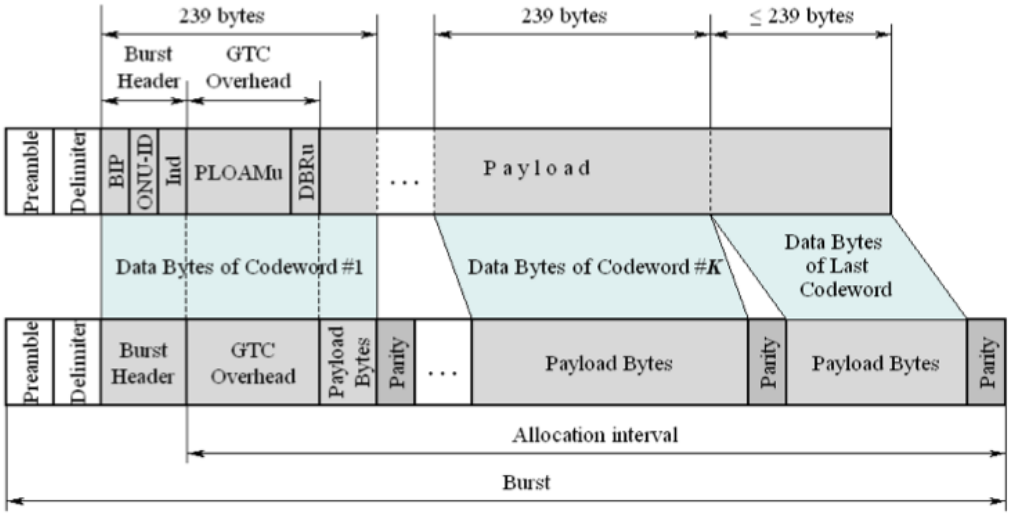

Figure 2.14 Upstream transmission with parity bytes insertion **[ITU-T G.984.3, 2008]**

For GPON Downstream frames all the bits are used for the FEC coding, but in GPON Upstream frames the Delimiter and Preamble are excluded as presented in Figure 2.14.

The coexistence scenario presented in section 4 strongly depends on the correcting performance of the RS (255,239). The correcting performance depends on the theoretical relationship between the BER after and before FEC function correction, respectively BER_{Output} and BER_{Input}. The relation can be mathematically computed with

the assumption that errors occur independently from each other and that the decoder never fails (probability of incorrect decoding equal to zero). [ITU-T G.975, 1996]

Thus:

$$\begin{cases} P_{UE} = \sum_{i=9}^{N} \frac{i}{N} \cdot \binom{N}{i} \cdot P_{SE}^{i} \cdot (1 - P_{SE})^{N-1} \quad with\ N = 255 \\ BER_{Input} = 1 - (1 - P_{SE})^{1/8} \\ BER_{Output} = 1 - (1 - P_{UE})^{1/8} \end{cases}$$

with:

P_{UE} = Probability of an Uncorrectable Error
P_{SE} = Probability of a Symbol (byte) Error
N= Codeword length (255)

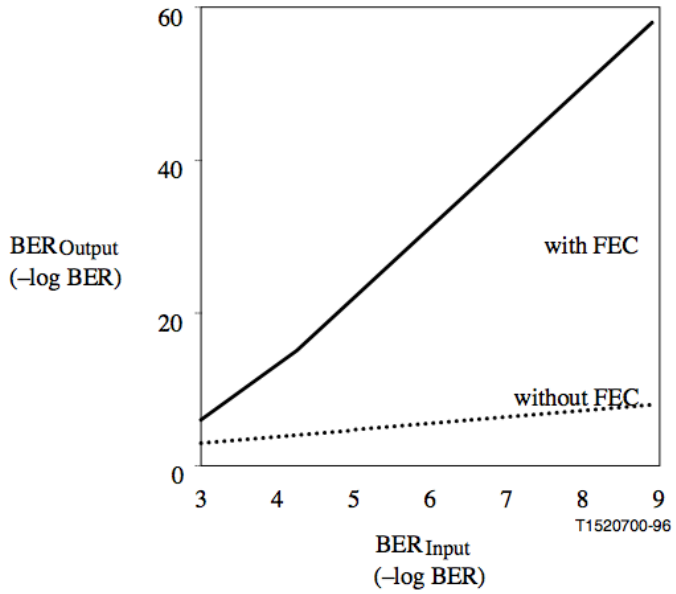

Figure 2.15 Theoretical output BER versus input BER **[ITU-T G.975, 1996]**

For BER_{Input} above 10^{-3}, the probability of incorrect decoding strongly increases because the error pattern is beyond the capacity of the decoder to correct the codeword. In such cases, the BER_{Output} versus BER_{Input} curves are even located below the "without FEC" curve in Figure 2.15. For a BER_{Input} bellow 10^{-3} the FEC shows great correcting performance, for example a BER_{Input} in the order of 10^{-4} is converted into a BER_{Output} around 10^{-24}. [ITU-T G.975, 1996]

2.3.10. GEM Data Mapping

The GPON Encapsulation Method (GEM) allows GPON systems to transport payload data from different formats such as ATM traffic and Ethernet over the GTC layer in a transparent way [Leonid G. Kazovsky, 2011]. The Ethernet frames are carried directly in the GEM frame payload and as it can be seen in Figure 2.16 the preamble and SFD bytes are dropped prior to GEM encapsulation. Table 2.5 presents the GEM fields and the respective functions.

One of the Advantages of GPON over EPON is the fact that fragmentation is possible, thus one Ethernet frame can be mapped into a single GEM frame or multiple GEM frames, but one GEM frame shall not carry more than one Ethernet frame.

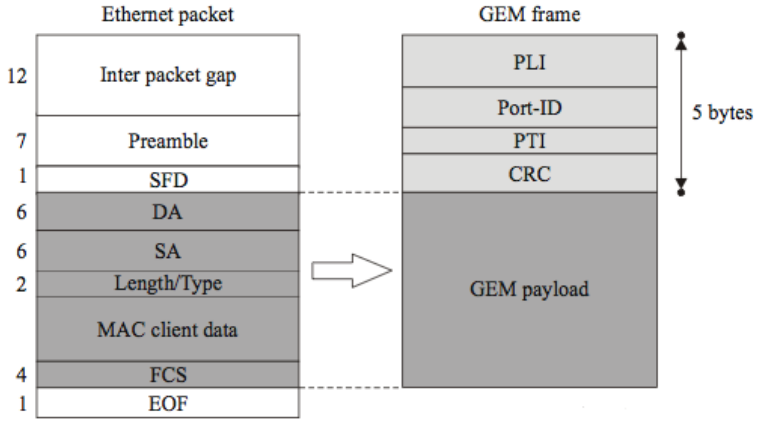

Figure 2.16 GPON Encapsulation Method (GEM) **[Boomsma, 2006]**

Table 2:5 GPON Encapsulation Method (GEM) **[ITU-T G.984.3, 2008]**

Field Name	Function
PLI	12 bit field to Indicate the length of the payload.
Port-ID	12 bit field to indicate the payload destination.
PTI	3 bit field to indicate the content type of the fragment payload and its appropriate treatment
CRC	13 bit field to provide error detection and correction functions.
GEM Payload	Carries Ethernet fragments striped of Preamble, SFD and extension fields

2.4. Ethernet Passive Optical Network (EPON)

Following the same structure presented for the GPON, we will present the EPON system accordingly to the protocol stack defined by the IEEE 802.3ah recommendation and depicted in Figure 2.17.

The IEEE 802.3ah recommendation is an extension to the 802.3 Ethernet standard where the physical and data link layers of the EPON network are specified.

Unlike ITU standards, such as BPON or GPON, IEEE 802.3ah specifies only a small portion of an EPON system. This creates significant interest from the research community and fabricants, to address interesting challenges that are omitted from the standard, but on the other hand makes the compatibility between equipment from different vendors a problem.

The EPON stack is significantly more complex than the GPON as can be seen in both Figure 2.7 and 2.17. The Physical medium dependent (PDM), physical medium attachment (PMA) and physical coding sublayer (PCS) are used to adaptation and conversion from the physical medium to a standardized interface, the so called gigabit media independent interface (GMII).

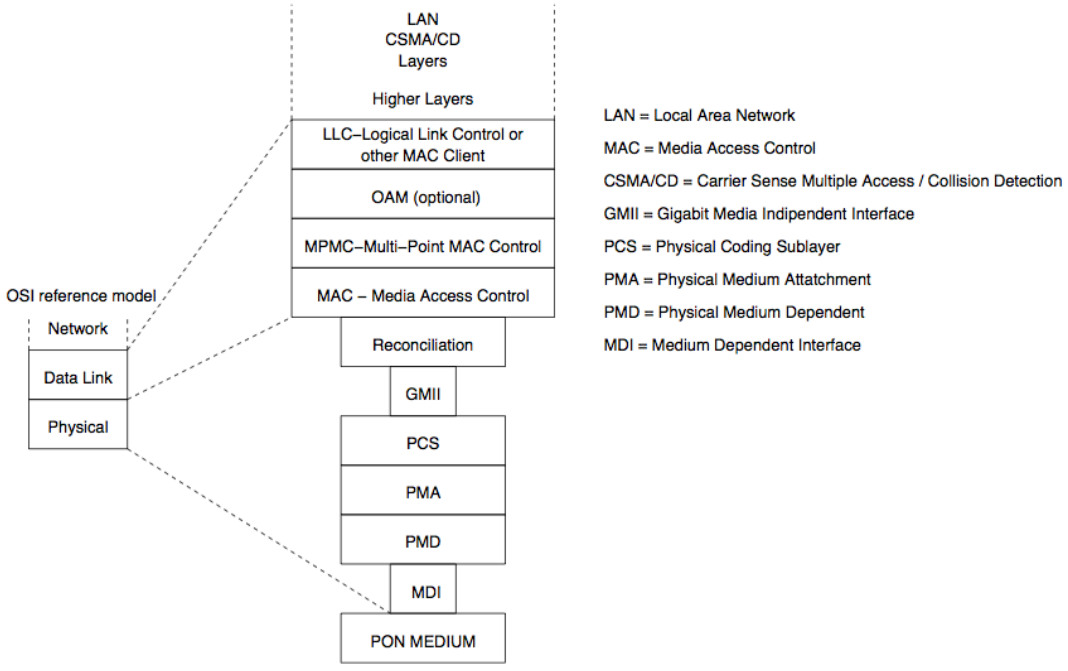

Figure 2.17 EPON stack **[Boomsma, 2006]**

In table 2.6 the functionalities associated to the different stack sub-layers are presented.

Table 2:6 EPON Stack fields **[Boomsma, 2006]**

Sublayer name	Function
LLC	Used to rout the packages to the corresponding MAC client.
OAM	Operation, Administration and Maintenance”
MPMC	Allows P2MP instead of P2P connections, and implements the DBA.
MAC	Responsible for framing, addressing, error detection and access control
RECONSILIATION	Translates the GMII and presents them to the MAC layer.
GMII	Standard interface used to allow data medium Independence.
PCS	Decodes/encodes the data into the 8B/10B line code
PMA	Bit level synchronization using CDR process and autocorrelation process, and clock recovery.
PMD	Controls the modulation of the data on the carrier.

2.4.1. EPON Physical Medium Dependent (PMD) Layer

PMD layer is specified in clause 60 of the IEEE 802.3ah standard. Two implementations [PON, 2008] are defined, namely 1000BASE-PX10 and 1000BASE-PX20, being the 10 and 20 the correspondent length in km between OLT and ONUs.

Table 2.7 summarizes the EPON system specifications defined in the clauses of the IEEE 802.3ah standard. The difference between the PX10 and PX20 specifications are inside the OLT, which in the PX20 case uses a better transmitter and an APD receiver, instead of a PIN. Since the difference in the specifications is inside the OLT, the ONU can be similar, lowering the cost of network.

Unlike GPON that has several transmission rates, EPON adopted a fixed 1.25Gbit/s but, due to the 8B/10B line encoding, the bit rate for data transmission is 1Gbit/s. The splitting ratio is not defined in the standard but 1:16 without FEC or 1:32 with FEC are the usual configurations.

Table 2:7 EPON System specifications

Standard	IEEE 802.3ah
Rate	1.25/1.25Gbit/s
Split Ratio	1:16 ~1:32 (32767 limit by LLID address space 2^{15}
Data encapsulation mode	Ethernet
Broadband efficiency	72%
Line encoding	8B/10B
Ranging	Round trip time
DBA	Defined by vendor
TDM support	CESoP
ONT interconnectivity	None
OAM	Weak, extended by vendors
FEC	Reed-Solomon (255,239)
Logical reach (Maximum logical reach)	Unlimited (krammer)
Differential logical reach (Maximum logical range)	Unlimited (Krammer)
Maximum channel insertion loss	PX10: 20 dB PX20: 24dB
Fragmentation	No

The operating wavelength range is the same as the one for ITU-T B/GPON and it is presented in Figure 2.18. The wavelength range overlapping is the main issue in the stacked-PON scenario, as it will be presented in section 2.5

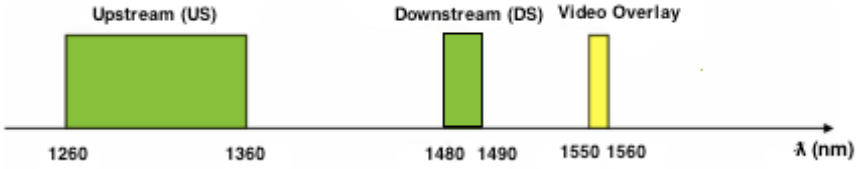

Figure 2.18 EPON wavelength allocation

2.4.2. Multi Point Mac Control (MPMC)

To allow Point-to-Multi-Point (P2MP) topology over the Point-to-Point (P2P) topology presented in the previous releases of the 802.3 standard, EPON systems makes use of a layer called Multi Point Mac Control (MPMC). This layer is defined in clause 64 of the 802.3ah standard and performs ranging, bandwidth arbitration, and discovery functions.

2.4.3. Multi Point Control Protocol (MPCP)

The MPCP is a TDMA multiplexing scheme, in which the upstream channel is divided into time-slots allocated to the ONUs as it is presented in Figure 2.19. During the time slots allocated to a specific ONU, the upstream channel is dedicated to that ONU. MPCP uses two types of messages, the REPORT message is used by the ONUs to report the status of its queues to the OLT, and GATE messages sent by OLT, indicating the ONUs upstream transmission windows [Leonid G. Kazovsky, 2011] [Kramer, 2004]. GATE messages are sent in-between regular Ethernet frames, and each frame specifies the ONU by its LLID and also the start and length of the upstream window. Upon receiving the grant, the ONU transmits as many Ethernet frames as it can fit into the allocated transmission slot. As fragmentation is not allowed, only full frames can be transmitted [Kramer, 2004].

The ONU can request additional grants by sending REPORT messages. In EPON systems, the traffic streams that arrive at the ONUs from the customer premises are kept in queues. There are up to eight different queues with different priorities and QoS requirements [Kramer, 2002]. The queues follow the IEEE 802.1p recommendation.

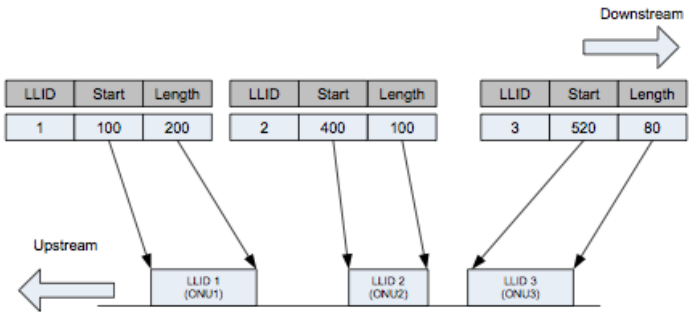

Figure 2.19 EPON Multi Point Control Protocol **[Kramer, 2004]**

2.4.4. EPON Frame

In EPON systems there are two types of frames that should be noticed. The data and control frames, presented respectively in Figure 2.20 and Figure 2.21.

The upstream and downstream data frames are equal and very similar to the common Ethernet frames. Both generic Ethernet frames and EPON frames contain the destination and source MAC address (DA and SA), payload length/type, a variable-size payload section, and CRC.

The differences reside in the modifications of the EPON header. The preamble and start of the frame delimiter (SFD) are modified to include LLID and to enable the point-to-point-emulation (P2PE) function. The SFD byte is moved to the third byte of the preamble, which is renamed to start of the LLID delimiter (SLD). The LLID is used by the ONUs to filter the received packets, and forward them to the upper layers. The LLID is assigned to each ONU by the OLT. [Boomsma, 2006]

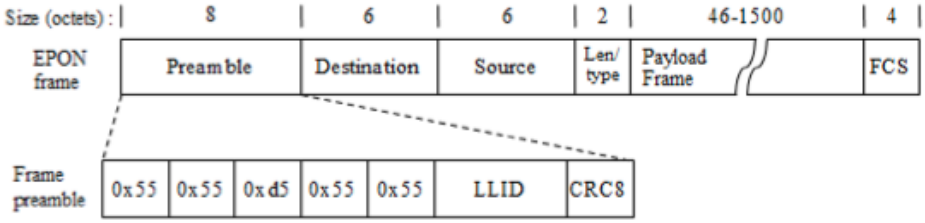

Figure 2.20 EPON Data Frame **[Boomsma, 2006]**

The control frames are called multi-point control protocol data unit (MPCPDU) and are constructed from the standard IEEE 802.3 MAC-CONTROL frames. The control frames are identified by a certain Opcode in the Opcode field which is 2 bytes long. The most important MPCPDU frames are the GATE and the Report frames. [Boomsma, 2006]

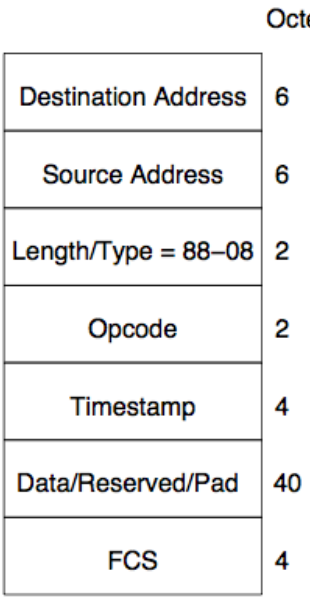

Figure 2.21 EPON MPCP Control Frame **[Boomsma, 2006]**

2.4.5. Interleaved Polling with Adaptive Cycle Time (IPACT)

In the majority of the EPON systems some sort of dynamic bandwidth allocation scheme is implemented but it is important to notice that the 802.3ah standard does not specify any algorithm, instead it leaves it open to the implementation of each vendor or manufacturer [Kramer, 2002] [IEEE 802.3ah, 2004] [Leonid G. Kazovsky, 2011].

As the bandwidth allocation is not specified by the standard, different options can be used, from an even division of the bandwidth among all ONUs, to the allocation of all the bandwidth to a single ONU. The best-known DBA algorithm is called interleaved polling with adaptive cycle time (IPACT) DBA and it is presented in Figure 2.22 [Leonid G. Kazovsky, 2011] [Kramer, 2002].

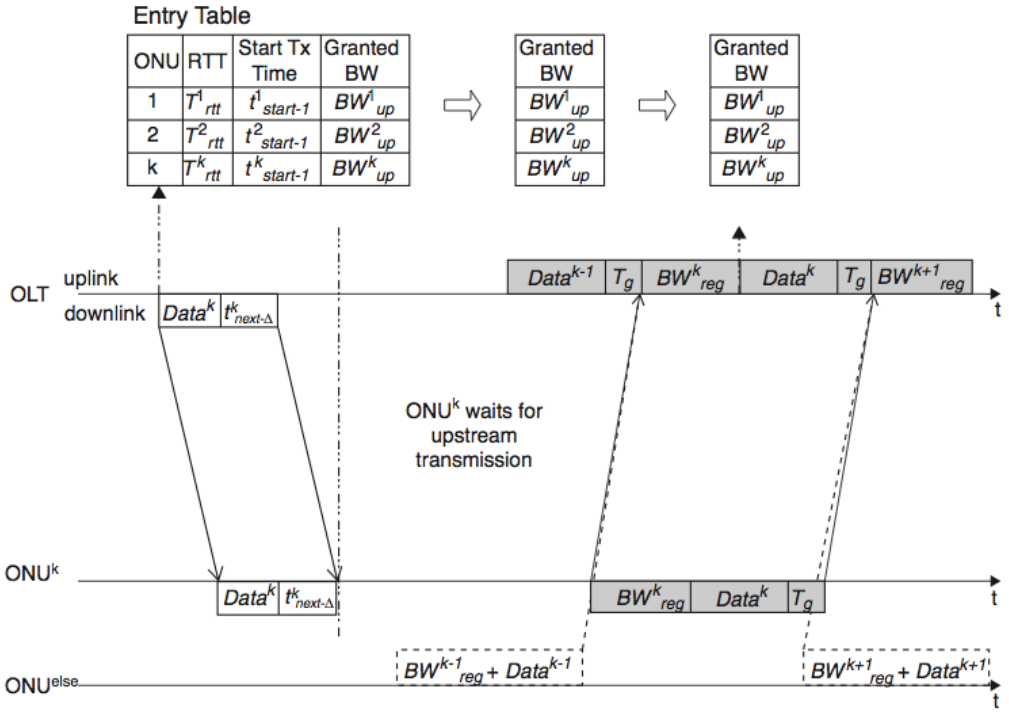

Figure 2.22 EPON DBA Process **[Leonid G. Kazovsky, 2011]**

The IPACT allows bandwidth allocation by keeping track of the bandwidth requests sent from the ONUs and granting them in the next traffic cycle. To avoid upstream collisions the GATE messages are timed according to the respective round trip time (RTT) of each ONU.

As the IPACT schedules upstream traffic bursts in a pipelined fashion, the successive bursts are separated by a minimum specified guard time, allowing upstream bandwidth utilization to be maximized. [Leonid G. Kazovsky, 2011]

The grants are conceived according to different algorithms, which may support functions such as bandwidth fairness, QoS etc. Some of the most used algorithms are described in table 2.8.

Table 2:8 DBA Scheduling services **[Kramer, 2002]**

Service	Description
Fixed	Ignores the BW requests from the ONUs. Divides the BW evenly by all the ONUs connected.
Gated	Grants the BW requests from the ONUs without time window limitations.
Limited	Grants the BW requests from the ONUs up to a certain limit. Implemented to overcome channel monopolization by one ONU.
Elastic	Grants the BW requests to one ONU, up a window which size can be as big as the size of all grants from all the ONUs combined in the previous cycle, (if just one ONU is transmitting)

2.4.6. 8B/10B Coding

The 8B/10B coding of the data is performed at the GMII. During the 8B/10B encoding and decoding, each set of 8 bits (octet) is converted into a 10 bit value. The goal of this process is to ensure that there are sufficient zero-to-one or one-to-zero transitions to allow an easy clock recovery and the balance of the DC level. The major drawback is the associated wasted bandwidth that is 25% [Kramer, 2004] [Leonid G. Kazovsky, 2011].

2.4.7. Forward Error Correction

EPON systems do not have Forward Error Correction (FEC) defined in the standard, however to allow the splitting ratio to increase from 16 to 32 users, or to increase the distance from OLT to the ONUs FEC must be used [IEEE 802.3ah, 2004]. The FEC encoding technique usually used in EPON is also the Reed-Solomon (255,239), used in GPON systems, allowing the same improvement of 3 to 4 dBs in the link budget [Leonid G. Kazovsky, 2011].The correcting performance presented in Figure 2.15 can also be applied for EPON systems.

2.5. Stacked-PON

The Stacked-PON scenario presented in the Figure 2.23 is composed by one EPON network (OLT and ONUs) and one GPON network, sharing the same fiber span, from the optical splitter situated close to the OLTs, to the optical splitter close to the ONUs. As a consequence of both PONs sharing the same wavelength plan, it is impossible to connect them without serious packet losses.

For the sake of clarity the EPON and its elements are going to be designated as the “base PON”, and GPON and its elements called as “interference PON”.

As presented in section 2.2.3, upstream and downstream communication employ different methodologies, thus different coexistence scenarios were studied and proposed. In the downstream direction, traffic is transmitted in continuous mode, thus it is impossible to directly connect for example a GPON OLT to an EPON network, without prohibitive degradation of the respective traffic flows. The solution presented for the downstream communication is based on the use of all-optical wavelength conversion at both ends of the interference PON as presented in Figure 2.23.

In the upstream direction one of two solutions can be explored, the wavelength conversion as it is presented in Figure 2.23 or the possibility of upstream coexistence taking advantage of channel “free window times” between bursts from different ONUs. The coexistence scenario is further studied due to its simplicity and unprecedented approach.

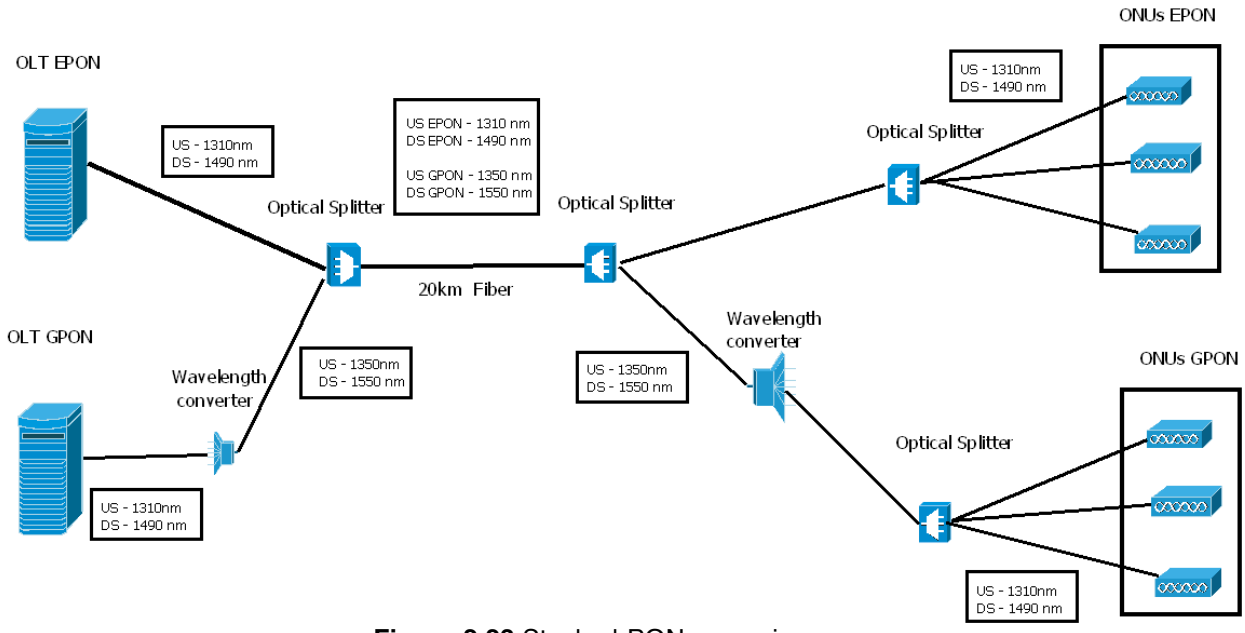

Figure 2.23 Stacked-PON scenario

In the downstream direction wavelength conversion is mandatory. Various possibilities can be used, such as opto-electronic conversion through the use of optical transceivers, or all-optical wavelength conversion. The latter presents several advantages such as higher bit rates, bit rate transparency and low power consumption.

The wavelength hop studied for the upstream transmission is from 1490nm to 1550nm due to the low attenuation, Figure 2.24, and great availability of optical devices in the C Band, such as SOAs, MZI-SOAs and EDFAs.

For upstream transmission the wavelength conversion proposed is from 1310 nm to 1330 nm, due to the similar characteristics of the fiber for neighbor CWDM channels (CWDM, 2012) and because higher wavelength hops would imply increased difficulties in the wavelength conversion process.

In section 4 upstream communication coexistence is simulated (section 4.2) and physically assessed through an experimental setup (section 4.3).

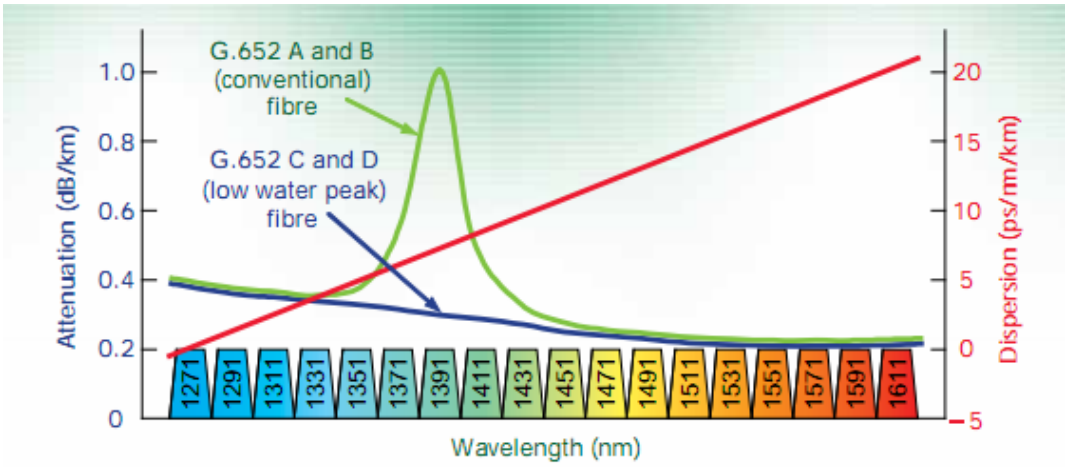

Figure 2.24 Fiber Attenuation and dispersion per wavelength channel **[CWDM, 2012]**

2.6. Conclusions

In the current chapter are presented the PON standards that currently experience higher deployment rates, EPON and GPON. Section 2.2 presents a general overview on PON topology, functionalities and upstream/downstream data transmission and management.

Section 2.3 and 2.4 presents in greater detail, respectively the GPON and EPON networks, focusing on the different aspects such as traffic encapsulation, bandwidth allocation, line coding and physical media layer specifications. These two sections are

important for both the comprehension of the stacked model proposed and the correct setting of the simulation model presented in section 4.2

Section 2.5 presents the Stacked-PON model proposed and explains the methodology followed for the upstream and downstream EPON/GPON coexistence over the same fiber.

3. Downstream communication

3.1. Wavelength Conversion

Wavelength converters (WC) are key components in this dissertation scenario, as they will allow the coexistence of both EPON/GPON upstream and downstream signals, in the same fiber span between the OLTs and ONUs, without packet losses inhibitive of communication.

WC are devices that convert one input modulated signal (usually called pump), at a certain wavelength λ_1, to another wavelength λ_2 (usually called probe), without modifying the information of the pump signal. They can be divided in two groups, optical-electro-optical converters (OEO-WC), where the input signal is converted from the optical domain to electrical and then back to optical again, and all-optical WC (AO-WC), where there is no conversion to the electrical domain.

In OEO converters, the input signal at λ_1 is detected using a PIN or APD receiver, then the obtained electrical signal is usually regenerated and modulated in the new desired wavelength λ_2 .The drawbacks of OEO converters are the low conversion bit rate, transparency and high power consumption. To overcome these problems, all optical conversion is presented as the solution and it will be studied in detail during this chapter.

The most important characteristics for wavelength converters are indicated bellow [Durhuus, 1996], [Silveira, 2011] :

- Bit rate independence;
- low extinction ratio degradation;
- Reduced signal to noise ratio degradation;
- Moderate input power required;
- Operation over a large input and output ranges of wavelengths;
- Operation over a large input power range;
- Low chirp;
- Simplicity;

Semiconductor optical amplifiers arise as the optimum medium for wavelength conversion, especially due the non-linearities and the different employment possibilities for optical processing, such as regeneration and amplification.

Section 3.1.1 begins with an introduction to SOAs structure and basic principles of operation and section 3.1.2 presents the theoretical principles for cross gain modulation

(XGM). Section 3.1.3 and 3.1.4 present respectively the theoretical principles for cross phase modulation (XPM) and cross polarization rotation (XPR)

3.1.1. Semiconductor Optical Amplifiers (SOAs)

Semiconductor optical amplifiers (SOAs) are key devices in all-optical data processing, and from their intrinsic properties arises the wavelength conversion possibilities studied over the next sections. SOAs are very attractive amplifiers and signal processing units, especially for access networks, because of their low cost, high gain, fast response and compact size, allowing an easy integration in photonic circuits.

The first semiconductor optical amplifiers, dated from the 60s, were made from GaAs junctions and operated in the so-called first window, ranging from 800nm to 900nm. Due to the high fiber losses presented in this window and the existence of a more suitable window that ranges from 1300nm to the 1600nm, a new generation of SOAs was developed in the 80s using InP/InGaAsP junctions.

The SOAs are usually a double heterostructure with different band gap energies, and an active layer responsible for the amplification between them. The input signal is confined to the active region that acts as a waveguide, and due to the reflections from the end facets the process adds considerable noise. [Connelly, 2002]

Semiconductor optical amplifiers work in a similar way to semiconductor lasers. The light beams are produced, in the laser case, or the light is amplified in the SOAs, through a stimulated emission process inside a resonant cavity. The major difference between SOAs and the lasers are the reflectance of the cavity end-facets that in the case of the SOA are low and for the lasers is very high (mirror). Hence the, fabrication and design are very similar. The process of amplification resides on the transitions of free carriers between the conduction band and the valence band, and the consequent energy radiation. The most important carrier transactions between the energy bands are spontaneous emission, stimulated emission and stimulated absorption. Figure 3.1 shows the described transitions.

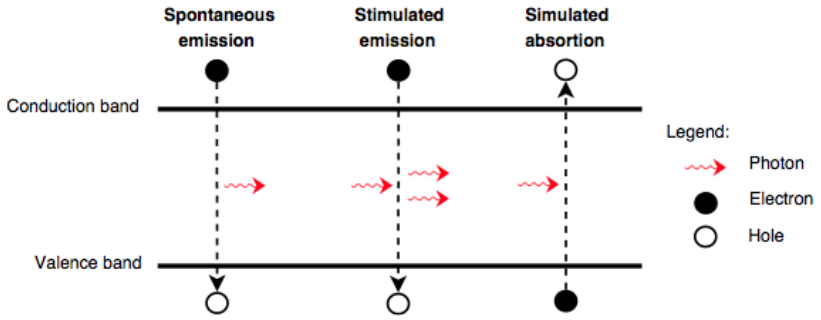

Figure 3.1 Carrier transitions between valence band and conduction band **[Connelly, 2002]**

In the spontaneous emission process an electron in the conduction band recombines with a hole in the valence band, lowering the energy state and emitting a photon with the energy correspondent to the transaction from conduction to valence band. This photon has random phase, direction and frequency and it is responsible for the amplified spontaneous noise (ASE).

In the stimulated emission a biasing current is applied to the active region to allow population inversion, i.e from the valence to conduction band. When a photon incident in the semiconductor has suitable energy to cause a carrier in the conduction band to recombine with a valence bands hole, a new photon is emitted with identical phase, direction and frequency as the incident one. This process repeats itself along the active region in an avalanche way allowing coherent light emission.

The last process is the absorption, and occurs when the injected current is low and the incident photon energy is higher than the energy defined by the band gap difference. The photon is absorbed by the carrier in the valence band instead of contributing to the amplification of the input signal.

Besides the linear amplification, SOAs are very attractive to perform signal processing due to the non linearities associated, such as four wave mixing (FWM), cross polarization rotation (XPR), cross gain modulation (XGM) and cross phase modulation (XPM) [Durhuus, 1996], [Dutta, 2006].

The latter three will be presented next in detail, as they will be studied as different possibilities for wavelength conversion.

3.1.2. Cross Gain Modulation

The cross gain modulation technique takes advantage of the third order optical nonlinearities (χ^3) presented in the SOAs to perform wavelength conversion [Durhuus, 1996]. The principle used is very simple compared to other modulation techniques such as

XPM, FWM and XPR. As can be seen in Figure 3.2, a modulated input signal (λ_1) will saturate the gain of the SOA, thus the number of active carriers in the excited state will decrease, resulting in a decrease of gain. The modulation of the probe signal is proportional to the gain, so the output signal, at λ_2, will be an inverted copy of the signal at λ_1. (A maximum in the pump input wave corresponds to a minimum in the converted output signal). Usually after the SOA a filter selects the probe wavelength and drops the pump.

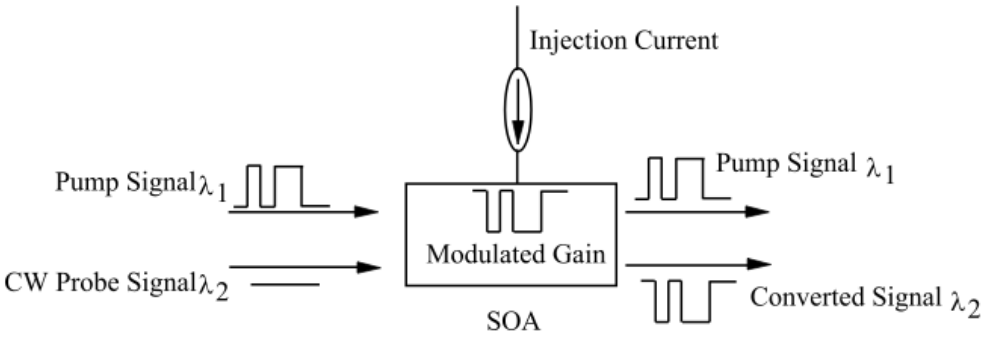

Figure 3.2 Scheme of wavelength conversion in SOA based in XGM **[Sun, 2002]**

The XGM wavelength conversion is illustrated in Figure 3.3. In the first image (i) an input signal containing the bit stream 01001010 is applied to the SOA. Due to this input bit stream, the carrier density variations will present the pattern pictured in (ii). As it is possible to observe, the density variation appears as a reversed stream of the input signal, 10110101.

The probe signal will be modulated according to the carrier density induced variations, thus the converted probe signal will contain the bit stream 10110101 as shown in (iv). The converted probe signal will be an inverted replica of the original intensity-modulated input signal.

Figure 3.3 on the right represents the transfer function characteristic for the XGM wavelength conversion. The ideal transfer function is shown as well as one more similar to an experimental one. The shape of the real transfer function is due to the slow gain recovery of the SOA.

XGM wavelength conversion presented in Figure 3.2 is configured as a co-propagating scheme i.e pump and probe signals both enter the SOA in the same side, and propagate in the same direction, but is also possible to obtain XGM conversion using a counter-propagating scheme, where the probe and pump signals enter/travel the SOA in opposite sides/directions. The counter-propagation scheme avoids the use of output optical filter, due to the different propagating directions. In both configurations the XGM

conversion generates noise due to the ASE within the SOA as well as degradation of the extinction ratio [Senior,2009]

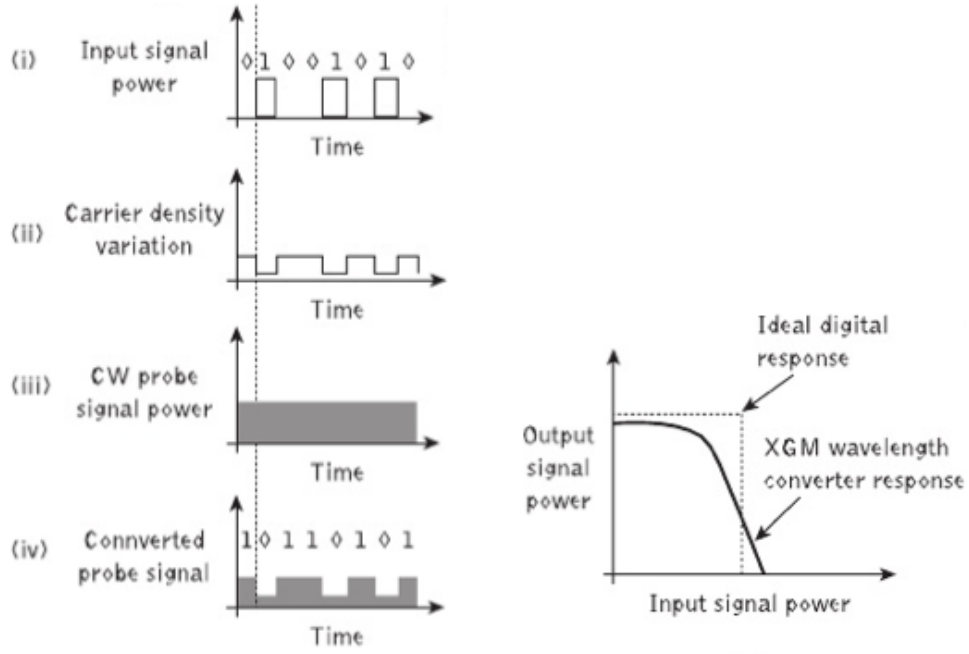

Figure 3.3 Signal time chart showing the operating principle of XGM wavelength conversion (left) and transfer function characteristic for the XGM wavelength conversion (right) **[Senior, 2009]**

The main advantages of wavelength converters based on XGM in SOAs are the simplicity of operation, high conversion efficiency, polarization independence (if the SOA used is also polarization independent) and high range of input and output wavelengths acceptance [Durhuus, 1996]. On the other hand, the speed of operation is determined by the carrier dynamics of the SOA, which is restricted due to its relatively slow carrier recovery (tens of picoseconds) [Durhuus, 1996]. The other disadvantages are the small extinction ratio (because the gain is never reduced to zero, Figure 3.3 (II)(IV)), degradation due to spontaneous emission and frequency chirping due to the variations in the refractive index, caused by changes in carrier density inside the SOAs. [Durhuus, 1996] [Dutta, 2006]

3.1.3. Cross Phase Modulation

Cross phase modulation (XPM) is a cross modulation technique that allows the output signal not to be inverted, contrarily to the previously presented XGM. XPM can be implemented taking advantage of the non-linearities presented in optical fibers or semiconductor devices such as MZI-SOAs, Michelson interferometers or a Delayed Interference Signal Converter (DISC) [Durhuus, 1996]

Whereas XGM wavelength converters take advantage of the gain modulation

presented in semiconductor optical amplifiers, due to an input modulated signal, the cross phase modulation is based on the variation of the refractive index of the semiconductor medium, due to the input signal. The variation of the refractive index of the nonlinear medium is proportional to the amplitude of the input signal and inversely proportional to carrier density variations. [Senior, 2009]

The working principle used in XPM wavelength converters is presented in Figure 3.4. A pump signal, intensity modulated (IM) at (λ_1) and a probe signal, CW at (λ_2) are simultaneously injected into an SOA. Due to the high power of the pump signal the SOA saturates and the output signal at (λ_2) experiences phase modulation accordingly to the input information [Joergensen, 1996]. The output signal should be intensity modulated as the pump signal, thus after the phase modulation inside the SOA a phase to intensity stage is necessary.

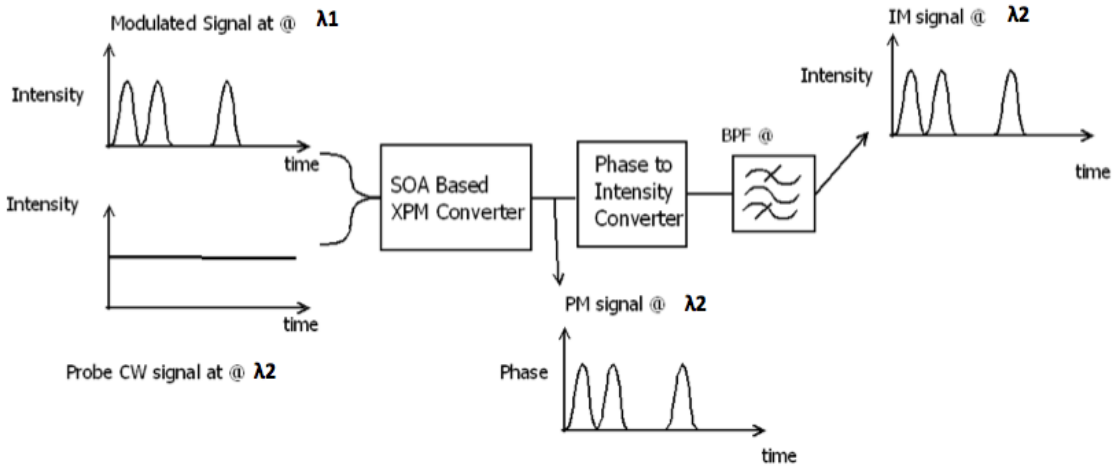

Figure 3.4 Cross-phase modulation (XPM) working principle based on **[Silveira, 2011]**

As it was presented previously the main advantage of XPM based converters is the possibility of not inverting the information presented in the pump signal, but also high conversion efficiency and high output extinction ratio are achieved [Cartledge, 2002]. The major drawbacks of the XPM conversion are the narrow input power dynamic range, and the increased complexity due to the conversion from phase to intensity modulation [Hanfoug, 2003]. It is also important to note that XPM wavelength conversion experience XGM non-linearitys in the probe signal. This gain modulation is highly undesired since it introduces patterning effects and degradation of the output signal.

Cross Phase Modulation in MZI-SOA

In XPM converters based on MZI-SOAs, a CW signal, called probe, at the wavelength λ_2 is split equally and passes simultaneously in the two arms of the MZI (Figure 3.5). These two beams are amplified by the SOAs and then merge and interfere at the output coupler. A modulated signal λ_1 passes through one of the arms, and during the "one" bits, both the gain inside the SOA and the refractive-index change. These changes will modulate the phase of the CW signal that passes through this arm. The different phase introduced in CW is obtained because the saturation gain induced by λ_1 reduces de carrier density inside the SOA, and thus the refractive index increases. If during the "one" bits the phase shift is equal to π, the two CW signals will interfere at the output creating an exact replica of the input modulated signal with the new desired wavelength.

The relation between the output signal P_o to the input signal P_i is described by [Dutta, 2006]:

$$\frac{P_o}{P_i} = \frac{1}{8}\left\{G_1 + G_2 - 2\sqrt{G_1 G_2}\,\cos(\emptyset_1 - \emptyset_2)\right\} \quad (3.1)$$

where G_1 and G_2 represent the amplifiers' gains and $\emptyset_1$, $\emptyset_2$ are phase changes induced by nonlinear effects in the two amplifiers. The phase difference, at the output is given by [Dutta, 2006]:

$$\Delta\emptyset = \frac{\propto}{2P_s}\left\{-\frac{h\nu}{e}(I_1 - I_2) + \frac{P_c}{2}(G_1 - 1)\right\} \quad (3.2)$$

where $\propto$ is the linewidth enhancement factor, P_s is the injected power in one of the amplifiers, P_c is the saturation power in the amplifier and I_1, I_2 are the currents through the two amplifiers. Considering $I_1 \cong I_2$ and if the SOAs are equal, $G_1 \cong G_2 \cong G$.

$$\frac{P_o}{P_i} = \frac{G}{2}\sin^2\left(\frac{\Delta\emptyset}{2}\right) \quad (3.3)$$

where $\Delta\emptyset = \frac{\propto}{4}\frac{P_c}{P_s}(G - 1)$

Substituting by typical values [Dutta, 2006] such as 3 for α, 10 mW for P_s and saturated gains of G ≅ 40, we get P_c =1mW for $\Delta\emptyset\ of\ \pi$.

The carrier-induced changes are the major responsible for the refractive index variations, nonetheless there are some minor thermally induced refractive index changes. [Dutta, 2006]

A XPM modulator can operate at the same bit rates as XGM, 80 Gb/s [Veerasubramanian, 2008] [Contestabile, 2010], offering a large contrast, and small chirp due to the use of very small gain variations to induce a large phase shift.

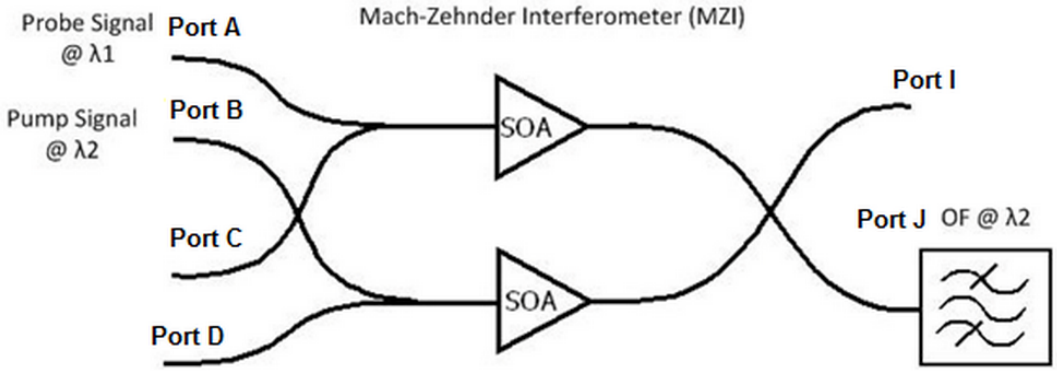

Figure 3.5 XPM WC using MZI-SOA [Dionísio, 2010]

Similar to XGM, XPM modulation can be implemented in a co-propagating scheme where both λ_1 (input signal) and λ_2 (probe signal) are launched in the interferometer and travel in the same direction or in a counter-propagation scheme where the input and probe signal travel in opposite directions. The operation principle is similar for both schemes, but the counter-propagating scheme has the advantage of reduced noise, since the probe signal does not appear at the output, sparing the use of an optical filter.

3.1.4. Cross polarization rotation

Besides cross gain and cross phase modulation, cross polarization rotation emerge as a very attractive way to perform the out-of-band wavelength conversion needed for this dissertation scenario. Tang et al [Tang, 2005] demonstrated out-of-band cross polarization modulation for a modulated signal at 1480nm, and using the probe signal in the 1520 to 1600nm range with good Q-factor and very low ER penalty.

The operation basics of the wavelength converters based in XPR can be seen in Figure 3.6 and are described below.

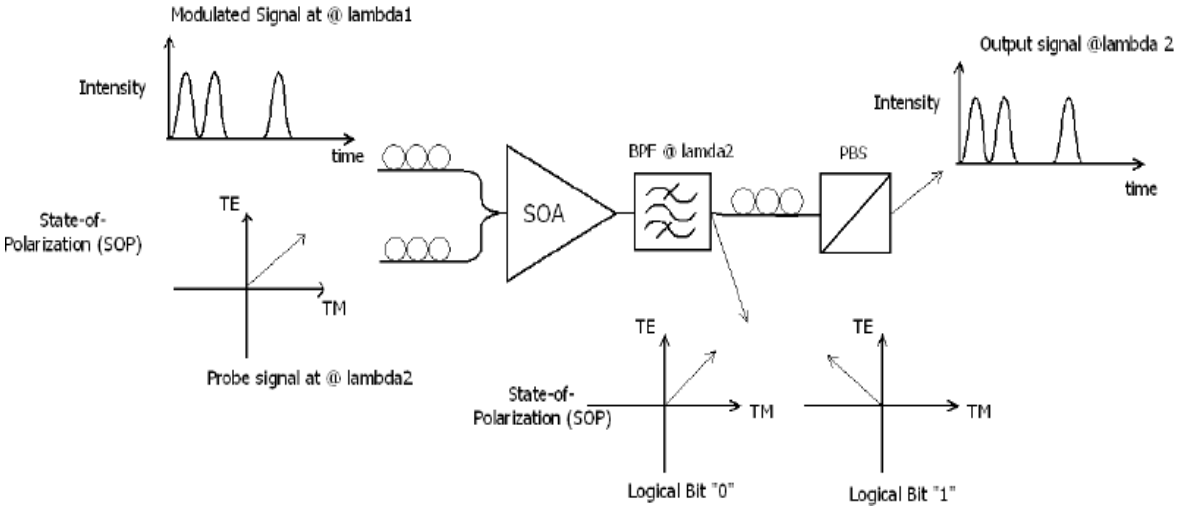

Figure 3.6 XPR wavelength converter working principle based on **[Silveira, 2011]**

When only a probe signal, with polarity adjusted to be approximately 45° (with respect to the axis of the SOA polarization) and low enough power not to experience transversal electric (TE) and transversal magnetic (TM) rotation, enters the SOA, the output polarization controller should be set to minimize the output signal at the beam splitter (the probe signal is not aligned with the output beam splitter). This represents the 'zero' in the modulated output signal.

When in the presence of both the previously referred probe and a pump modulated signal with its polarization aligned to the SOA polarization, in order to have the maximum gain possible, the probe beam will experience different gains in the TE and TM modes. If the different gains experienced by the two modes, and thus the different refractive indexes variations allow a rotation of the state of polarization in 90° in the probe signal at the output, a strong non inverted signal is obtained.

To clarify, when a probe and a pump signal during the "zero" bit is present at the entrance of the XPR WC, no signal is present at the output, since the beam splitter is not aligned the polarization of the probe. In the other hand, when the pump is at the "one" state, the probe will experience a polarization rotation, and if that rotation is equal to 90° ,a "one" bit will be present at the output.

"The difference between the TE and TM effective indices results from the guiding properties of the amplifier waveguides and a very small index difference (of the order of $2 * 10^{-4}$ *for a 2 mm long device at 1550nm) is sufficiently high to induce a significant birefringence (TE/TM phase shift* $> \pi/2$*)."* [Soto, 1999]

The dependence of the TE and TM phase shift and polarization rotation due to the SOAs gain compression and probe polarization is presented in [Soto, 1999].

3.2. Experimental Wavelength Conversion

Figure 3.7 presents two types of wavelength conversion that can be performed in practical situations, wavelength up-conversion that occurs when the probe signal and thus the output-converted signal are in a longer wavelength than the original modulated signal. On the other hand down-conversion is performed when the output-converted signal is situated in a shorter wavelength than the modulated input signal.

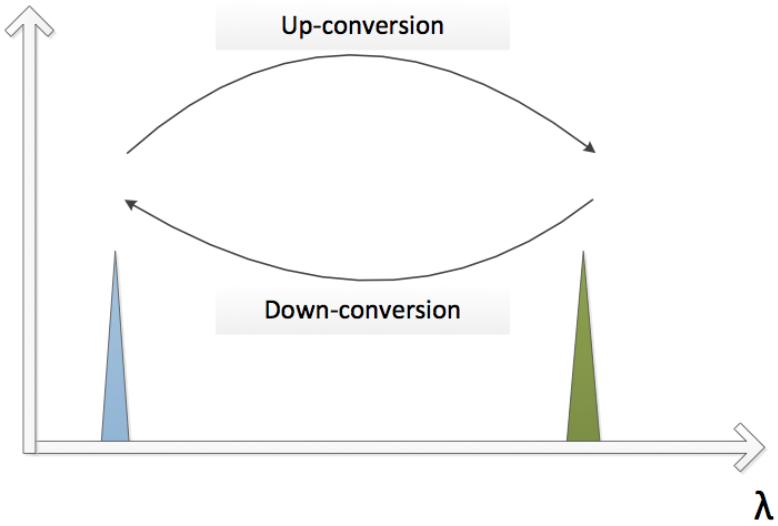

Figure 3.7 Wavelength Up and Down conversion

In this dissertation up and down conversion were assessed to fulfill the requirements for up-conversion in OLT side and down-conversion at the ONU side. During this chapter the wavelength converters will be assessed by the complexity of the WC itself but specially taking into consideration the performance characteristics such as the extinction ratio (ER), signal to noise ratio (SNR), and Q-factor.

Extinction ratio can be determined from the eye-diagram presented in Figure 3.8, and is defined as the ratio between the power of the logic level “1” and the power of the logic level “0”. In decibels we have:

$$Extinction\ Ratio\ (dB) = 10log_{10}\frac{power\ level\ of\ the\ "1"}{power\ level\ of\ the\ "0"} \quad (3.4)$$

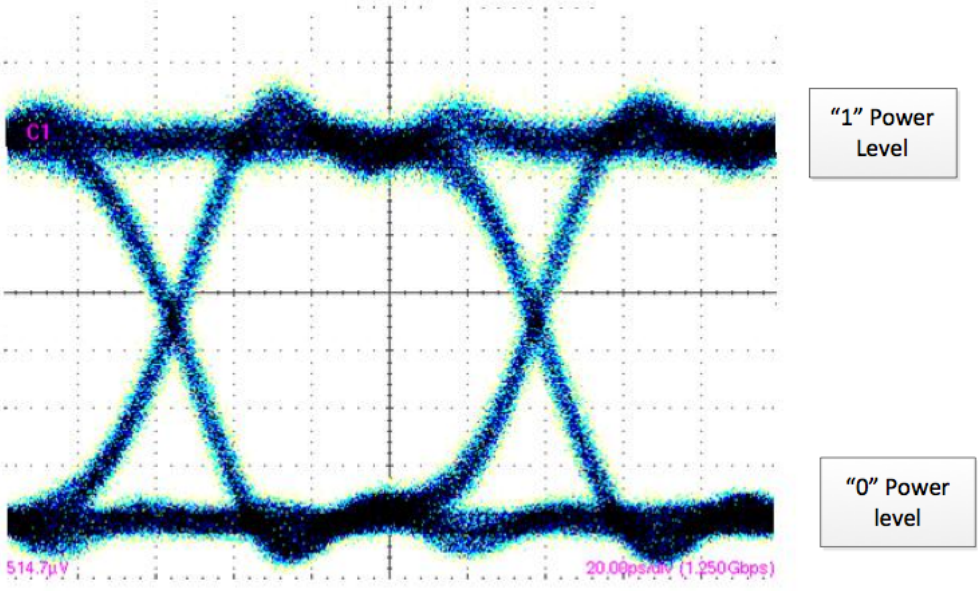

Figure 3.8 Eye Diagram

The quality of converted signal can be quantified by the signal Q-factor value which is extracted form the signal-to-noise ratio (SNR). This parameter is calculated by [Agrawal, 2002] as:

$$Q = \frac{I_1 - I_0}{\sigma_1 + \sigma_0} \approx \frac{I_1}{2\sigma_1} = \frac{1}{2}(SNR)^{\frac{1}{2}} \quad (3.5)$$

Where, I_1 and I_0 are the current level of the bits levels "1" and "0", respectively; and σ_1 and σ_0 are standard deviation of the level '1'and '0', respectively. The BER can be extracted from the Q-factor using the following expression [Agrawal, 2002]:

$$\text{Ber} = \frac{1}{2}\text{erfc}\left(\frac{\text{Q}}{\sqrt{2}}\right) \quad (3.6)$$

3.2.1. XGM Wavelength conversion

In the laboratory, all-optical XGM wavelength up-conversion, from 1490nm (λ_1) to 1549,32nm (λ_2) and down-conversion from 1549,32nm (λ_1) to 1490nm (λ_2), using a single stage semiconductor optical amplifier, were performed.

The setup used a external cavity laser (ECL) emitting at λ_1, that was modulated by a MZ modulator, using a PRBS at 2,5 Gbit/s with a pattern length of $2^{31} - 1$. The use of 2,5 Gbit/s makes this wavelength converter suitable for GPON/EPON scenarios.

After the signal modulation by the MZM and due to the low power of the modulated output signal, an amplification stage was introduced, using an S-Band Amplifier for the up conversion and an EDFA for down conversion. The S-Band Amplifier and EDFA response is presented with more detail respectively in Appendix II and [Carvalho, 2012].

Both pump signal λ_1 and probe signal λ_2 were controlled by different variable optical attenuators (VOA) and then coupled together before entering the SOA (Figure 3.9). The gain of the SOA and consequently the cross gain induced in λ_2 is considerably dependent on the polarization and power of both input signals, thereby to achieve the best conversion possible, a careful tuning of the polarization controllers and VOAs was made. The setup was mounted in a co-propagating scheme, thus after the SOA a band pass filter centered in λ_2, with 20nm bandwidth, was used, to discard the λ_1 signal. A PIN receiver was connected to a sampling oscilloscope to extract the eye diagram and performance characteristics such as Q-factor, signal to noise ratio (SNR) and extinction ratio. Figure 3.9 depicts the experimental setup used.

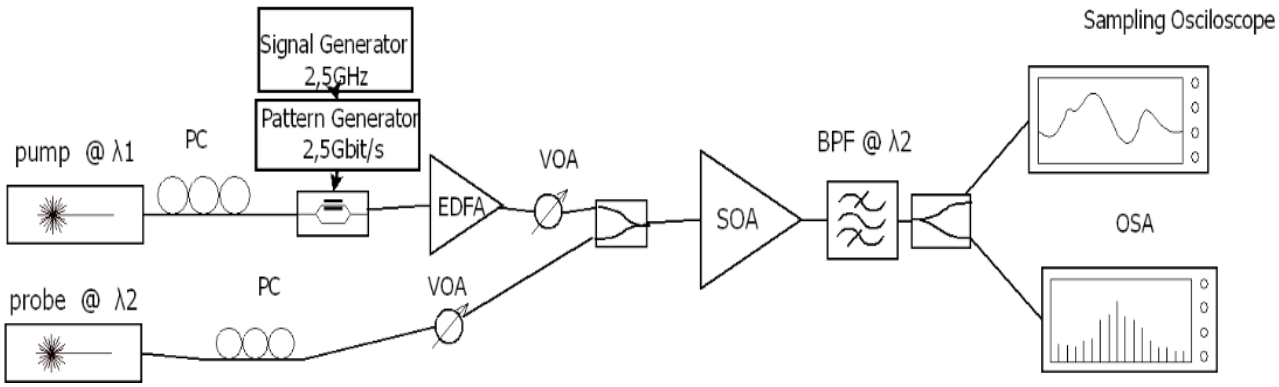

Figure 3.9 Experimental setup for analyzing WC considering XGM in an SOA

The cross gain modulation technique, presented in section 3.1.2, and analyzed in

this section is quite dependent of the SOA gain dynamics, such as carrier recovery time, the saturation output power and SOA wavelength range.

The SOA used for the XGM experiment is characterized in Appendix I and exhibits good performance operating in a wide bandwidth range, from tens of Mbit/s till 10Gbit/s and also high saturation power, around 7 dBm. When operating in S-Band, this SOA shows some limitations especially in gain and noise figure, due to not be intended to work in this band, as can be seen in Figure 3.10 and Appendix I.

In the experimental setup used the SOA was biased with 140mA, this choice was made taking in consideration the signals input powers and the amplifier gain and noise figure.

Regarding out-of-band wavelength conversion, the major problems faced were: the gain reduction when using a probe and pump signal at 1490nm, and the fact that the slope in the saturation part of the curve is less steep than when using a wavelength inside the operation region of this SOA.

For the cross gain modulation to operate at its best, the pump signal needs to be strong enough to saturate the gain, and the probe should not contribute decisively for the saturation output. Considering the different gain curves that are presented in Figure 3.10 an increased power difference between the pump and probe signals was required when compared to the in-band conversion.

The extinction ratio of the output signal depends on the difference between the “0” level and “1” level, and the gain that each of the states generates, thus the less steep gain curve presented at 1490nm creates an ER and Q-Factor penalties in both up and down conversions.

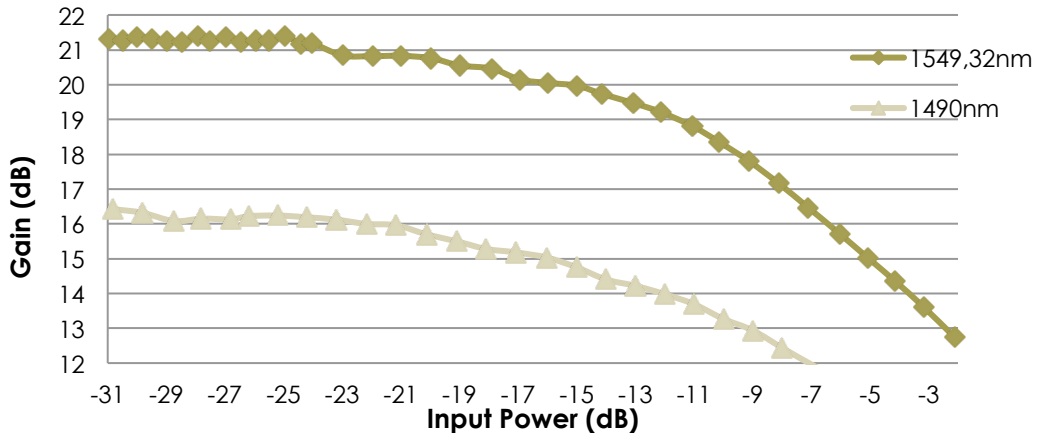

Figure 3.10 SOA optical gain as a function of input power

Figure 3.11 presents BER (extracted from the Q-factor) as a function of the received optical power (ROP) at the PIN, for the back-to-back situation, with original signal

at 1490nm and converted one at 1550nm. For low input powers (lower than -10dBm) the PIN works at the limit of it sensitivity, thus the differences in BER are not significant. As the ROP increases the BER decreases, and for log(BER) lower than -19 (which correspond to a Q-factor of 9) an excellent conversion is achieved. In this conversion the converted signal needs to be at least -4dBm whereas in the back-to-back situation it can be around -9dBm. This 5 dB penalty is usual in XGM conversions but accentuated in out-of-band WC. [Durhuus, 1996]

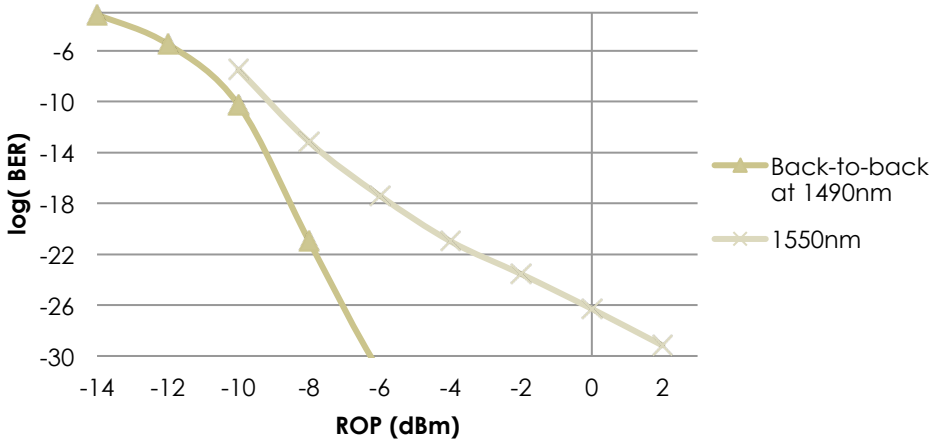

Figure 3.11 BER as a function of the received optical power (ROP) for the back-to-back situation at 1490 nm and 1490-1550nm conversion

For XGM conversion the ER is of the most importance, due to the degradation of the "1" and "0" level inherent to a cross modulation technique based in amplitude modulation. Figure 3.12 presents the ER degradation suffered by the converted signal. As is presented in equation 3.4, the ER is given by the ratio of the "1" level power and the "0" level power, as a consequence, an increase of the "0" level power, even with a corresponding increase in the "1" level, will decrease the ER. This is verified in the back-to-back curve, which presents a strong ER decrease for received power above -8dB. The converted signal ER curve is less dependent on the ROP at the PIN because it already presents a strong penalty (high value of the "0" level) when compared to the back-to-back situation for the same power.

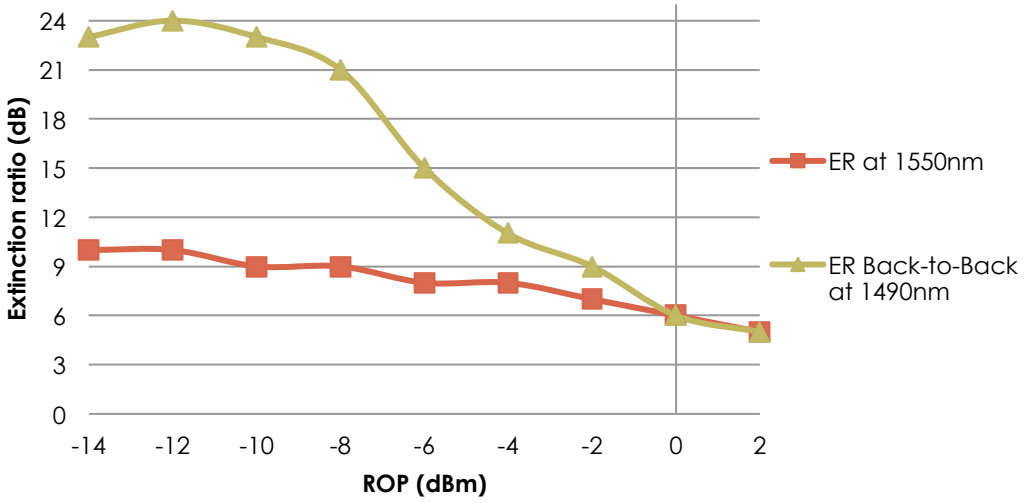

Figure 3.12 Extinction ratio as a function of the received power for the back-to-back situation at 1490 nm and 1490-1550nm conversion

For down conversion the back-to-back signal at 1550nm is located inside the SOA wavelength range, this allows an improvement of 1 to 3 dB for the same BER (Figure 3.13) when compared to the back-to-back signal at 1490nm (Figure 3.11). The overall wavelength conversion performance is similar, for both up and down conversion, because the increase in the BER and ER (Figure 3.14) in the back-to-back signal at 1550nm is counter-balanced with the poor gain exhibited by the probe at 1490nm.

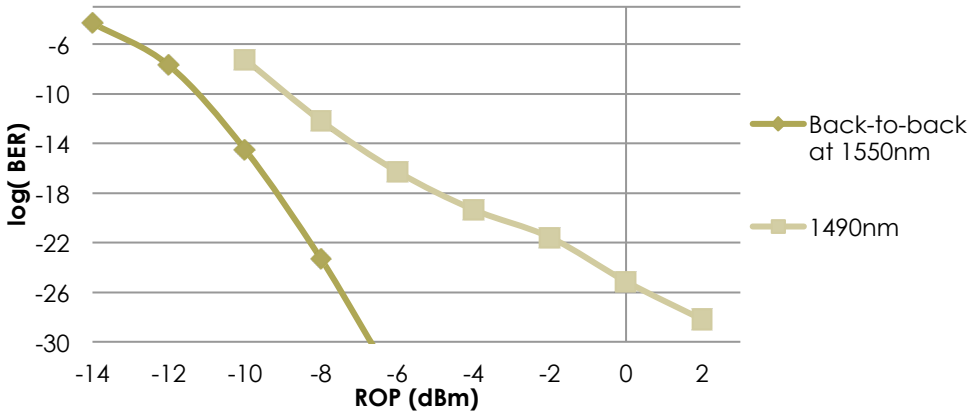

Figure 3.13 BER as a function of the ROP for the back-to-back situation at 1550 nm and 1550-1490nm conversion

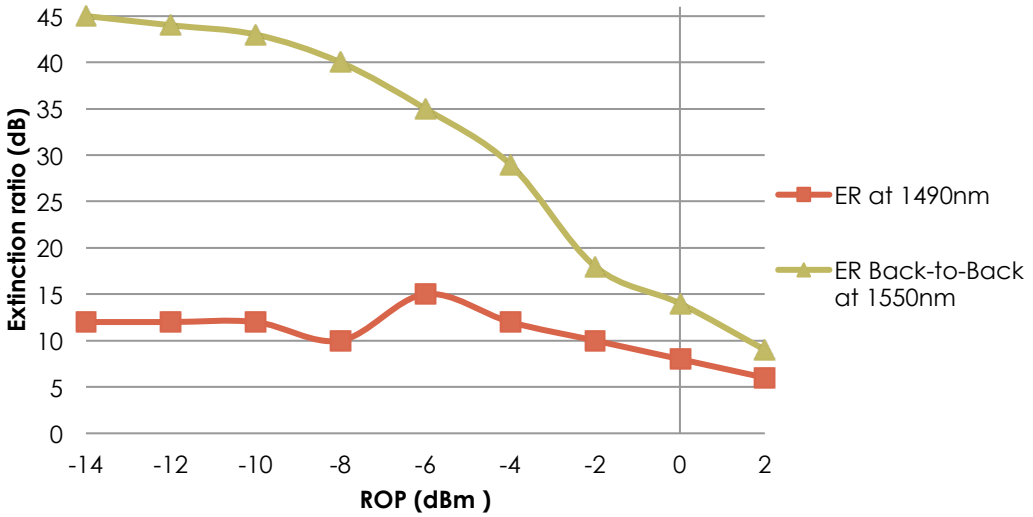

Figure 3.14 Extinction ratio as a function of the ROP for the back-to-back situation at 1550 nm and 1550-1490nm conversion

3.2.1.1. Non-Inverting XGM using a Two-Stage SOA

From the outline of this dissertation, it is possible to realize that the wavelength conversion previously presented in this section, does not suit the wavelength conversion necessary, since the converted signal is an inverted copy of the original signal. However, due to its simplicity further studies in XGM conversion have been deployed, with special focus in non-inverting wavelength conversion.

A Two-Cascaded WC presented by Hamié et al [Hamié, 2005] shows good ER values for a wide range of wavelength converted signals, but for the wavelength conversion targeted in this dissertation (from 1490 to 1550nm) a poor value of ER, less than 5dB, was achieved. Nevertheless, to achieve the wavelength conversion needed using XGM, it is here proposed a two-cascaded SOA wavelength conversion using in-band conversion.

The 60nm, from 1490 to 1549,32nm, hop needed could be divided in two 30nm hops, selecting the SOAs to have high gain over the 30nm hop of a single conversion. The signal experiences a double inverting conversion, thus at the final output the signal would be a non-inverted replica of the input signal, at 1550nm. The proposed scheme uses an intermediate probe (λ_3), at a wavelength around 1520nm. The use of two wavelength hops instead of just one allows best performance results, like higher ER, Optical Signal to

Noise Ratio (OSNR) and Q-Factor, but represents an increased cost due to the extra SOA and Probe laser needed.

It is mandatory that at the output of the first conversion the signal is filtered and regenerated, or at least the “zero” level must be low enough to be seen as a “zero” for the second SOA. If this is not ensured, and due to the ER penalization verified in the XGM conversion, the second stage can interpret the input signal as a continuous signal and no wavelength conversion is performed. This fact was assessed in the laboratory and although the output of the first stage presented good OSNR and Q-factor, the high power value of the “zero” made the wavelength conversion impracticable.

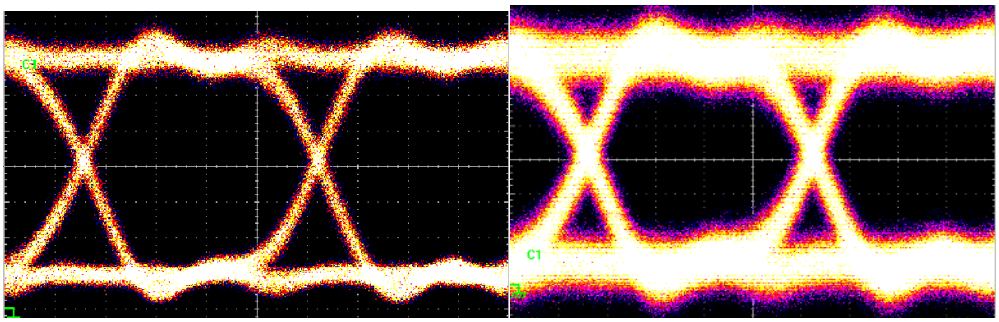

Figure 3.15 (Left) Back-to-back signal at 1490 **(Right)** Converted signal at 1520nm

Figure 3.15 presents the back-to-back signal at 1490nm and the output of the first stage at 1520nm. Although the converted signal presents a great eye diagram with good OSNR and Q-factor, the ER degradation is visible through the enlargement of the mean value of the “zero” level.

3.2.2. XPM Wavelength conversion

The Mach-Zehnder is an interferometric device that allows a probe signal to suffer a certain phase shift (phase modulation) in one of the arms, due to refractive index variations produced by a modulated signal. The phase modulation results in amplitude modulation due to the interference between the signals in the two arms in an output coupler.

This section is divided in static characterization, and dynamic characterization. In the static characterization section, elemental characterizations were made to better understand the MZI-SOA behavior and its bandwidth limitations. In the dynamic characterization a wavelength conversion over 25nm is presented (the maximum wavelength hop achieved with the equipment available) using 2,5 Gbit/s NRZ signal with low Q-factor and SNR penalty.

Static Characterization

In this section the Mach-Zehnder interferometer is characterized in static conditions, i.e. using a continuous wave (CW) instead of a modulated signal as the input signal. The aim of the static characterization is to evaluate the phase shift rotation that can be implemented in one of the arms, and to balance the MZM to improve the cross modulation. The use of continuous waves simplifies the understanding of the MZI-SOA because carrier dynamics are not taken into consideration.

To better understand the MZI-SOA behavior, even for a static mode evaluation, it is important to realize its structure, and the properties of its constituents. The MZI-SOA used, consists of three stages: an initial 2x2 coupler which splits the input signal equally, a central section composed by one SOA and a phase shifter in each one of the arms, and another 2x2 coupler at the end which recombines the signals at the output.

A MZI matrix representation is presented bellow, where the [P] and [Q] represents the couplers, and the [D] represents the temporal delay (τ) that the signal experiences when passing through each of the arms. To simplify, the delay (τ) can be assumed equal for both arms and set to zero, thus [D] is equal to 1 . [YAHAY, 2007]

$$\begin{bmatrix} H_{11}(f) & H_{12}(f) \\ H_{21}(f) & H_{22}(f) \end{bmatrix} = [P][D][Q] = \frac{1}{\sqrt{2}} \begin{bmatrix} 1 & -j \\ -j & 1 \end{bmatrix} \begin{bmatrix} \exp(-j2\pi f\tau) & 0 \\ 0 & \exp(-j2\pi f\tau) \end{bmatrix} \frac{1}{\sqrt{2}} \begin{bmatrix} 1 & -j \\ -j & 1 \end{bmatrix} \quad (3.7)$$

From the MZM matrix model it can be seen that if only one continuous signal is applied in the port B ($H_{11}(f)$), (Figure 3.5) and considering that both the SOAs have the same biasing thus the same gain and phase shift, the signals traveling in each arm are going to interfere at the output coupler. Port J ($H_{22}(f)$) will present the constructive interference (one) and Port I ($H_{12}(f)$) will present destructive interference (zero) (Figure 3.5). [YAHAY, 2007]

In Figure 3.16 can be seen the output powers for both ports using a 10dBm CW input signal and the same varying bias for both SOAs.

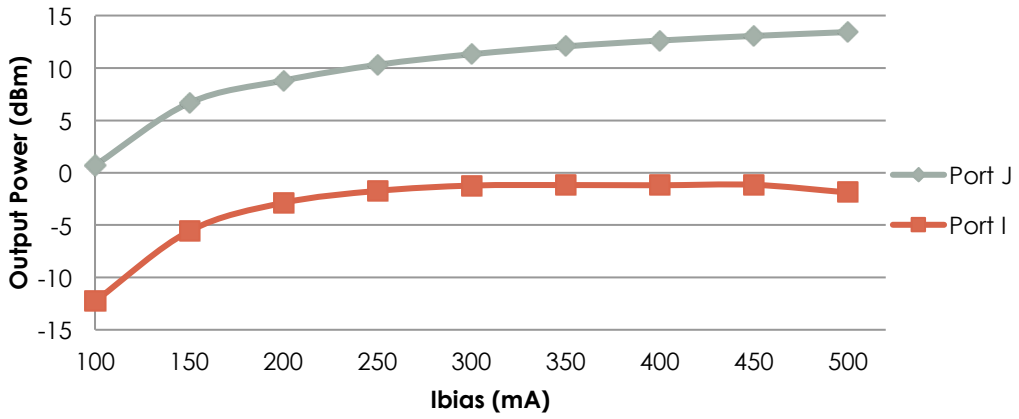

Figure 3.16 Output signal power for the two output ports of the MZI-SOA as a function of the SOAs biasing current

The best extinction ratio between Port J and Port I was achieve when both SOAs where biased with 500mA, thus this was the biasing point used for the rest of the static characterization.

The key element in XPM is the phase rotation inside the interferometric device, such phase rotation can be measured by performing the two next measurements. For the first measurement a 0 dBm continuous wave is applied at port B, for 0 V applied to the phase shift. Port J represents the constructive interference (maximum power) and Port I represents destructive interference (minimum power).

When varying the phase shift in the upper arm, the phase difference between the signals travelling in both arms changes, for a phase shift equal to 180ºan inversion of ports is obtained. Figure 3.17 presents the port inversion which occurs for a phase shifter voltage of 6,56 V. For values higher than 6,34 V the phase difference between the two arms increases and a new inversion in the output ports occurs. The maximum power contrast between the constructive and destructive interference conditions in each port, due to phase shift variation, is around 21 dB.

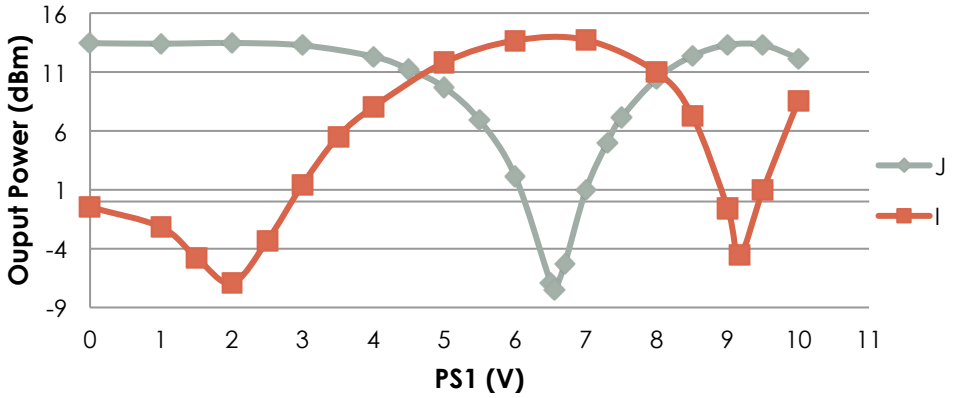

Figure 3.17 Output probe signal power for the two output ports of the MZI-SOA as a function of the phase shift voltage applied to the upper arm

The influence of the probe signal polarization (polarization sensitivity) in the output signal was observed by rotating the polarization controller (PC) to obtain the maximum power variation at the output. When the PS voltage was 6,54 V (destructive interference) the polarization sensitivity was around 15 dB, for a PS voltage of 0 V (constructive interference) the polarization sensitivity was 1,1 dB.

The phase shift inside the SOA is also considerably dependent on the power of pump signal (modulated input signal), but in this case, since only the static properties are being assessed, the modulated signal that is used in the wavelength conversion is substituted by a continuous wave applied at Port A. In the second measurement made the output power was assessed as a function of the input pump power without changing the phase shifter PS1, that was fixed in the inversion point found before, 6,56 V. The aim of this measurement was to evaluate the power needed during the "1", for a given wavelength, to allow a phase rotation of 180º in the probe wave. The results are presented in Figure 3.18.

Analyzing Figure 3.18 is possible to observe that at 1535nm, i.e inside the bandwidth of the MZI-SOA, it was possible to realize a 180º phase shift which corresponds to an output power value equal to 13dBm.

When the probe is at 1525nm, the 180º shift was not achieved, but with extra phase shift allowed by the use of a second phase shifter at the lower arm, wavelength conversion was possible, as it is presented in the dynamic characterization section. For probes at shorter wavelengths than 1525nm, as 1500nm, it is not possible to achieve the 180º shift even using a second PS.

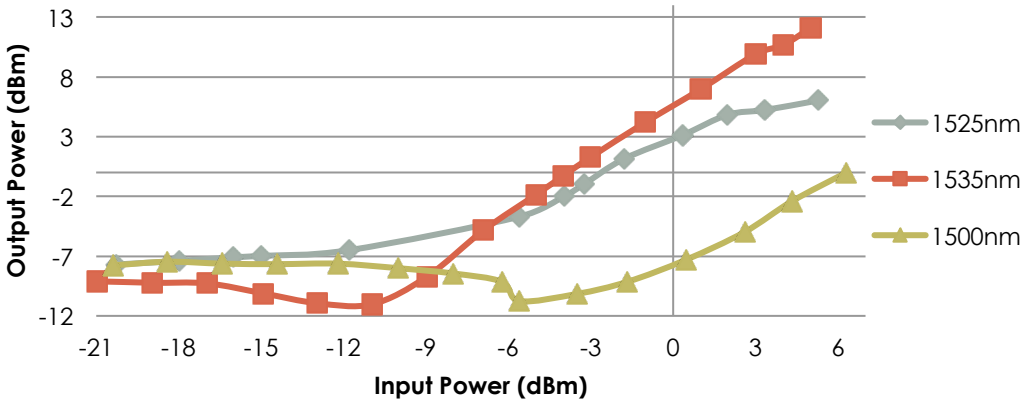

Figure 3.18 Output probe signal power @ port J as a function of the pump signal power

The extinction ratio results here presented are not observed in the dynamic characterization that will be presented next, because of the carrier dynamics influence when the WC operates at 2,5 Gbit/s.

Dynamic characterization

In the dynamic mode characterization the highest wavelength hop with reasonable performance was pursued. The setup presented in Figure 3.19 was optimized for wavelength conversion from 1525nm(λ_1) to 1549,42nm(λ_2) and from 1549,42nm (λ_1) to 1525nm (λ_2) at 2,5 Gbit/s.

The setup used an external cavity laser (ECL) emitting at λ_1 that was modulated by a MZ modulator using a PRBS at 2,5 Gbit/s, with a pattern length of $2^{31} - 1$. The use of 2,5 Gbit/s allows this wavelength converter to be used in GPON/EPON scenarios.

As it was proven in the static characterization section, the power of the input modulated signal has great influence in the phase rotation inside the upper arm of the MZI-SOA, thus, due to the limited output power of the modulator, an EDFA had to be used to amplify the pump signal. Both modulated signal λ_1 and continuous signal λ_2 were controlled by different variable optical attenuators (VOA) and were connected to the MZI-SOA in a counter-propagation scheme (λ_1 at port A and λ_2 at port I) to spare the use of an output filter for the λ_1 signal.

The gain of the SOAs inside the MZI-SOA is dependent on the polarization, thus, to achieve the best conversion possible, a careful tuning of the polarization controllers was made. The output signal is extracted in port B where a PIN receiver was connected to a

sampling oscilloscope, to observe the eye diagram and performance characteristics, such as Q-factor, OSNR and ER.

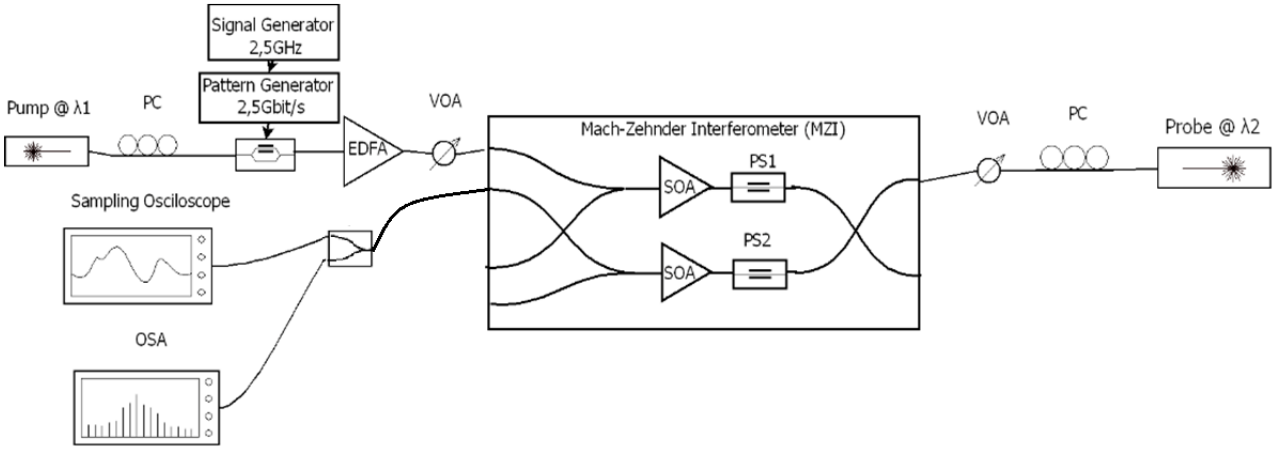

Figure 3.19 Experimental setup for WC using XPM in a MZI-SOA

The correct setting of both probe and pump signal powers has a great influence over the wavelength conversion performance. Figure 3.20 presents the variation of the Q-factor as a function of the probe signal power for several powers of the pump, considering down conversion. Similar results were attained for up conversion.

For low pump powers the output signal will be also low, thus at the receptor the noise will dominate and the BER will be penalized. In the other hand for higher values of the probe signal the high gain compression will reduce the phase shift thus also penalizing the BER. For each pump signal power a 14dBs lower probe power optimizes the conversion.

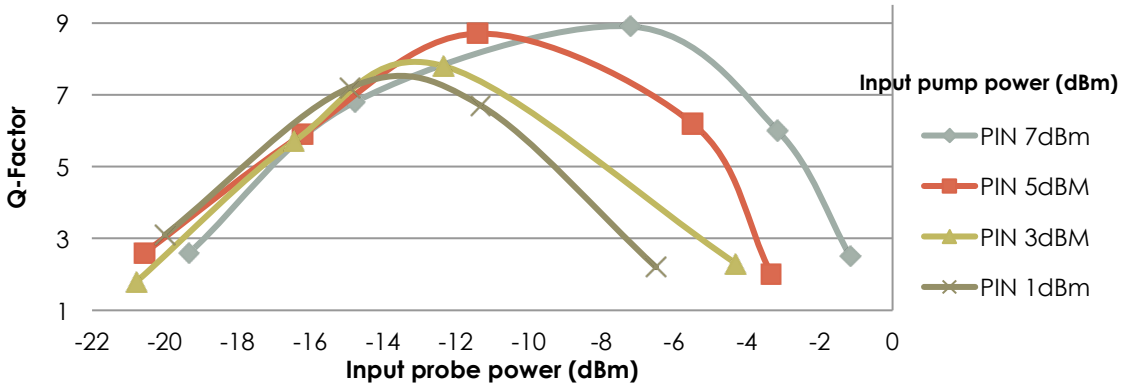

Figure 3.20 WC using XPM: Q-factor as a function of the pump (lambda 1 @ 1525nm) and probe (lambda 2 @ 1550nm) powers

For higher values of pump and probe powers BER decreases due to the better response of the SOA when saturated, and also to the increased power of the output modulated signal when received at the PIN. From figure 3.20 we can also conclude about the dynamic input of the MZI-SOA (the range of input probe and pump powers that can be converted).

Figures 3.21 and 3.22 present BER as a function of the ROP at the PIN, for the up and down conversion, respectively. The back-to-back curves at 1525nm and 1550nm present similar behavior as ROP increases, however with a better performance for the back-to back at 1550nm. The converted signal at 1550nm exhibits an approximately constant power penalty around 2dB, for the different BER. For the converted signal at 1525nm the power penalty varies from around 2 dB at lower ROP (higher BER associated) to 4 dB at higher ones (lower BER). Based on these results, we can conclude that proper conversion performance was achieved for both up and down conversion, with even better results obtained for up conversion (1525nm-1550nm).

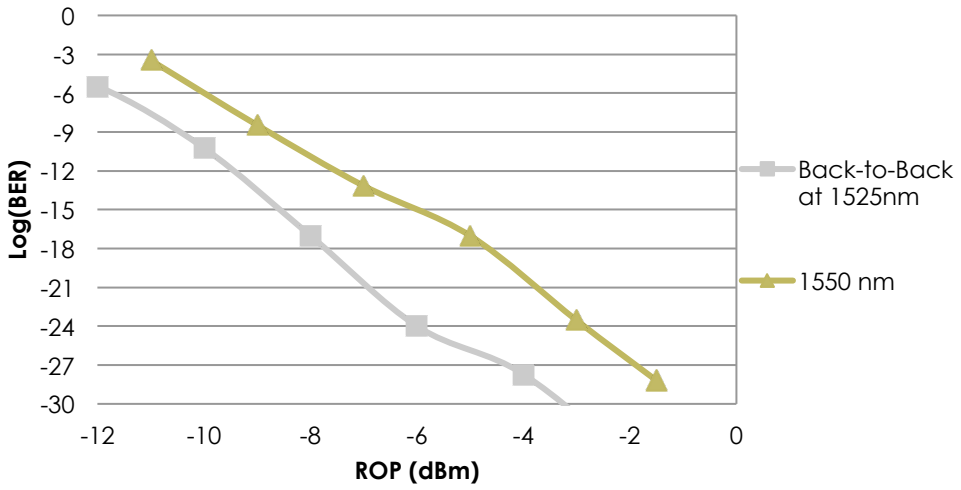

Figure 3.21 BER as a function of the ROP for the back-to-back situation at 1525 nm and for 1525-1550nm conversion

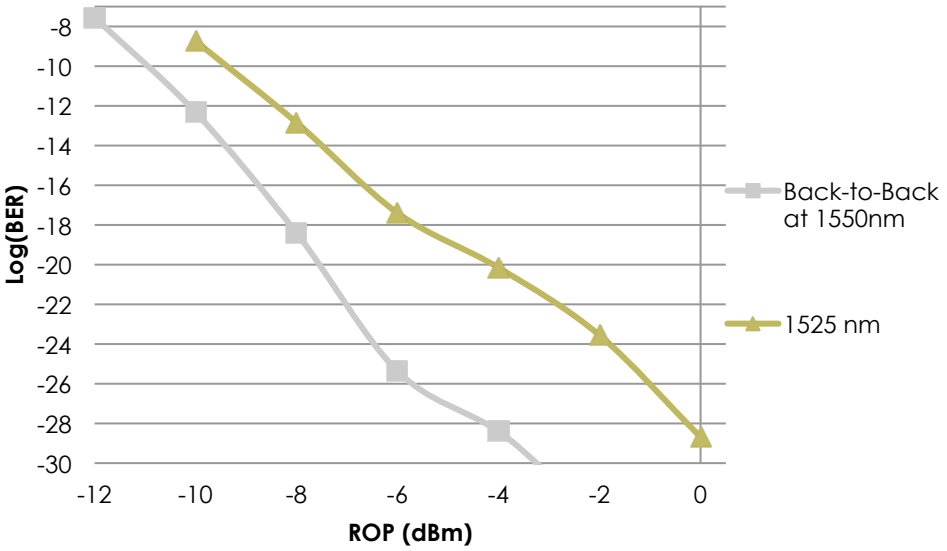

Figure 3.22 BER as a function of the ROP for the back-to-back situation at 1550 nm and 1550-1525nm conversion

Comparing to WC using XGM, a performance increase (BER, SNR and ER) was verified for the XPM technique.

ER of the converted signals for both directions is constant over the power range (-10 to 0 dBm), around 15 dB. This presents a minimum increase of 4 dB when compared to XGM up and down conversion.

In XPM conversion the ER is degraded from 20 dB in the static measurement to about 15 dB in the dynamic measurement. There are two reasons for the degradation. First, the SOA carrier number can reach a steady-state value in the static tests, leading to a small output value in the “0” level. On the other hand, in dynamic operation, the SOA carrier population does not reach this steady-state value due to the slow carrier recover lifetime. Second, noise in the PIN receiver and the oscilloscope limit the smallest signal that can be observed, thus further degrading ER and BER.

3.2.3. Cross Polarization Wavelength conversion

In this section the principles of the XPR conversion are presented, using an experimental setup to verify the potential of this technique.

It is important to notice the similarities between the characteristics of a wavelength converter based on nonlinear polarization rotation in a single SOA, and MZI-SOA wavelength converters. Both are based on interferometric principles, in XPR the

transverse electric (TE) and transverse magnetic (TM) modes, that independently propagate through the SOA, behave similarly to the different light paths in the arms of the MZI-SOA converters [Liu, 2003].

The major advantage of the interferometric WCs is the possibility of getting both a non-inverting, as well as an inverting, wavelength conversion [Liu, 2003]. In this section the wavelength converters based in XPR are characterized in static conditions, i.e. using a continuous wave (CW) instead of a modulated signal as the input signal. This characterization allows us to understand the effect of the pump signal in the output probe signal.

During the static characterization three different measurements were made, first was assessed the best input probe signal power to be used in a non-inverting wavelength conversion, second the same measurement was made but for the inverting wavelength conversion, third, was evaluated the variance of the non-inverted ER with the input probe wavelength.

The setup used was based on the presented in [Tang, 2005], but the circulator was replaced by an optical coupler, the output polarizer by a polarization beam splitter (PBS) and an optical band pass filter (OBPF) centered in the probe signal was introduced. The probe signal was a 1490nm continuous wave from the ECL and the pump signal was the 1549,32nm CW used in previous sections.

In all the three measurements taken the probe PC was adjusted to be approximately 45º with the orientation of the SOA polarization, and the pump PC was adjusted to maximize the gain (allowing the biggest polarization rotation). Without a polarization analyzer, this was achieved controlling the gain of the SOA for different positions of the PC wave plates.

The PC placed after the SOA is used to adjust the polarization of the SOA output with the orientation of the PBS. For non-inverting conversion, in the absence of pump signal, the PC is set to minimize the output signal, on the other hand, for the same conditions, but inverting conversion, the PC is set to have the highest output power possible.

In Figure 3.23 is possible to evaluate the response of the WC for different input pump and probe powers. The largest ER was around 8dB achieved for a -15dBm probe and a 7dBm pump.

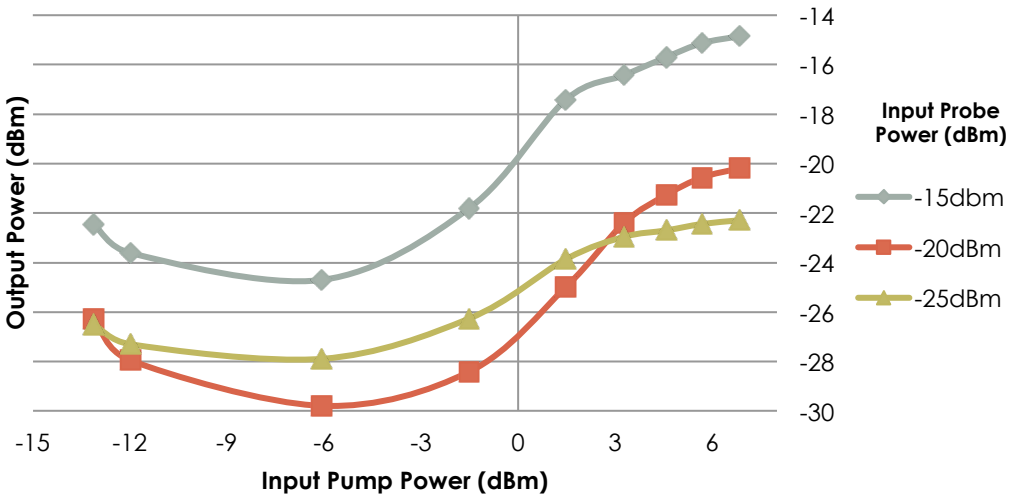

Figure 3.23 Output Power as a function of the pump and probe powers in an Non-inverting configuration

In both inverting and non-inverting conversion, XGM takes place, regarding non-inverting wavelength conversion it opposes to the effect of polarization rotation, decreasing the ER. In the inverting conversion, presented in Figure 3.24, it can be noticed that XGM enlarges the effect of polarization rotation, thus the slope of the curve is sharper and the ER is considerably larger (best case around 20 dB).

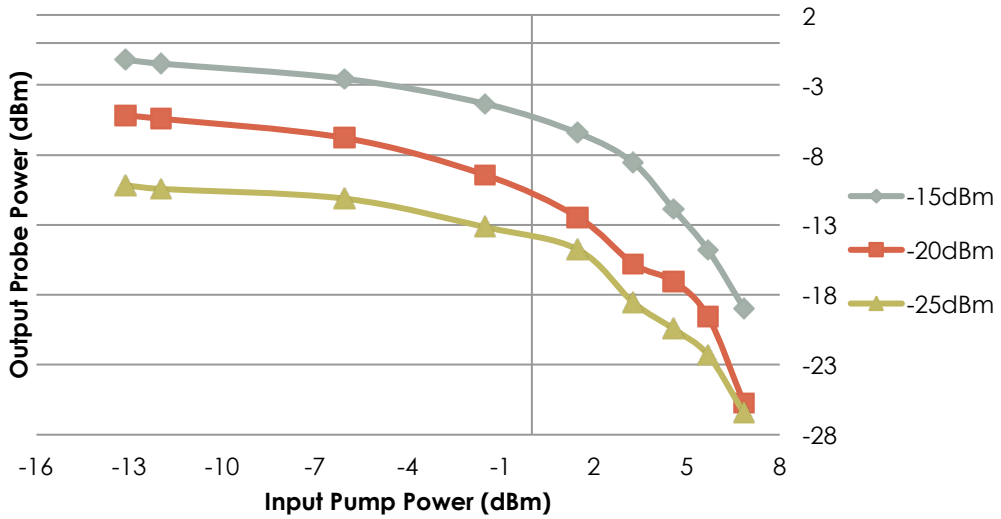

Figure 3.24 Output power as a function of the pump and probe powers in an inverting configuration

Analyzing Figure 3.23 and 3.24, and the respective maximum ER achieved, it is possible to conclude that XPR in a inverting scheme will present better conversion performance that in a non-inverting one, due to the increased ER provided by the carrier depletion [Tang, 2005].

In Figure 3.25 the efficiency of the conversion was assessed for three different wavelengths. For all the wavelengths the polarization was again set to maximize the gain and allow the maximum polarization rotation.

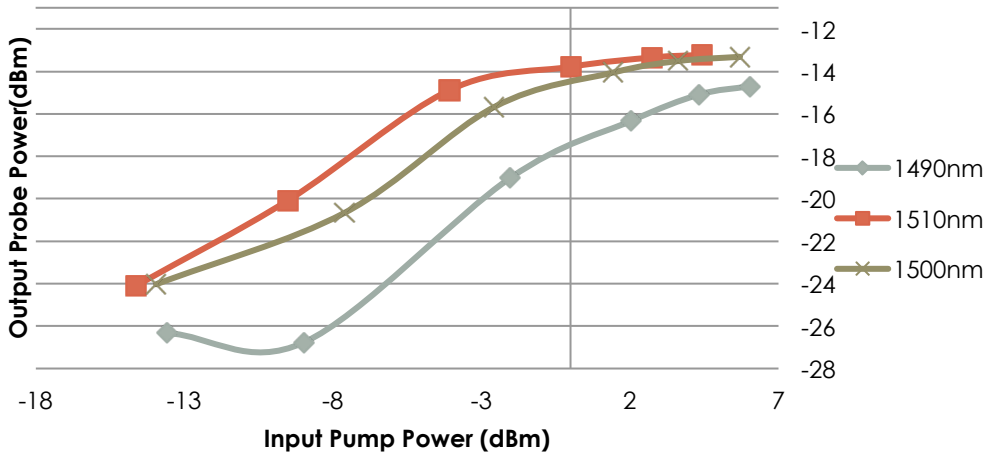

Figure 3.25 Output power as a function of the pump power for different wavelengths in an non-inverting configuration

Analyzing Figure 3.25 is possible to consider that the ER of the converted signal when using XPR is not seriously dependent of the input wavelength. The differences observed for the three input wavelengths are due to the S-Band amplifier used for the pump amplification, which exhibits greater gain and less noise for wavelengths above 1490nm. The fact that XPR is almost wavelength independent is supported by the results presented in [Tang, 2005] and [Liu, 2003].

3.3. Conclusions

In this section three different types of wavelength converters were presented, based on the non-linearitys presented in SOAs, as the solution for the Stack-PON downstream inoperability. The SOA arises as the optimum medium to perform the wavelength conversion due to his low cost, cross modulation possibilities, fast response and compact size that allows an easy integration in photonic circuits.

XGM is presented as the simplest WC, allowing large wavelength hops and high bit rate conversion, but at the cost of information inversion at the output, ER degradation and thus BER penalization.

XPM is a more complex WC technique, which implies two stages, first amplitude to phase modulation and second phase to amplitude modulation. The increased complexity is further penalized by the short wavelength hops allowed, but is compensated by an

increased conversion performance, better BER, SNR and ER, and a non-inverted output.

At last XPR wavelength conversion fits the wavelength conversion requirements for the stacked PON scenario in terms of bit rate, wavelength hop and non inverted modulation [Tang, 2005] and [Liu, 2003] but unfortunately dynamic wavelength conversion was not attained in the lab due to the high complexity involved in this technique.

4. Upstream Coexistence

4.1. Introduction

As it was presented in section 2.2.3, upstream access in PON systems was implemented using TDMA, and depends on the OLTs bandwidth assignment, to avoid the potential overlapping of ONU transmissions.

Due to the different protocols used for EPON and GPON systems, it is not possible to grant the upstream bandwidth control of both types of ONUs to a single OLT, as each one of the OLTs would only grant bandwidth upstream windows to the respective ONUs, without taking notice of the remaining ones. One possible solution would be the implementation of an independent PON upstream scheduler, that would have to be placed between the ONUs and the OLTs, and would be responsible for the management of the ONUs report messages, as well as the OLTs grants, avoiding packet collisions to happen. This independent scheduler would need both EPON and GPON interfaces and a very complex scheduling mechanism. Further studies about the independent scheduler are out of scope of this dissertation.

A simpler way to allow upstream communication without serious packet losses is based on the study of the upstream bandwidth procedures, and controlling the transmission parameters of each PON system. The method here presented takes advantage of the “free time windows” that the fiber medium presents due to the burst nature of the upstream communication flows, to send bursts of information from another type of ONU without prohibitive collision rates (Figure 4.1).

In this section, a statistical study of the packet error rate (PER) and bit error rate (BER) for the upstream direction flows is presented, using $Matlab^{®}$ simulation. In this simulation the influence of different traffic profiles in the performance of the coexistence scenario is evaluated.

4.2. Upstream Communication Simulation

The aim of the $Matlab^{®}$ simulation created is to assess the viability of the Staked-PON upstream communication. The key point in this simulation is the “free time windows” between bursts of one type of ONU (for example EPON) that allows bursts from a different type of ONU (GPON) to be transmitted, (Figure 4.1). As presented in section 2.3.5 and section 2.4.5 both GPON and EPON systems can employ static bandwidth allocation (SBA) or dynamic bandwidth allocation (DBA), the latter method dynamically assigns

upstream transmission windows to the respective ONUs, enabling bandwidth enhancements, but minimizing the so called “free time windows”. (Figure 4.1)

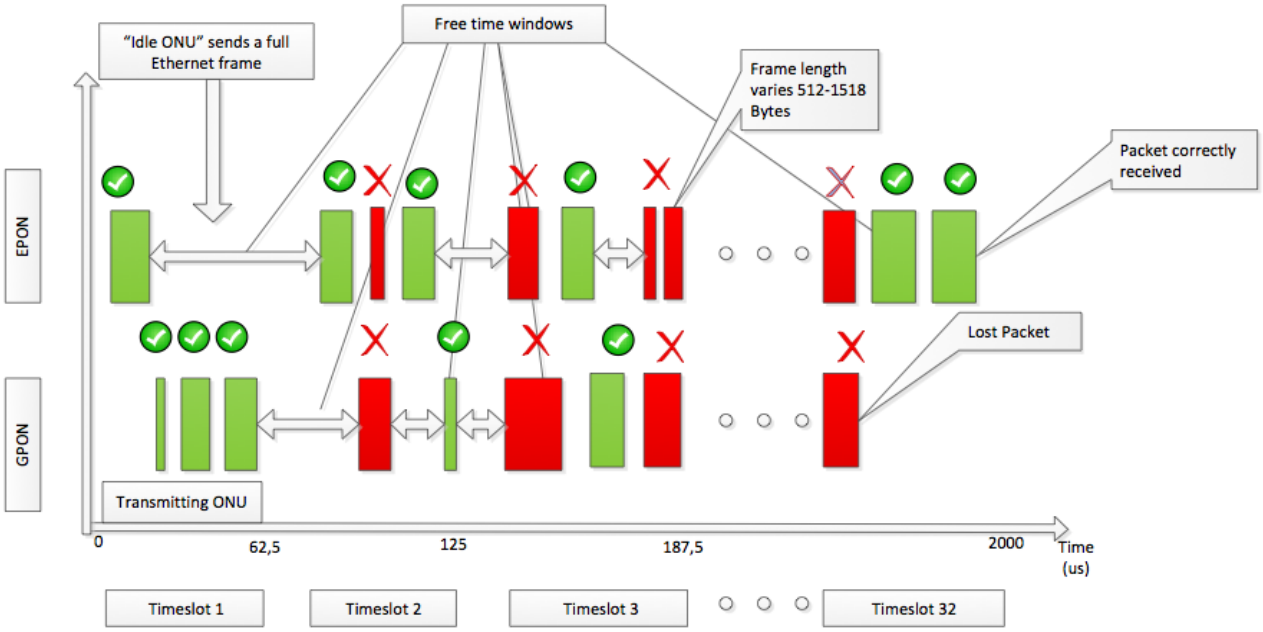

Figure 4.1 Schematic representation of the upstream coexistence scenario in a full 32 ONUs scenario

For the considered modeling, both EPON and GPON ONUs use static bandwidth allocation (SBA). The drawback of using SBA is the increased packet delay, and buffer overflow that can happen as it is described in [Kramer, 2005]. Independently of the fact that one ONU has information to send or not, a certain transmission window is always reserved, thus during that transmission window the ONU has the medium for itself. Due to the fact that the stacked PON scenario is composed by two different OLTs, and both of them grant upstream transmission windows to the subsidiary ONUs, without taking notice of the allocation plan of the other OLT, at each moment two ONUs have the medium reserved for itself, one is a GPON ONU and another is a EPON ONU.

The model proposed utilizes the EPON network as the base PON and evaluates the performance degradation that it suffers, due to the interference from the GPON ONUs. A 32 ONUs EPON was considered because it represents the operator ideal scenario (network cost/number of users)

Along this section different traffic parameters, such as the number of transmitting ONUs, the payload size, the inter-frame gap size and the guards times (Figure 4.2 and table 4.1) will be assessed taking in mind its relative “weight” in the overall network

performance. The general conditions assumed to modulate the network are presented bellow.

Assumed Conditions

- The bit pattern created to fill the Payload section, as well as the majority of the other headings, are composed by pseudorandom sequences drawn from a uniform distribution.
- The bit rate used for EPON was 1,25Gbit/s and for GPON 1,24416Gbit/s.
- 2ms “service cycles” in which every ONU transmits information.
- When the ONU has no data to send or has already finished the data to send, the remaining of the slot is stuffed with zeros.
- For each number of GPON ONUs transmitting, 32 PER measurements were made and an average value was presented.
- The ONU can be in one of two states: “idle” or “transmitting”.
- Idle ONUs transmit one full Ethernet Frame with 1518 Bytes and the rest of the slot is stuffed with ’0’ bits.
- Payload size is variable between 512 and 1518 bytes
- Number of frames from one ONU is variable between 3 and total number of frames that can be inserted into one transmission window without fragmentation.
- One bit is wrong if it is received a “1” when was transmitted a zero, but if two “1” collide no bit error is detected.
- GPON traffic was considered to be exclusively composed by Ethernet frames.
- Packet is considered to be equal to an Ethernet frame.
- One packet is considered wrong if one or more bits are wrong in the Logical Link Identifier (LLID) or in the DA or SA.
- In each Payload, if more than one bit is detected wrong, the packet is considered lost (due to the CRC and FEC correction)
- The considerations above were based on [ITU-T G.975, 1996]:

For a full Payload:

1518*8=12 144 bits

for a $BER_{Input}\ of\ \ 10^{-4}$ the BER_{Output} of $5 * 10^{-15}$ is obtained so:

in 12 144 bits only one can be wrong.

- The guard time is the channel idle period between the transmission slots from two different ONUs, the inter frame gap is the channel idle period between two different frames transmitted by the same ONU, both parameters are presented in Table 4:1 and Figure 4.2

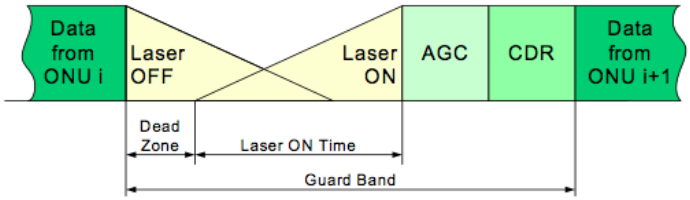

Figure 4.2 Structure of the guard band **(Kramer, 2006)**

Table 4:1 Guard time simulation parameters

	EPON	GPON
ACG	96/**192**/288/400ns	44 ns (70.7ns)
CDR	96/**192**/288/400ns	
Laser ON/OFF	512ns	25.7 ns (4 Bytes)
Dead Zone	128 ns	
Interframe Gap	72ns (12 Bytes)	
Guard Time	1024ns (160 Bytes)	8 Bytes

One of the most sensitive parameters when considering a PON simulation is the distribution of the number of “idle” ONUs and “transmitting” ONUs. In order to achieve the most reliable simulation, different ONU distributions were considered, such as Gaussian, Gama and uniform distribution. Additionally a distribution that here is named as “standard” was also assessed.

The above referred traffic distributions have been already employed for the study of network traffic distributions, especially wireless networks, and can be also considered for PONs [McAvoy, 2010]. Pareto distributions are extensively referred for the modeling of self-similar traffic [Hadi Ghauch, 2009], which is used for analyzing packet switching networks. Due to its increased complexity it would be inadequate for the simulation proposed.

4.2.1. Gaussian traffic distribution

The objectives of this simulation are to evaluate the evolution of the packet destruction with the number of connected ONUs, and thus evaluate the feasibility of the upstream-stacked scenario. Figure 4.3 presents the number of transmitting EPON ONUs, and it is important to note that for each number of GPON ONUs connected, a random number of EPON ONUs are transmitting. The number of EPON ONUs transmitting follows a Gaussian distribution with mean value 16 and standard deviation around 2,8. The use of a Gaussian distribution to model the number of EPON ONUs transmitting is due to the fact that in a 32 ONUs network the probability of a small number (less than 7) or a big number (more than 25) of ONUs transmitting at the same time are very low.

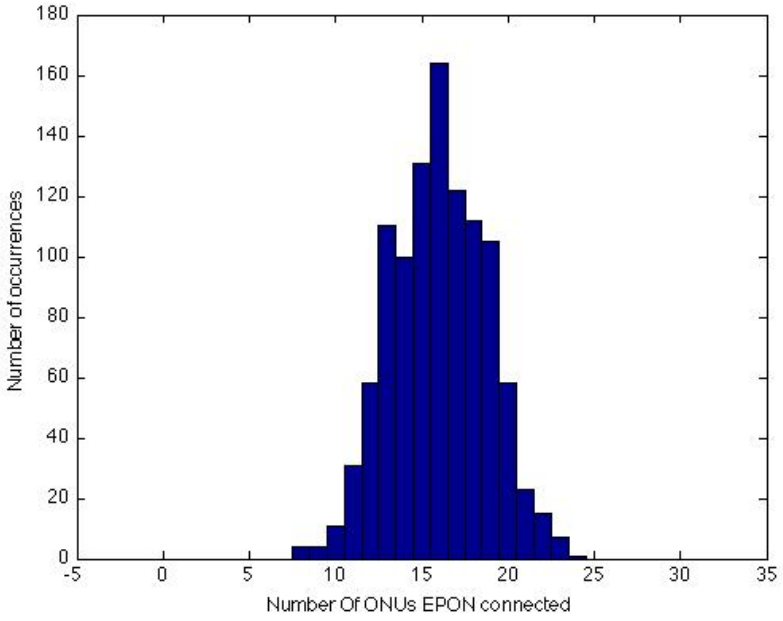

Figure 4.3 Number of EPON ONUs transmitting, following a Gaussian distribution

Figure 4.4 presents PER as a function of the number of GPON connected ONUs for 4 different traffic setups. The “normal” setup represents the case where the different ONUs transmits variable size frames and variable number of frames in each time slot. In the “maximum number of frames” setup each time slot is divided into parcels with the size of a full frame (1518 bytes), each parcel is filled with a variable sized frame. The “maximum frame size” setup uses a random number of frames, with constant size equal to 1518 bytes. As expected, the last setup “maximum number and frame size” combines the latest two and presents a full utilization of the channel, since all the ONUs use the full time slot to send data. From Figure 4.4 is clear to verify the linear relation between PER and

the number of GPON ONUs connected. As the number of GPON ONUs increase the channel utilization and thus the packet interference also increases. As expected, the setup referent to the maximum channel utilization presents the highest PER.

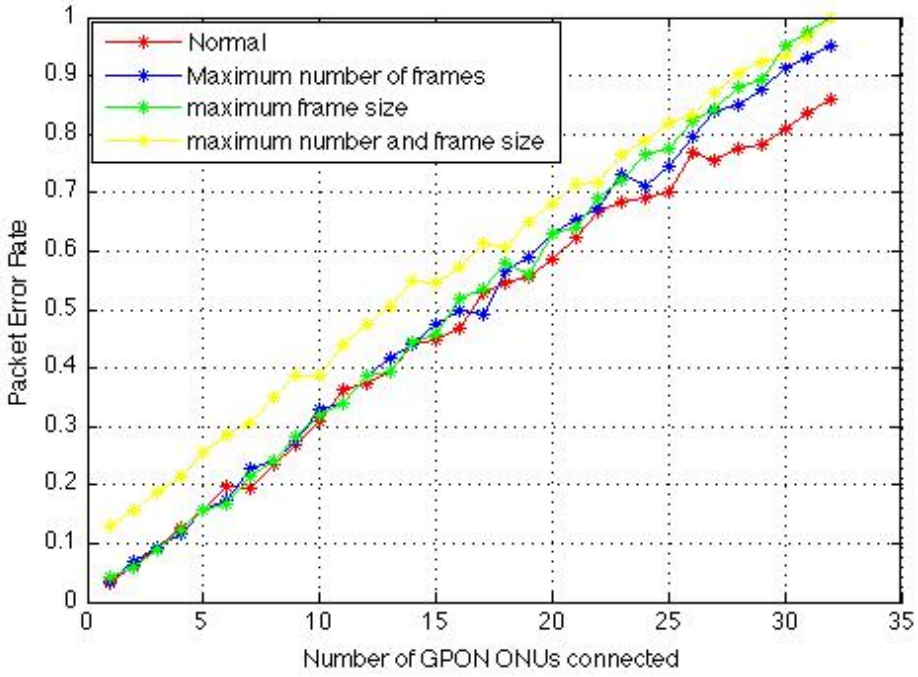

Figure 4.4 Mean PER as a function of the number of plugged GPON ONUs

Considering that a PER value lower than 10% allows upstream communication with fair performance, it is possible to connect up to 3 GPON ONUs in a 32 EPON system. Considering “maximum number and frame size” the PER is never lower than 10%, thus is impossible to implement the stacked-PON scenario in a extremely loaded network.

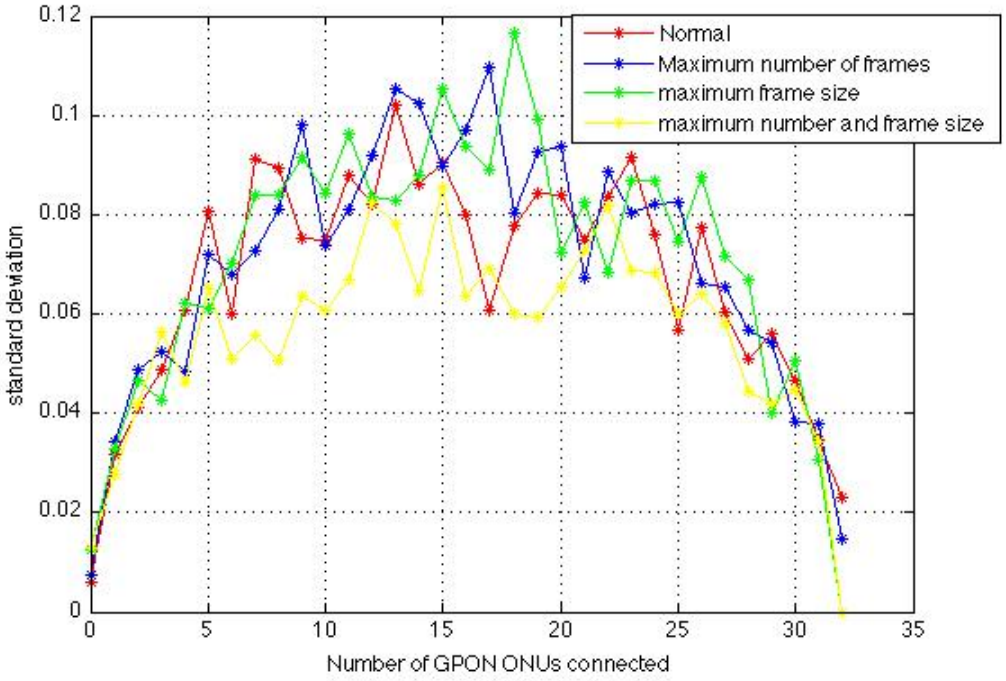

Figure 4.5 PER standard deviation as a function of the number of plugged GPON ONUs

Additionally, figure 4.5 presents the standard deviation for the referred situations. The high variation that is quantified by the standard deviation curve is explained by several factors, such as the random number of EPON ONUs in “idle” or “transmitting” state (Figure 4.3), the variable Ethernet packet size and the number of frames transmitted by each ONU during the correspondent time window. For the maximum channel utilization the variance is slightly lower because of the constant number of frames and frame size, thus the variance is only due to the random number of EPON ONUs in “idle” or “transmitting” state.

For a better understanding of the traffic properties and variations Figure 4.6 presents the number of GPON ONUs and EPON transmitting ONUs pairs and Figure 4.7 presents every PER measurement made as a function of the number of GPON ONUs connected (instead of Figure 4.4 that presents mean values) for the “normal” setup.

Analyzing Figure 4.6 we may clarify the working principles behind the simulation performed. The number of GPON ONUs is incremented from 0 to 32 and the number of EPON ONUs is set to 32, but as in a real network, not always an ONU as data to send, so we have the “idle” state previously presented. During the “idle” state, synchronization must be maintained, thus some traffic is always present. In Figure 4.3 the number of EPON transmitting ONUs varies from 8 to 24, due to the random process that arbitrates the number of “transmitting” ONUs.

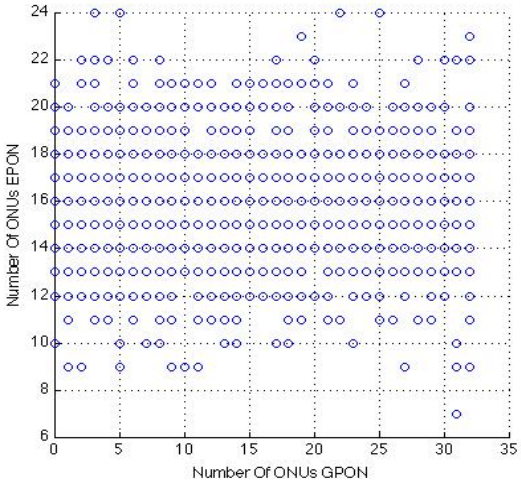

Figure 4.6 Number of GPON ONUs and EPON transmitting ONUs pairs

Figure 4.7 presents PER as a function of the GPON/EPON transmitting ONUs and, as it can be noticed, the highest variations occur between 8 and 24 ONUs. This is explained by the " interference weight" of the idle ONUs relative to the all ONUs connected. For low number of ONUs the relative interference variations are low, due to the number of ONUs, on the other hand, for high number of ONUs, the interference variations are also low because of the already very high destructive interference associated to the high number of ONUs connected.

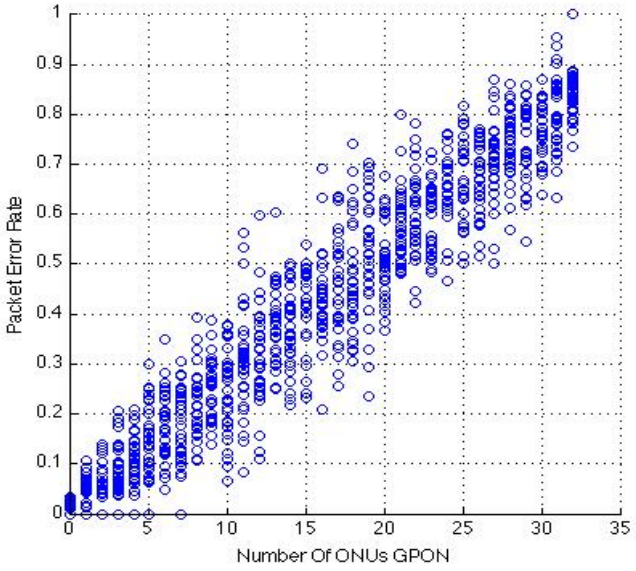

Figure 4.7 PER absolute values as a function of the number of connected GPON ONUs

Figure 4.8 presents the BER as a function of number of GPON ONUs connected.

The different setups considered present a high variation in the BER values, but, even for the worst case, the BER is less than 12%, that represents a considerable low value compared with the PER of 100% correspondent (Figure 4.4). If the considerations made about the number of wrong bits associated to packet loss were too pessimistic, the value of PER could be considerably lower (the packet loss considerations are presented in the last point in the assumed conditions).

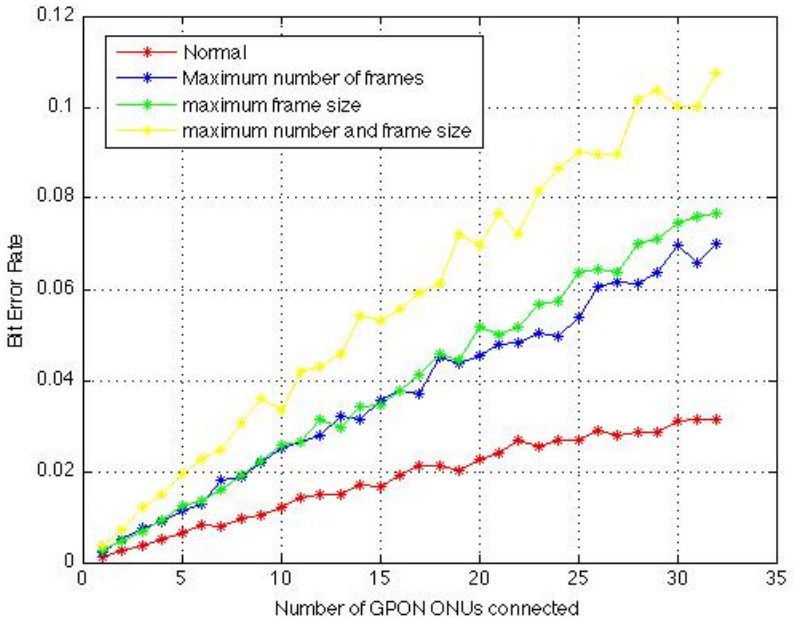

Figure 4.8 BER as a function of the number of the connected GPON ONUs

4.2.2. Uniform Traffic distribution

It is also interesting to evaluate the staked-PON behavior when the number of EPON ONUs presents approximately a uniform distribution. Although this distribution is not suitable to simulate network traffic, it works as a reference for comparison to the other distributions. Figure 4.9 presents the distribution of the transmitting EPON ONUs and Figure 4.10 presents the PER measurements.

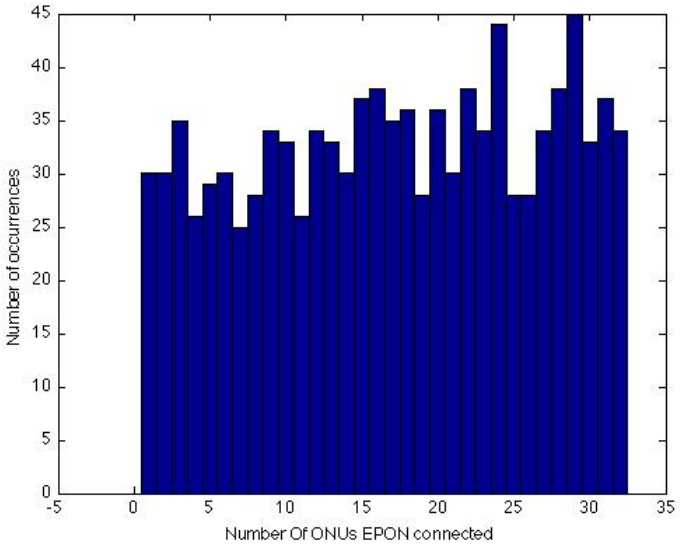

Figure 4.9 Number of EPON ONUs transmitting, following a Uniform distribution

As expected the mean PER curves present some differences when compared with the Gaussian distribution. For high number of GPON ONUs connected all the curves converge to the 100% packet loss, this was not experienced in the first simulation. The fact that the number of EPON ONUs connected could be, with similar probability, any number from 1 to 32 increases the variation of PER values as can be seen in Figure 4.11. This fact is corroborated because all the 4 curves present similar values, thus, when compared with the variation introduced by the number of frames and frame sizes, the variance associated with the number of ONUs transmitting is the major source of variation.

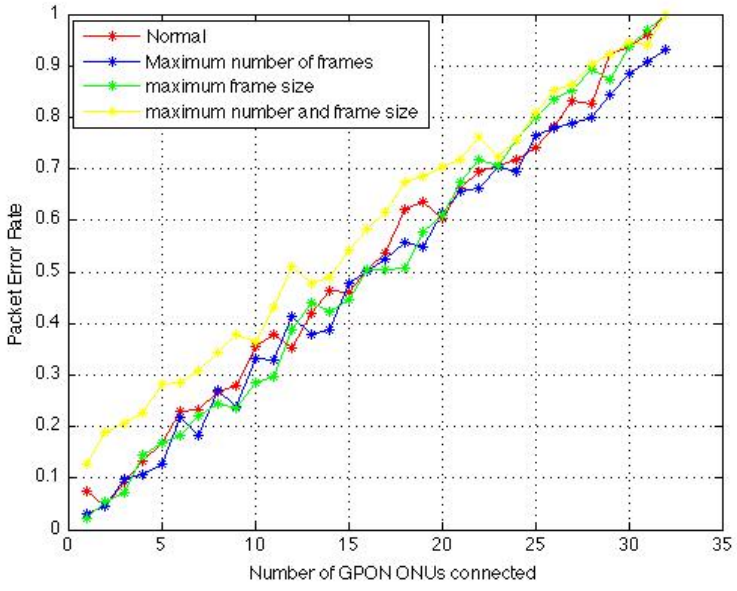

Figure 4.10 Mean PER as a function of the number of plugged GPON ONUs

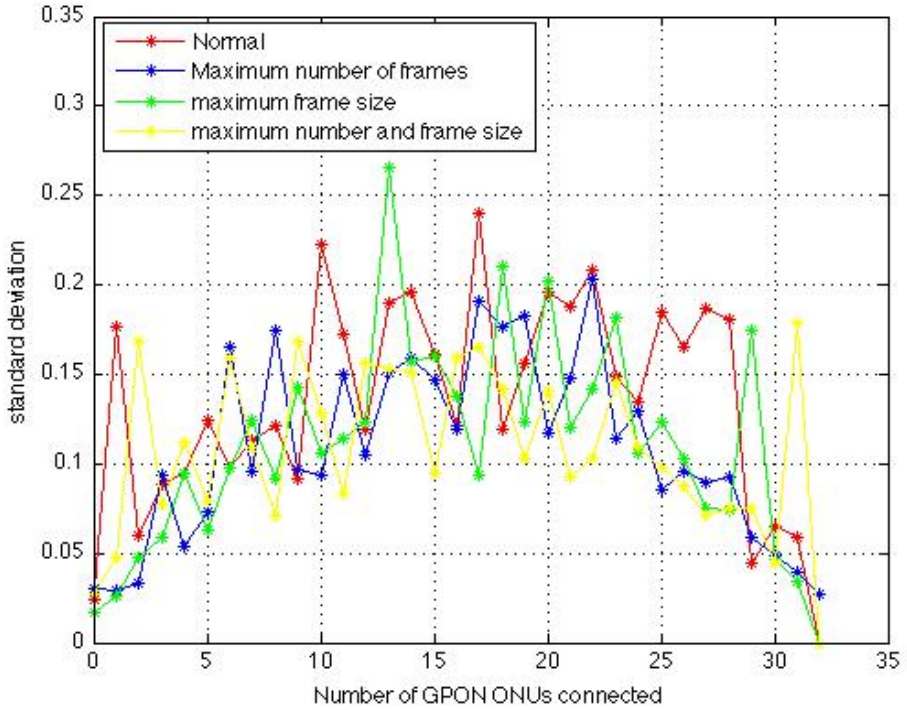

Figure 4.11 PER standard deviation as a function of the number of plugged GPON ONUs

The BER curves present similar behavior as in the Gaussian distribution.

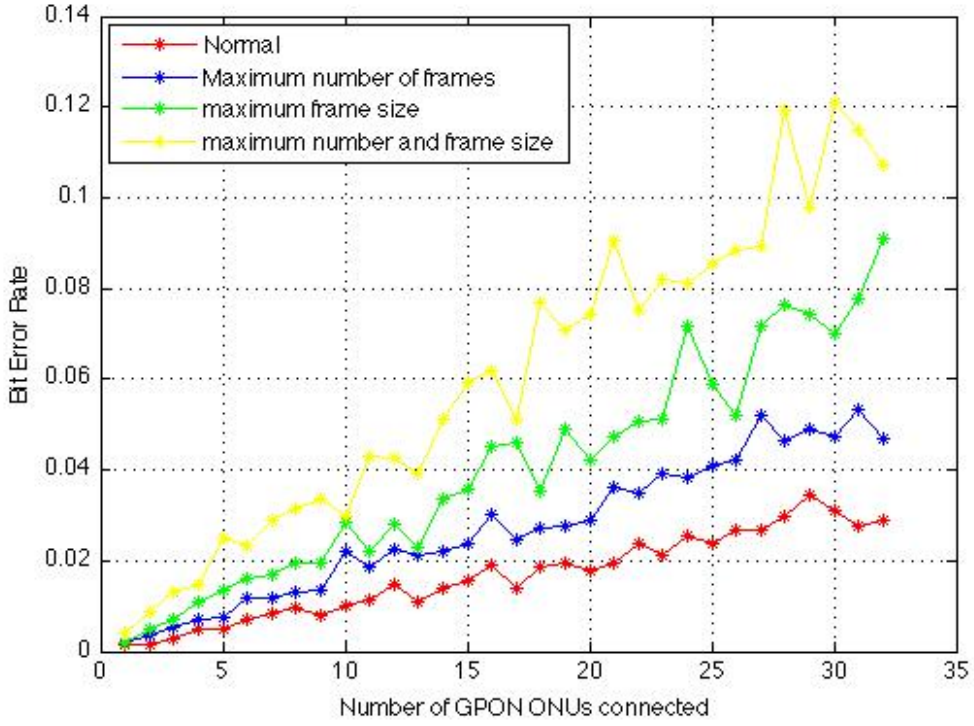

Figure 4.12 BER as a function of the number of connected GPON ONUs

4.2.3. Gama traffic distribution

Gama distribution is a general type of statistical distribution used for processes in which the waiting times between Poisson distributed events are relevant. Gamma distributions have two controllable parameters, k and θ, which correspond to shape and scale, respectively [Weisstein] [Statistics: The Poisson Distribution].

When any of these parameters are integers, a special case of distribution arises, called Erlang distribution. [Weisstein] In the simulation presented the k and θ parameters were set to 3,0 (Figure 4.13).

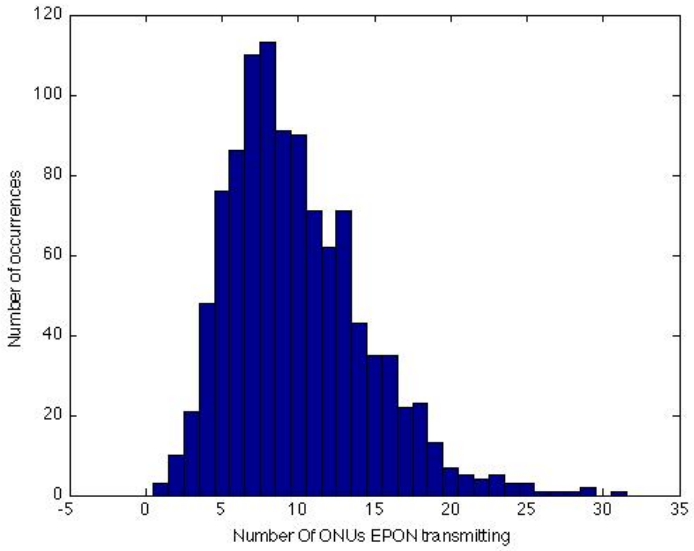

Figure 4.13 Number of EPON ONUs transmitting, following a Gama Distribution

Figure 4.14 presents the PER as a function of the number of GPON ONUs connected. The different traffic setups present an increase in the mean value when compared with the previous simulations, because the mean value of the number of EPON ONUs transmitting is lower. Due to the lower number of EPON ONUs transmitting the total number of frames sent in one cycle strongly decreases. For example, the lost of a certain amount of packets considering the Gama distribution represents a higher value of PER when compared to the loss of the same amount of packets for the uniform and Gaussian distributions.

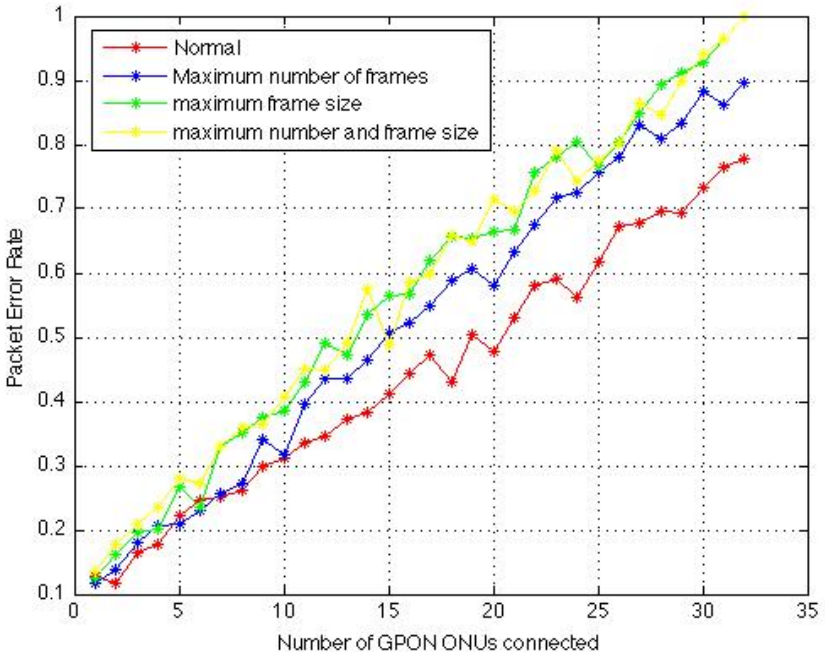

Figure 4.14 Mean PER as a function of the number of plugged GPON ONUs

Figure 4.15 presents higher peak values of standard deviation comparing with the ones presented for the Gaussian distribution (Figure 4.5) due to the long tail presented in the Gama distribution, which implies that in some cases up to 32 EPON ONUs are in the transmitting state.

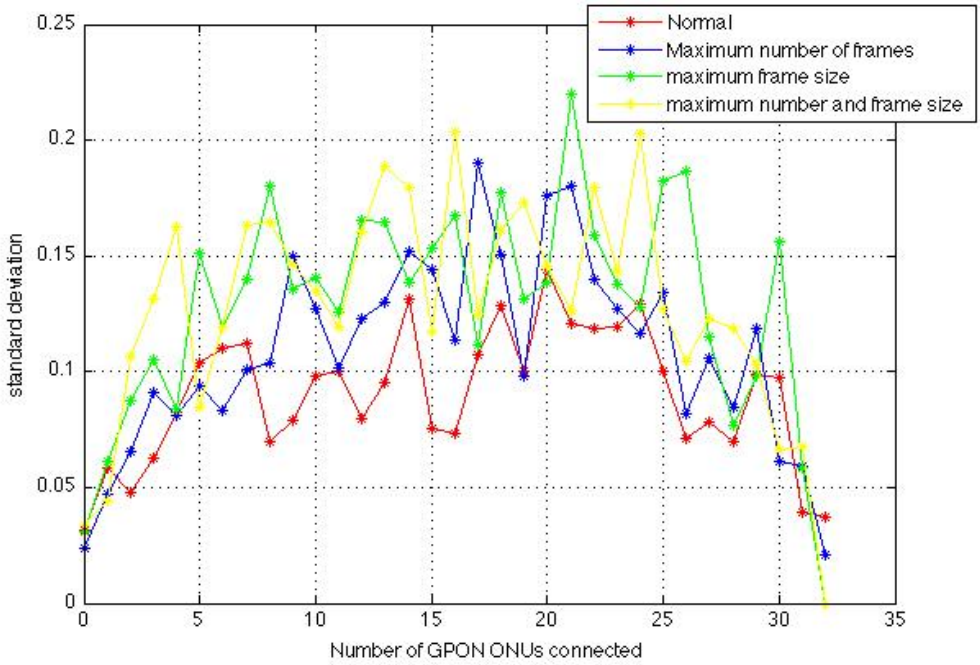

Figure 4.15 PER standard deviation as a function of the number of plugged GPON ONUs

Figure 4.16 presents lower values of BER when compared with the previous distributions due to the fact that lower values of data are sent in each network cycle.

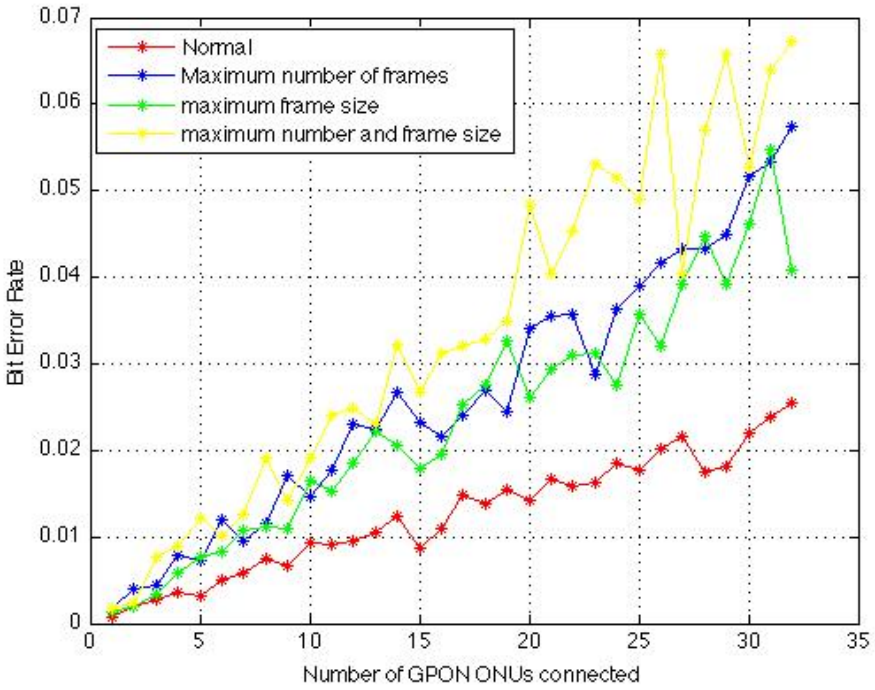

Figure 4.16 BER as a function of the number of connected GPON ONUs

4.2.4. Standard Traffic distribution

The Gaussian EPON ONU distribution considered before neglect's the fact that a low number of EPON ONUs could be connected during the lowest congestion hours, even lower than 7. The Gama distribution considered focus specially in a low number of EPON ONUs transmitting as can be seen in Figure 4.13. Thus, a new model is presented in this section, called "standard" traffic distribution. The proposal of this new distribution has in mind the variation of traffic presented over a day cycle [Gebert]. This model presents high probability for the number of transmitting ONUs to be in the range of 1 to 20, as it is presented in Figure 4.17.

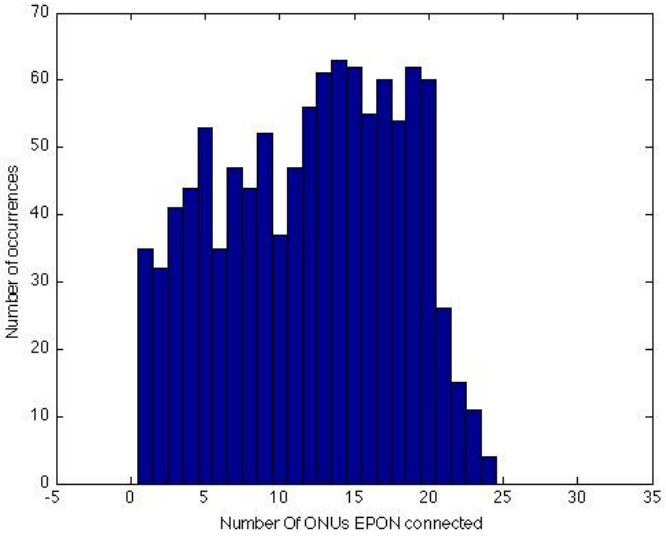

Figure 4.17 Number of EPON ONUs transmitting, following a "Standard" Distribution

Figure 4.18 presents a linear relation between the number of interfering ONUs and PER. It is important to notice that, once more, for "maximum number and frame sizes" PER is never lower than 10%, thus no stacked-PON scenario can be implemented. In the "normal" setup, up to 3 GPON ONUs can be connected for a PER lower than 10%.

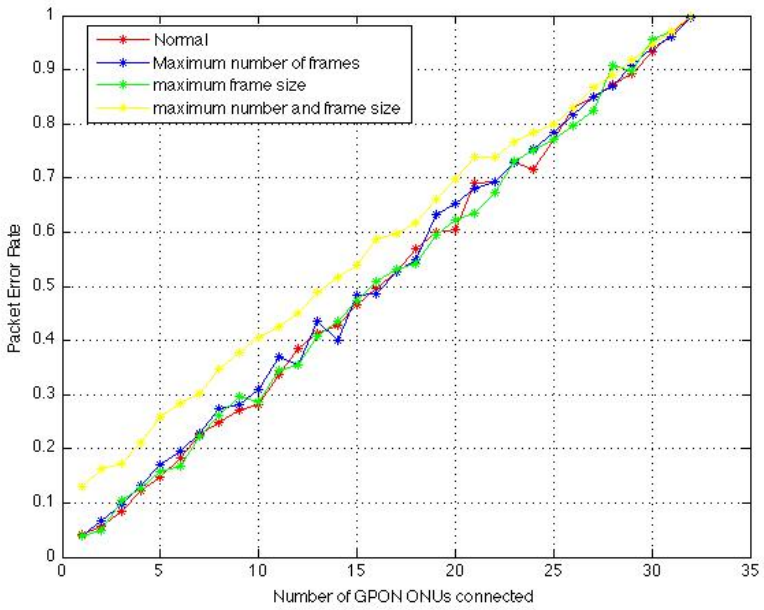

Figure 4.18 Mean PER as a function of the number of plugged GPON ONUs

Figure 4.19 presents similar values as the ones presented for the standard deviation graphic for the Gaussian distribution in Figure 4.5.

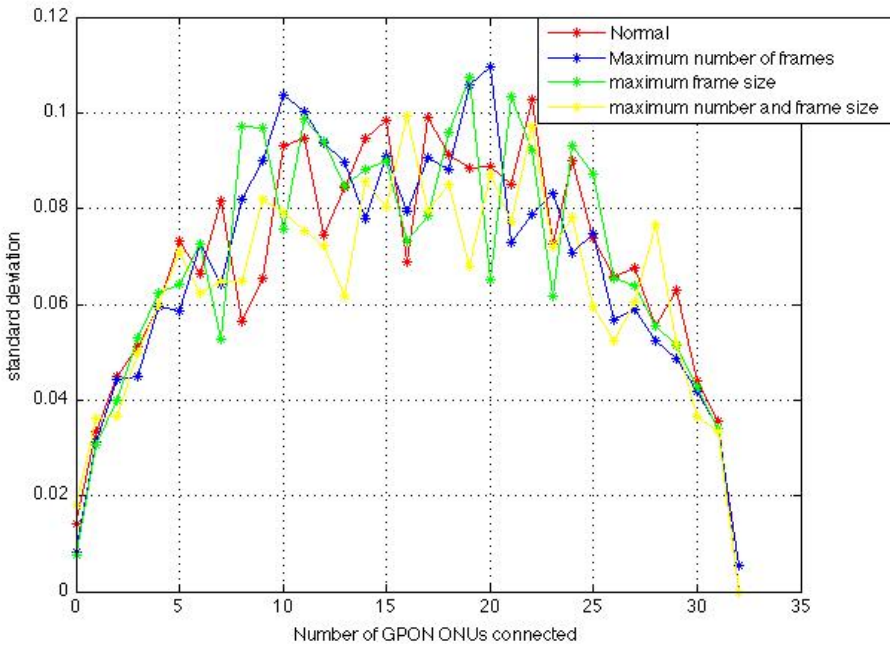

Figure 4.19 PER standard deviation as a function of the number of plugged GPON ONUs

Regarding the BER values achieved for the standard traffic distribution, a small decrease was detected, caused by the possibility of lower number of ONUs EPON connected. It is important to notice that the BER values are also mean values.

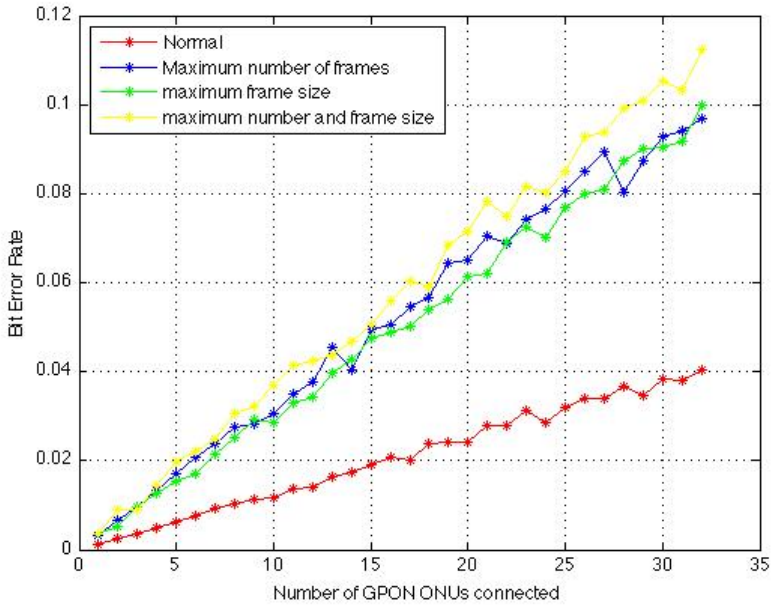

Figure 4.20 BER as a function of the number of connected GPON ONUs

4.2.5. Conclusions

In this section the upstream coexistence scenario without optical conversion was assessed and proved feasible. To allow the stacked-PON scenario to be viable, the traffic patterns and the subsequent channel “free window times” should be carefully controlled. For the scenario presented in 4.2.4, which corresponds to a generic traffic model, stacked-PON was proved possible for up to 3 GPON interferometer ONUs in a 32 EPON network.

In the presence of a network where all the ONUs send data at its full potential, PER is never lower than 10%, thus no stacked-PON can be implemented.

4.3. Upstream experimental emulation

In this section the stacked-PON upstream coexistence scenario was assessed, using the laboratorial setup presented in Figure 4.21 The EPON and GPON system’s characteristics are presented in Appendix III. A traffic analyzer, which is not pictured in Figure 4.21 was connected to both EPON and GPON OLTs and ONUs, in order to generate traffic and evaluate the performance of the stacked-PON scenario.

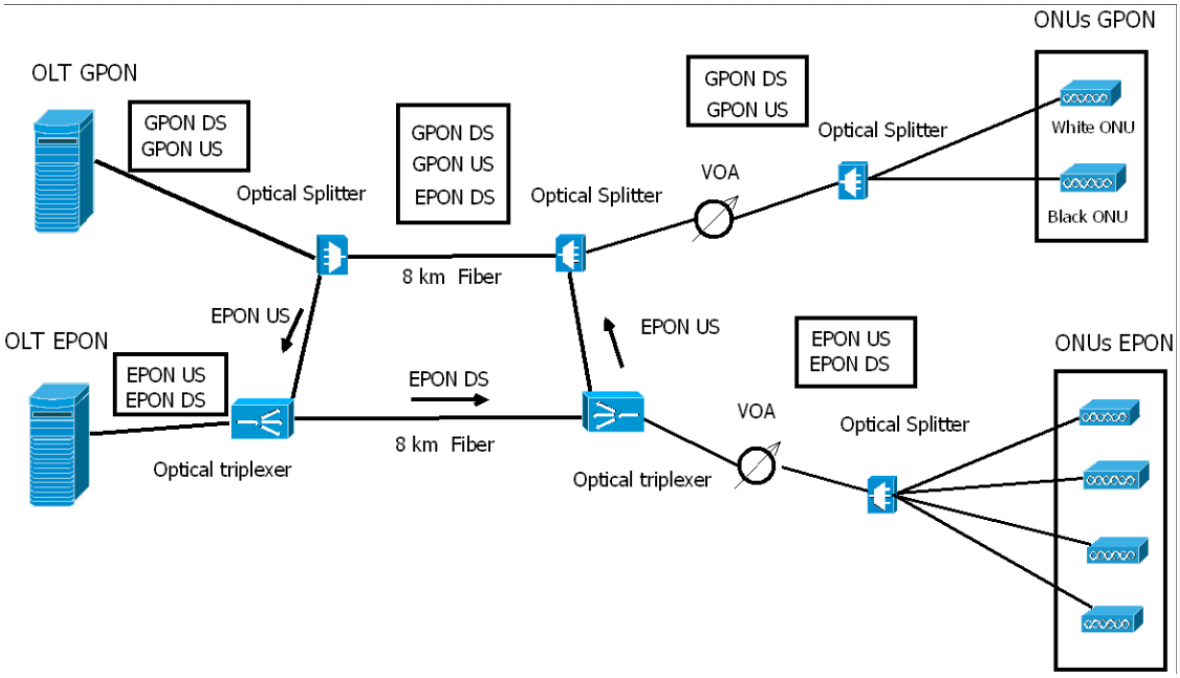

Figure 4.21 Upstream experimental emulation setup

EPON and GPON OLTs are responsible for the registration and upstream scheduling process of the subsidiary ONUs, thereby, for testing the upstream coexistence scenario, the downstream channel has to be free of interferences. To allow this, EPON downstream channel was separated from the upstream, by means of optical triplexers, then both signals were sent separately using fibers with similar length not to unbalance the ranging processes [ITU-T G.984.3, 2008].

In section 4.2 the upstream bursts' power in both PON systems are considered to be equal, since further power differences would greatly increase the complexity of the desired model. On the other hand, in a real context, simulated by the experimental setup presented in Figure 4.21, the upstream power settings of the different ONUs are of the most importance. Figure 4.22 assesses the power setting configurations by presenting the packet loss and number of EPON registered ONUs as a function of the relative power difference between the EPON and GPON ONUs. The GPON ONUs, that are referred in this dissertation as white and black, present different packet losses, due to the different sensitivities, -26 dBm and -25 dBm, respectively. EPON ONUs, differ not only in the sensitivity but also in the upstream signal power.

To better evaluate the accuracy of the simulations performed in section 4.2, the minimum gap between ONUs and the gap between bursts were set to the simulated values (table 4.1), and are presented below:

- Minimum GPON gap 12 Bytes
- GPON Burst gap 75 ns
- GPON bitrate 100 Mbit/s

- Minimum EPON gap 160 Bytes
- EPON Burst gap 192ns
- EPON bitrate 80 Mbit/s

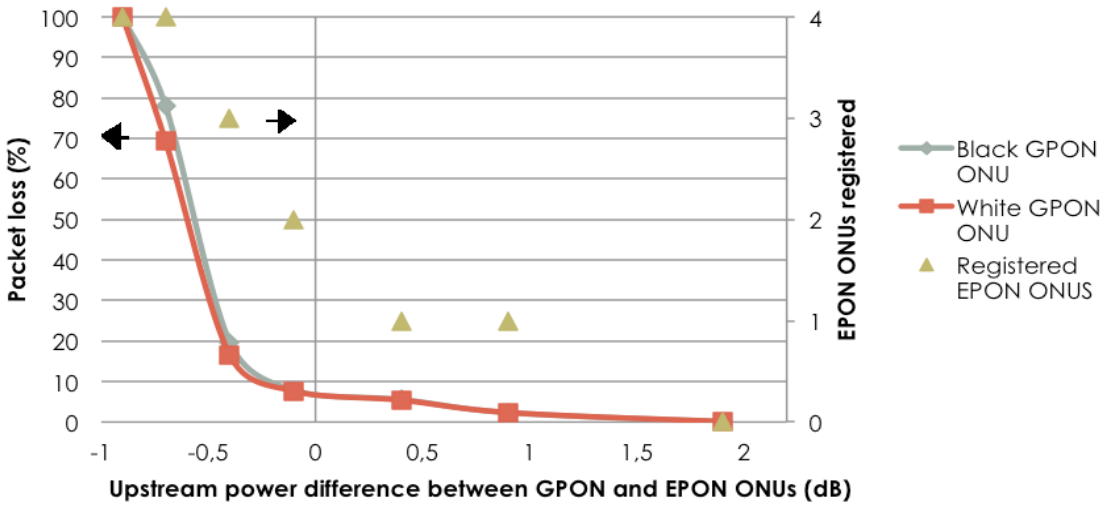

Figure 4.22 Packet loss as a function of the upstream power difference between EPON and GPON ONUs

In Figure 4.22 is presented the packet loss for both GPON ONUs, and the number of registered EPON ONUs, as a function of the difference between the upstream power of the EPON and GPON systems. The interference related to the EPON system is only due to the registration and synchronization process, because no traffic was applied to this system.

The GPON ONU upstream power was set to 2,7 dBm and the upstream power of the most sensitive EPON ONU was varied from 0,7 dBm to 3,7dBm. For a GPON upstream signal power 2 dB higher than the EPON signal, the packet loss is 0 and the EPON ONUs cannot register due to the low relative power. For a power difference around 0 dB, only two EPON ONUs are registered and the packed loss for the GPON systems is very low, less than 8%, this happens because the GPON ONUs are approximately 3 dB more sensitive than the EPON ones. When the EPON upstream power around 0,7 dB higher all the ONUs are registered and the GPON packet loss is around 70%.

Figure 4.23 presents EPON and GPON packet loss as a function of the number of connected GPON ONUs. Due to the equipment limitations, only two GPON ONUs and four EPON ONUs were available, thus the thirty-two ONUs scenario was emulated assigning an equal amount of traffic to each ONU and multiplying that amount of traffic for the connected ONUs, until thirty-two unitary amounts of traffic are reached. In EPON system only one EPON was connected due to the unbearable packet loss values attained for the upstream power difference, which allows all the EPON ONUs to be registered, Figure 4.22

In the test performed, the EPON ONU sent four million frames, representing a thirty-two EPON ONU network. In all packet loss measurements taken, the GPON traffic was incremented with 125 thousand frames in each ONU (white and black), thereby 2

more virtual GPON ONUs were simulated at each step.

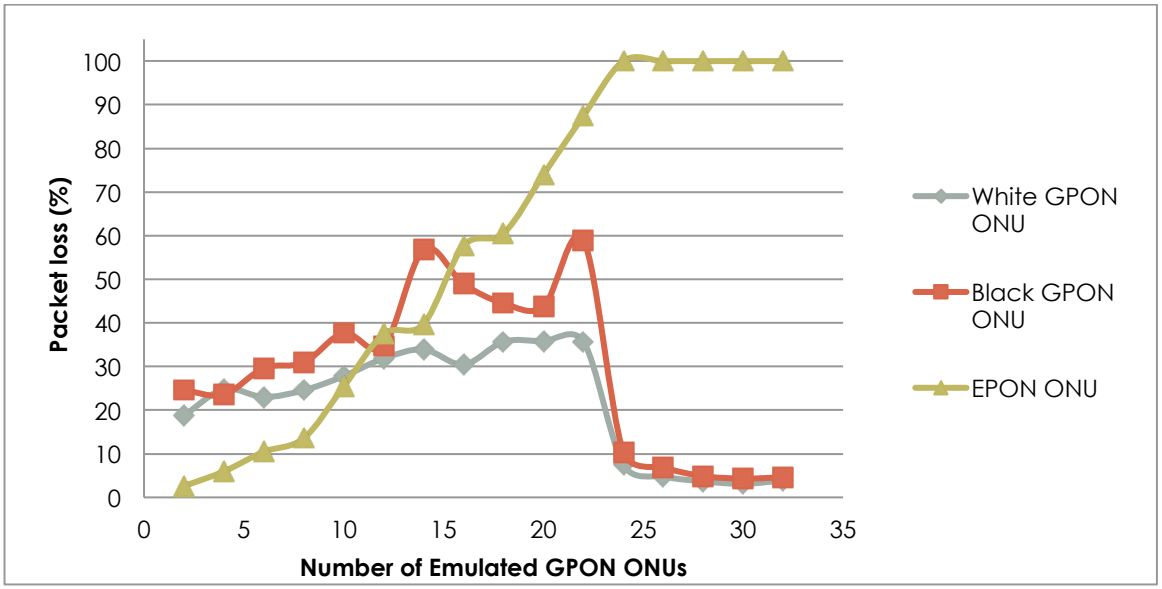

Figure 4.23 Packet loss as a function of the number of connected GPON ONUs

For up to six connected GPON ONUs, the packet loss is equal or bellow 10%, the condition previously assumed to be the maximum loss allowed for a upstream coexistence scenario feasibility. In the experimental part, the number of GPON ONUs that could be connected for the same 10% PER were 3, therefore the simulated and experimental results present a considerable difference explained by the power settings referred before.

The higher packet loss observed for the black ONU is explained by its lower sensitivity, In the case of the white ONU the PER was never above 40%, even when all the packets suffer interference from EPON traffic. This shows that with correct power setting and ONU sensitivity it may be possible to connect more that 6 GPON ONUs to the EPON system.

For more than 24 connected GPON ONUs the EPON ONU loses connectivity with the respective OLT, therefore all the packets were lost. On the other hand, GPON system controls the medium, as the EPON cannot connect, and the packet loss strongly decreases to less than 10% (this is due to the EPON registration and synchronization frames that corrupt some traffic).

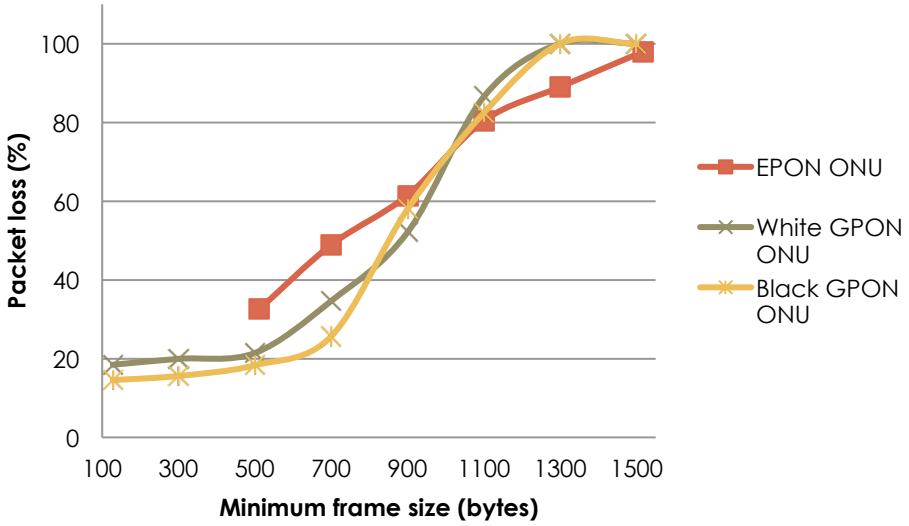

Figure 4.24 Packet loss as a function of the minimum EPON/GPON payload size

In the IXIA traffic analyzer, the frames generated when the payload is set to random, can vary from a minimum to a maximum value defined by the standards [ITU-T G.984.3, 200] (IEEE 802.3ah, 2004). For EPON systems the minimum payload size is 512 and the maximum is 1518 bytes due to the Ethernet specifications. For GPON systems the minimum payload size is 128 and the maximum is also 1518 Bytes.

Figure 4.24 presents the packet loss variations when the minimum payload size is increased from the minimum to the maximum value possible. The increased size of the payload implies a decrease of the inter frame gaps for the same amount of traffic transported, thus the medium will have less “free time” and the collisions will increase. When the minimum payload size is less than 512 bytes, the GPON and EPON systems maintain the packet loss in relative low values, whereas for minimum payload sizes above 512 a fast increase of the packet loss is verified, reaching 100% for 1300 bytes in the GPON case, and 1500 bytes for the EPON. Even when EPON starts with higher values of packet loss, the system is less dependent on the minimum payload size as is proven observing the less steep curve in Figure 4.24.

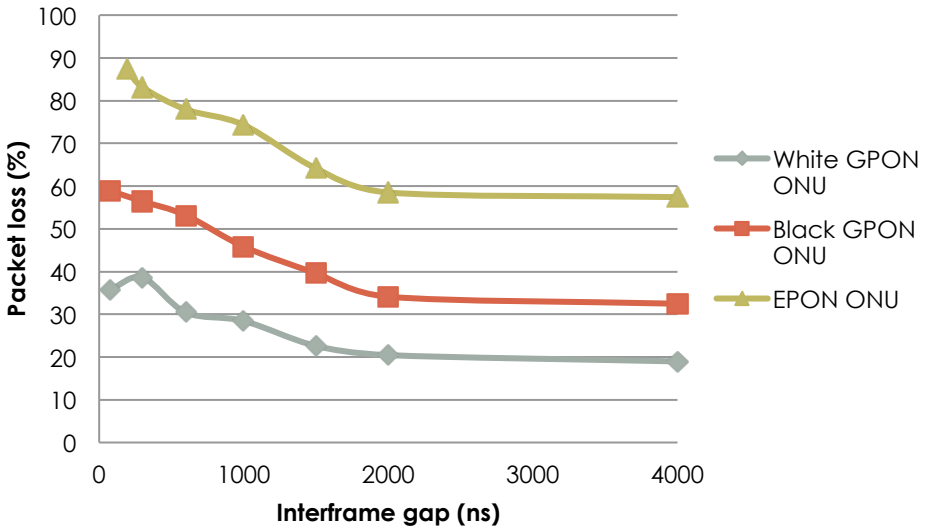

Figure 4.25 Packet loss as a function of the interburst gap

Figure 4.25 presents the relation between the interburst gap time between time slots from different ONUs and the packet loss value. Both EPON and EPON standards have defined a certain time when the channel is “empty”, in order for traffic flows from different ONUs not to overlap each other. In EPON there are different interburst gap possibilities, however, for the simulation realized in chapter 4.2 and for the experimental setup evaluation, 192 ns was used; in GPON the interburst gap used was 75 ns. For the EPON system a strong PER decrease occurs (30%) when the interburst changes from 192ns to 2000ns, but for higher values, such as 4000ns, just a slightly PER improvement happens. In GPON the same behavior is observed, but the PER decrease when the interburst gap increases from 75 ns to 2000 ns is not so evident, 24% for the black ONU and 15% for the white one.

4.4. Conclusions

In this section the coexistence of the stacked-PON upstream scenario was presented and proved feasible. Comparing the simulations presented in section 4.2 with the results presented in this section a major difference arises, due to the fact that the upstream power difference between ONUs from EPON and GPON and the respective sensitivity were not taken into account. This is very important since the relative upstream power difference between all the ONUs has the same importance, if not more, than the volume of interference traffic transported. This is observed in Figure 4.22

The evolution of the PER according to the number of ONUs connected is presented in Figure 4.23 and a similar behavior can be observed in Figures 4.4, 4.10, 4.14 and 4.18. The biggest difference between simulation and experimental evaluation is

visible when more than 24 GPON ONUs are connected to a full 32 EPON ONUs network, because the EPON system loses connectivity, due to the excessive interference from GPON ONUs, resulting in 100% packet loss for the EPON system, and a vestigial packet loss in the GPON one (which controls the medium access).

The dependence of the traffic lost (PER) with the medium “free time windows” is presented in Figure 4.24 and Figure 4.25 and are compliant to the principles behind the stacked-PON scenario.

5. Conclusions and Future Work

5.1. Conclusions

This work has been presented in a set of 5 chapters. In the first one were presented the context and motivation, structure and objectives along with the main contributions.

In the second chapter the main features of the passive optical networks were described along with the presentation of the stacked-PON environment, which is the main focus of this dissertation. This chapter starts with an overall presentation about the PONs architecture, transmission specifications and packet encapsulation, then followed by a more detailed study on the two most prominent PON systems, EPON and GPON. A careful study was taken over dynamic bandwidth allocation (DBA), upstream frame format and forward error correction (FEC) due to its importance for the upstream coexistence scenario presented in 2.5 and evaluated in chapter 4. Section 2.5 presents the stacked-PON environment proposal and divides the coexistence study into downstream communication presented in chapter 3 and upstream coexistence presented in section 4, due to the different communication methodologies used in the PONs.

Due to fact that PONs downstream transmission occurs in continuous broadcast, a straightforward pairing of two different PONs using the same wavelength plan is then out of the equation due to the underlying prohibitive collision rates. Thus chapter 3 of this dissertation is dedicated to the all-optical wavelength conversion, which is the process that enables the stacked-PON downstream communication to be feasible. Along this chapter were presented the semiconductor optical amplifiers (SOAs) as the optical medium to perform the wavelength conversion. What makes the SOAs so attractive to perform wavelength conversion are the presence of non-linearitys which enable cross modulation techniques such as cross gain, phase and polarization (sections 3.1.2, 3.1.4, 3.1.5) and also the possibility to employ in interferometric devices such as MZI-SOAs presented in section 3.1.4 and 3.2.2. This chapter presents the working principles behind the all-optical wavelength conversion in section 3.1 and the experimental validation in section 3.2. From the principles studied and the experimental validation is possible to conclude that XGM offers great wavelength hops over a large wavelength with the cost of a high penalization in the extinction ratio (ER) and an output inverted signal, XPM offers great overall performance (BER and ER) and also non-inverted output signal but does not allow the wavelength hop proposed because of the limited bandwidth of the MZI-SOA. XPR arises as a high bandwidth wavelength converter but no dynamic wavelength conversion was attained.

In chapter 4 was presented the upstream coexistence scenario, which takes advantage of burst nature of the upstream traffic flows. The burst nature of the traffic creates moments where the upstream channel is without use, thus another ONU can send information during those moments. Chapter 4 is divided into two sections, first is presented a simulation to assess the feasibility of the upstream coexistence scenario with interference of several ONUs. From this simulation and considering that a packet error rate bellow 10% enables the communication without prohibitive degradation, only up to 3 interference ONUs (GPON) can be connected to a full 32 EPON ONUs network. In the second section the experimental setup was set and evaluated using the available material, 2 GPON ONUs and 4 EPON ONUs. The upstream power transmitted and the ONUs sensitivity were not taken into consideration in the previous section, but from the experimental measurements performed (Figure 4.23) it is possible to conclude that the power balance between all the ONUs has the same importance, if not more, as the traffic congestion for the upstream coexistence.

5.2. Future work

This dissertation proposes a stacked-PON system employing the two PONs with more expression in the market today, EPON and GPON. Following the roadmap presented in Figure 1.1 a stacked PON using both current generation PONs and next generation PONs (XG-PON and NG-PON2) [ITU-T G.987.1, 2010] would be interesting.

In next generation WDM-PON systems, all optical wavelength conversion will become a key factor thus further studies in the wavelength conversion processes, with special focus on XPM, XPR and coherent wavelength conversion such as four wave mixing (FWM) [shikawa, 2008] [Dutta, 2006] will be of the most importance

Appendix I

CIP SOA-S-OEC-1550

The SOA used in section 3.2.1 and 3.2.3 is a bulk type SOA produced by CIP Technologies and the datasheet is presented here [CIP].

The cross modulation techniques presented in section 3.2.1 and 3.2.3 are considerably dependent on the properties of the SOA used and the operating points chosen, thus it is of the most importance to characterize the SOA in terms of bandwidth, gain, saturation point, amplified spontaneous emission (ASE) and noise figure (NF). Due to the out of band conversion performed in section 3.2.1, the characterization was performed for both in band wavelength (1550nm) and out of band wavelength (1490nm).

First it was characterized in terms of gain as a function of the input signal power, for a current of 145 mA, in order to find the best-input signal power for a 1550 nm and 1490 nm wavelength. In Figure I.1 it can be noticed that the saturation point, which occurs when a decrease of the gain of 3 dB is verified, is reached for -10dBm input power. Next characterizations were taken using this value as a reference input power.

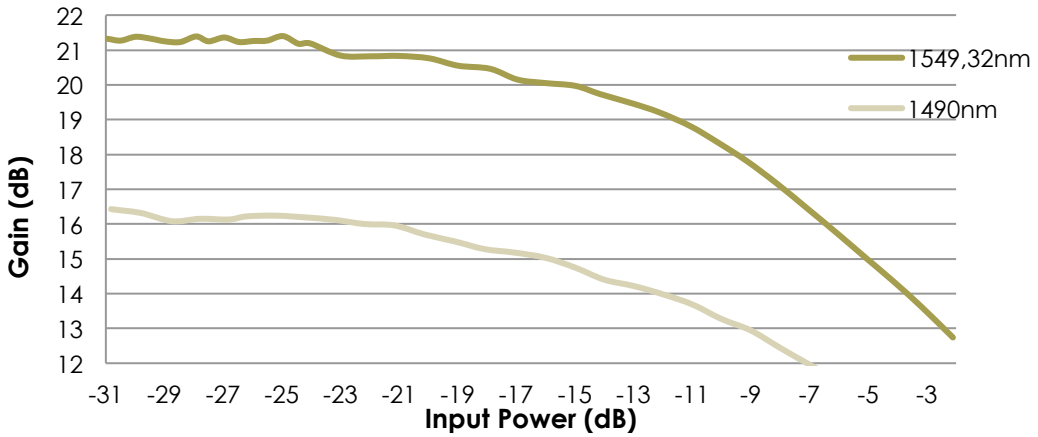

Figure I.1 SOA Gain as a function of the input signal power for 1550nm and 1490nm wavelengths

Next was assessed the variation of the gain, NF and ASE as a function of the biasing current using a fixed input power of -10dBm, as specified above and two different wavelengths, 1550nm and 1490nm. The results are presented in Figure I.2, Figure I.3 and Figure I.4.

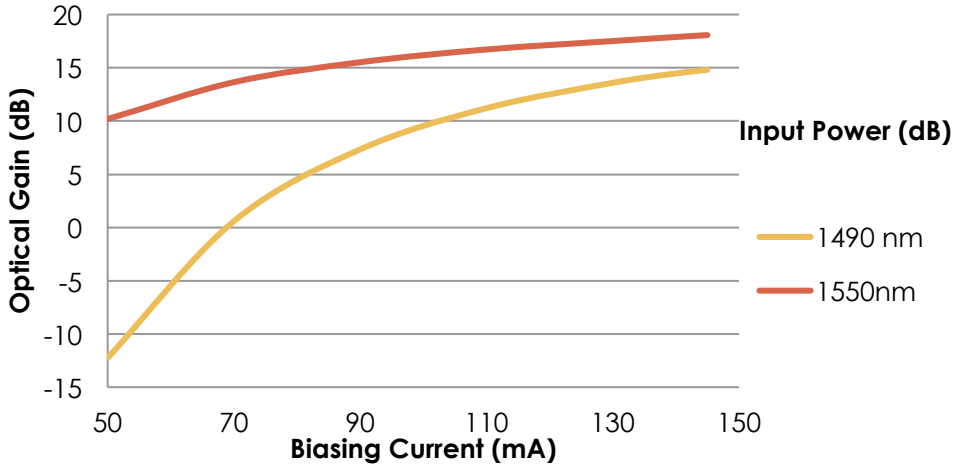

Figure I.2 SOA Gain as a function of the biasing current for 1550nm and 1490nm

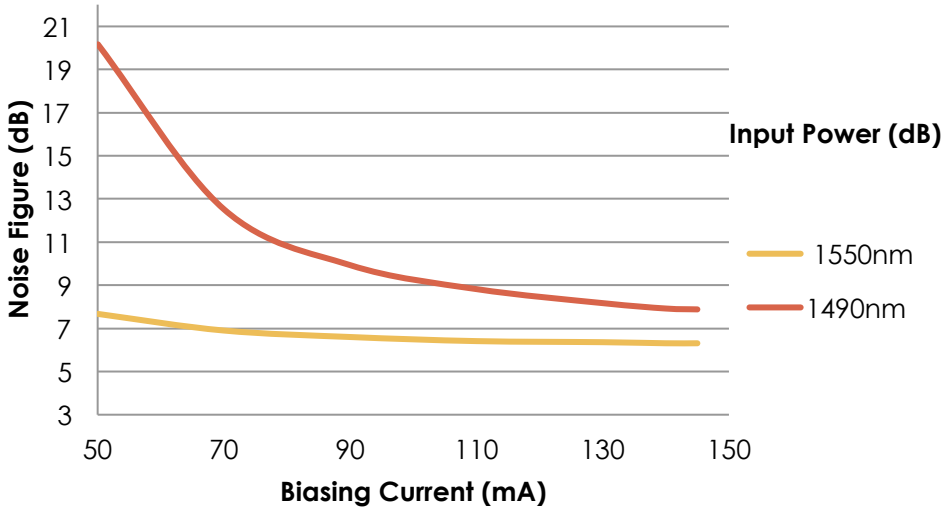

Figure I.3 SOA Noise Figure as a function of the biasing current for 1550 nm and 1490 nm

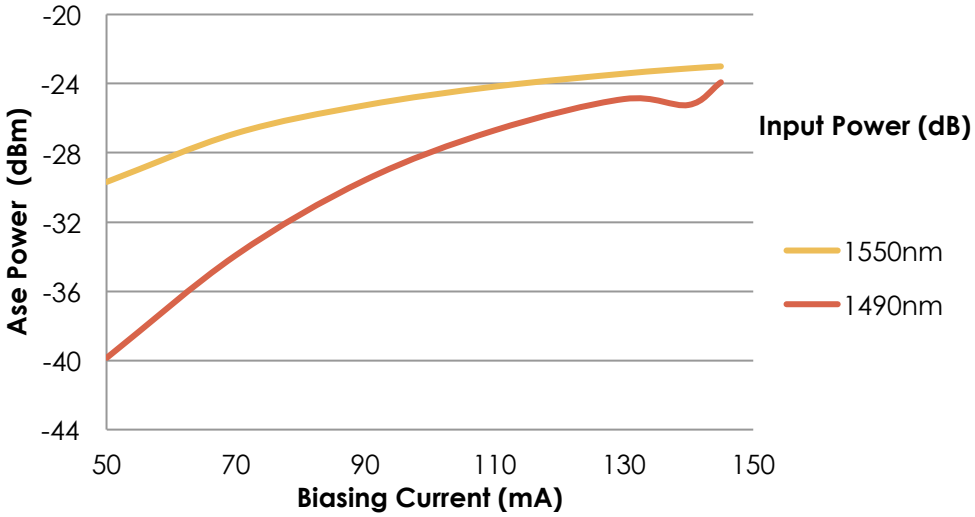

Figure I.4 SOA ASE as a function of the biasing current for 1550nm and 1490nm

From Figures-I 1,2,3 it can be noticed that the SOA properties assessed present less variations when working in the in band range (1550nm), compared to the out of band range (1490nm). For example, for the gain curve presented in Figure I the variation are 8 dB, from 50mA to 145mA, at 1550nnm, and around 25 dBs at 1490nm. As expected the SOA presents greater gain and less noise when a 1550nm signal is used as the input. The best operating point is undoubtedly when the SOA is biased with a 145 nm current, which corresponds to greater gain and less noise, the drawback is the increased ASE.

Figure-I 5 presents the SOA optical bandwidth over a 90nm window and for three different input optical powers that represent the unsaturated region (-20dBm), saturation edge (-10 dBm) and deep saturation region (0 dBm). The gain variation over the represented bandwidth is less accentuated for the deeply saturated region due to the great gain compression presented in that region.

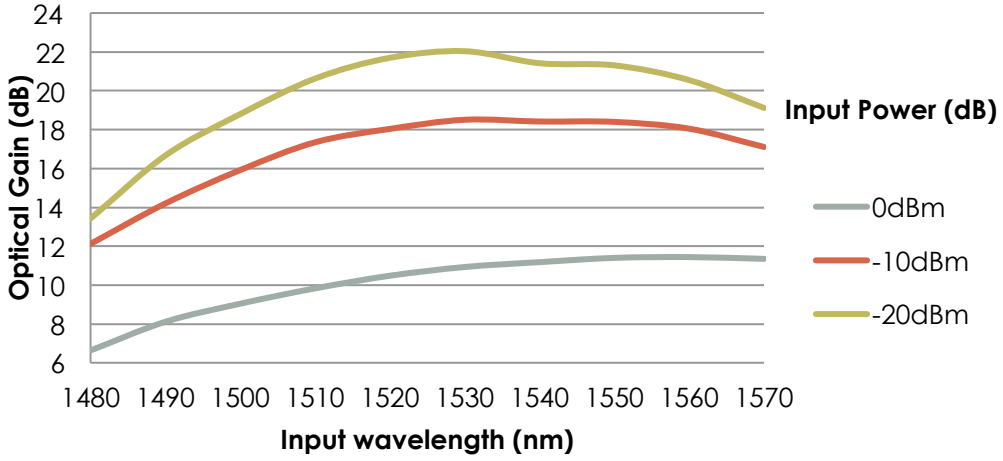

Figure I.5 SOA Gain as a function of the input wavelength for three different input powers

Appendix II

IPG Photonics TAD-20

The IPG TAD-20 amplifier is a doped fiber amplifier designed to work in the S-band (1460-1530nm), whose operating principle is similar to the EDFAs.

To clarify any misunderstandings, in the experimental sections where the IPG TAD-20 was referred (section 3.2.1 and 3.2.3) it was simply named S-band amplifier. Prior to its use in the respective setups the s-band amplifier was characterized and the results are present bellow.

First it was characterized in terms of gain, noise figure and ASE, as a function of the biasing current and input signal power, in order to find the best operating point for a 1490nm wavelength. In Figure II.1 can be noticed that the biggest gain, thus the best operating point, is reached for a biasing current of 0,5 A.

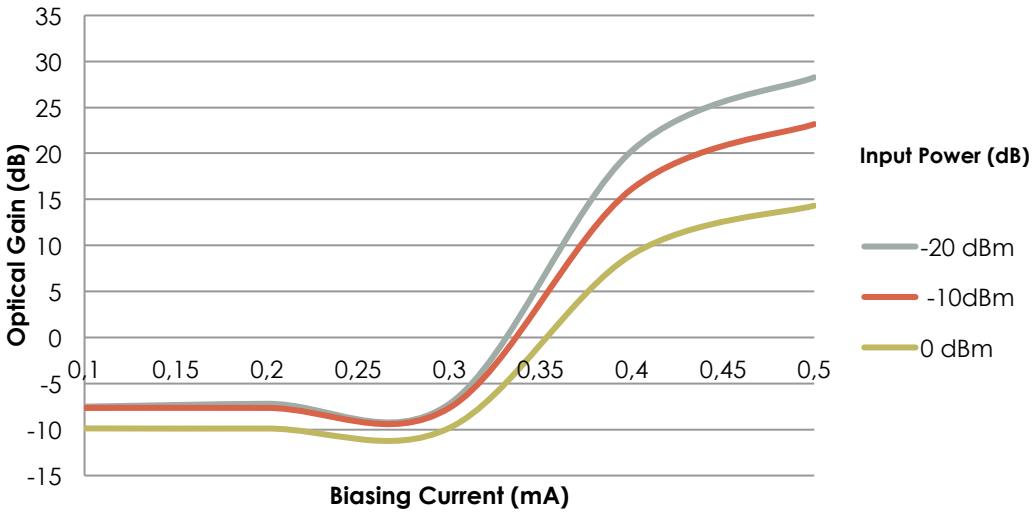

Figure II.1 Optical Gain as a function of the biasing current and input power

As the noise figure decreases with the increase of the polarization current, the best polarization point in terms of NF is also 0,5 A. The S-band amplifier shows the same NF behavior for the three input powers studied, but for 0dBm a 1,5 dB increase is verified.

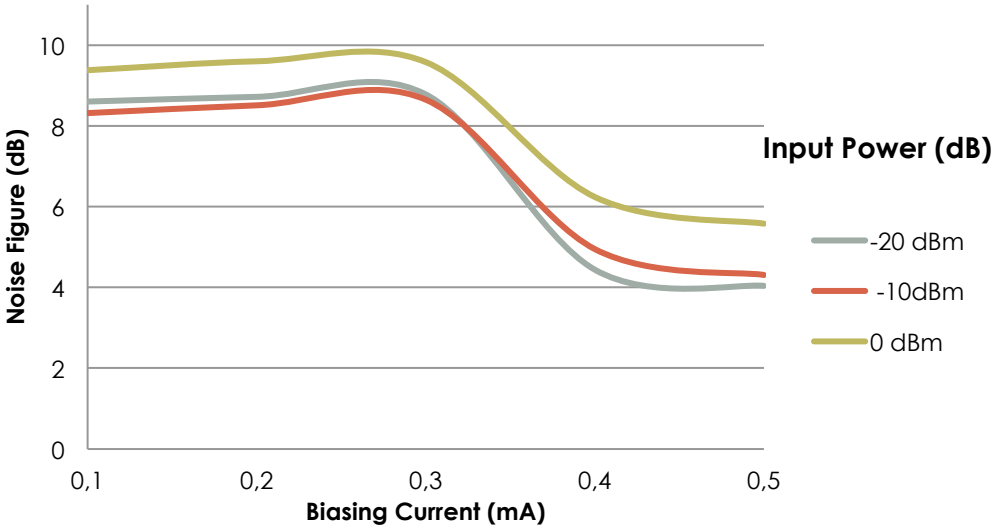

Figure II.2 Amplifier Noise Figure as a function of the biasing current for different input powers

Similarly to what was registered in the SOA, the S-band amplifier ASE also increases with the polarization current. Considering the presented characterization, the chosen operating point for the S-band amplifier applied to the sections 3.2.1 and 3.2.3 was 0,5 A.

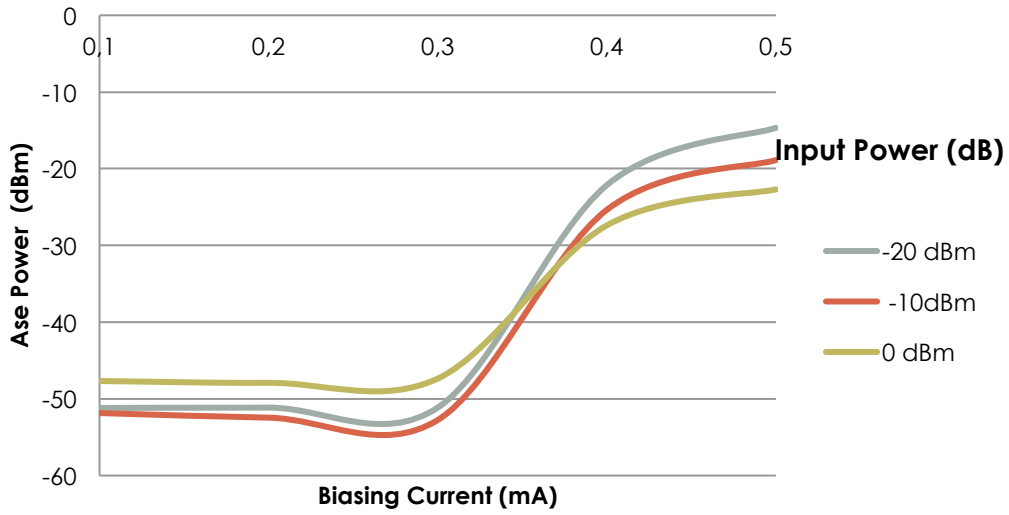

Figure II.3 Amplifier ASE as a function of the biasing current for different input powers

As for the SOA case, it is important to assess the output saturation power of the amplifier. Figure II.4 presents the optical gain as a function of the input signal power.

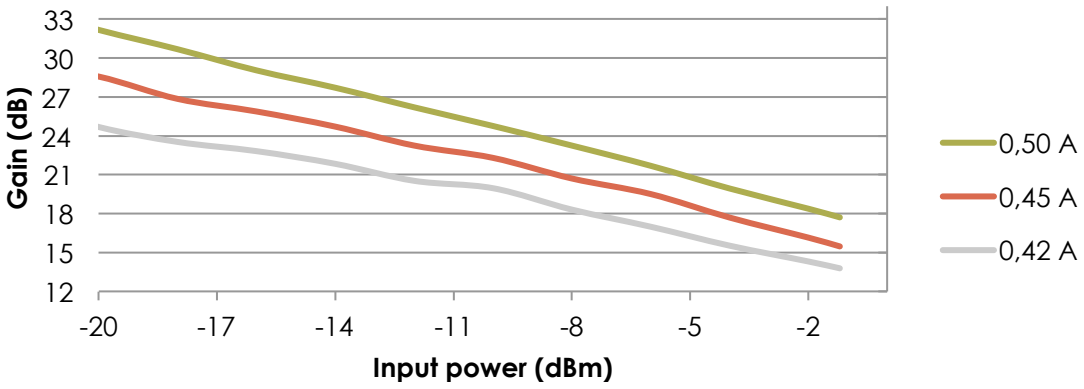

Figure II.4 Optical Gain as a function of the input signal power for different biasing currents

Although the S-band optical amplifier was only used for amplification of 1490nm wavelength, it is important to assess its optical bandwidth. Figure II.5 presents the optical bandwidth for different input powers. Here we can observe the gain compression due to the input power and also the fact that for out-of-band the gain is independent of the input power.

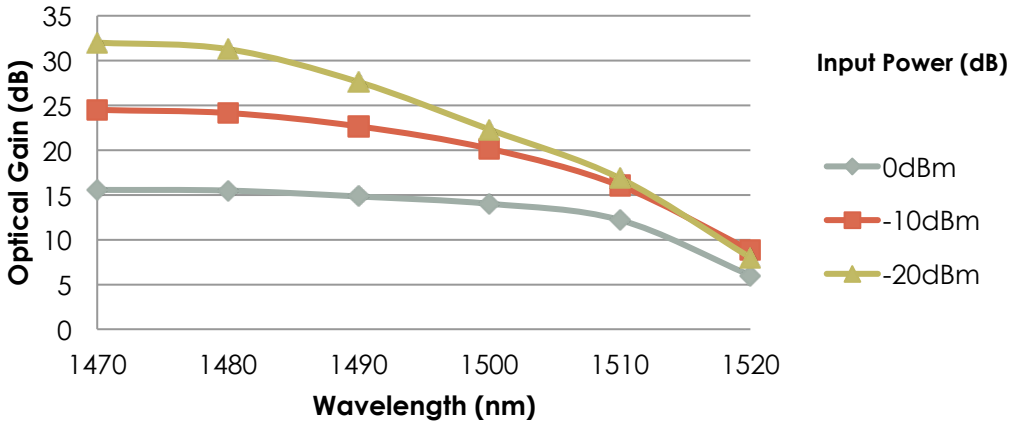

Figure II.5 Optical Gain as a function of the input wavelength for a fixed PIN and biasing current

Appendix III

Appendix III resumes the main operating characteristics that should be taken into consideration when using both EPON and GPON networks. This appendix is divided into EPON and GPON section presenting the OLT and ONU transmission characteristics separately.

EPON

Figure III.1 (left) OLT-AN5116-02 rack and power supply (right) ONU – AN5006-074

Table III:1 EPON OLT Characteristics

Fabricant / Model	FiberHome / AN5116-02
Transmitter/ Receiver Wavelength	1490 nm / 1310 nm
Transmit power (datasheet)	+2 to +7 dBm
Transmit power (measured)	+3 to +5 dBm
Maximum receive power	-6 dBm
Receive sensitivity (datasheet)	-27 dBm
Receive sensitivity (measured)	-27 dBm
Transmit / Receive Rate	1.25 Gbps / 1.25 Gbps
Connector Type	SC-PC

Table III:2 EPON ONU characteristics

Fabricant / Model	FiberHome / AN5006-05
Transmitter/ Receiver Wavelength	1310 nm / 1490 ± 10 nm
Transmit power (datasheet)	-1 to +4 dBm
Transmit power (measured)	+4 dBm
Maximum receive power	-3 dBm
Receive sensitivity (datasheet)	-24 dBm
Receive sensitivity (measured)	-28 dBm
Transmit/ Receive Rate	1.25 Gbps / 1.25 Gbps
Connector Type	SC-PC / SC-APC

NOTE: The ONU sensitivity has shown a variance with time (temperature) and also hysteresis with the input power.

GPON

Figure III.2 (left) OLT-7-8CH rack and power supply (right) ONU – PTINONT7RF1GE

Table III:3 GPON OLT characteristics

Fabricant / Model	PT Inovação /OLT7-8CH
Transmitter/ Receiver Wavelength	1490 nm / 1310 nm
Transmit power (datasheet)	+1.5 to +5 dBm
Transmit power (measured)	+3 to +4 dBm
Maximum receive power	-8 dBm
Receive sensitivity (datasheet)	-28 dBm
Transmit / Receive Rate	2.5 Gbps / 1.25 Gbps
Connector Type	SC-PC

Table III:4 GPON ONU characteristics

Fabricant / Model	PT Inovação /PTINONT7RF1GE
Transmitter/ Receiver Wavelength	1310 nm / 1490 nm
Transmit power (datasheet)	+0.5 to +5 dBm
Maximum receive power	-8 dBm
Receive sensitivity (datasheet)	-27 dBm
Receive sensitivity (measured)	-31 dBm
Transmit / Receive Rate	1.25 Gbps / 2.5 Gbps
Connector Type	SC-APC

References

A. M. Ragheb, M. E. (2010). Performance Evaluation of Standard IPACT for Future Long Reach Passive Optical Networks (LR-PON). International Conference on Communication Tecnologies, (p. 1). Riyadh.

Agrawal, G. P. (2002). In Fiber Optic Communication Systems (third ed., p. 491). Willey Interscience.

Alves, A. (2010, July). Redes Opticas Passivas de Próxima Geração. MSc. Thesis .

Boomsma, C. (2006, May). Ethernet over Passive Optical Networks. MSc. Thesis , 22 - 40.

Boucher, Y. G. (2007, January). Extended Transfer Matrix Formalism Applied to Active Mach-Zehnder Interferometers with Built-in Semiconductor Optical Amplifiers. INTERNATIONAL JOURNAL OF MICROWAVE AND OPTICAL TECHNOLOGY .

Cartledge, S.-C. C. (2002). Measurement-Based Method for Characterizing the Intensity and Phase Modulation Properties of SOA–MZI Wavelength Converters. IEEE PHOTONICS TECHNOLOGY LETTERS , 14 (11).

Carvalho, H. R. (2012). Distribuição ótica de sinais vídeo. Msc. Thesis , 12-15.

CIP. (n.d.). SOA-S-OEC-1550. Retrieved from http://www.eeng.dcu.ie:8888/ee454/872-EE/version/default/part/AttachmentData/data/SOA.pdf

Connelly, M. (2002). Semiconducor Optical Amplifiers. Netherlands: Spriger.

Contestabile, G. (2010, December). Cross-Gain Modulation in Quantum-Dot SOA at 1550 nm. IEEE explore , 46 (12).

CWDM. (2012, June). COARSE WAVELENGTH DIVISION MULTIPLEXING CWDM. Retrieved from ITU-T: http://www.itu.int/dms_pub/itu-t/oth/1D/01/T1D010000030002PDFE.pdf

Dionísio, R. (2010). Experimental Study of a Phase Modulator Using an Active Interferometric Device. MELECON 2010 - 2010 15th IEEE Mediterranean Electrotechnical Conference.

Durhuus, T. B. (1996, June). All Optical Wavelength Convertion by SOA. JOURNAL OF LIGHTWAVE TECHNOLOGY .

Dutta, N. K. (2006). Semiconductor Optical Amplifiers.

FTTH Council. (2012, July). FTTH Business Guide 2010 Archive/Why Fibre? Retrieved from http://wiki.ftthcouncil.eu/index.php/FTTH_Business_Guide_2010_Archive/Why_Fibre%3F

Gebert, S. Internet Access Traffic Measurement and Analysis. University of Wurzburg, Institute of Computer Science, Germany.

Hadi Ghauch, V. K. (2009). Self Similar Traffic Packet Switching & Computer Networks .

Hamié, A. (2005, June). All-Optical Inverted and Noninverted Wavelength Conversion Using Two-Cascaded Semiconductor Optical Amplifiers. IEEE PHOTONICS TECHNOLOGY LETTERS, VOL. 17, NO. 6, .

Hanfoug, R. (2003). Static extinction ratio bandwidth of Mach-Zehnder interferometer wavelength converters. IEEE/LEOS Benelux.

Idate. (2012). FTTX 2012 Markets & Trends Facts & Figures.

Idate. (2009). FTTx Market Report .

IEEE 802.3ah. (2004). Retrieved from http://www.ieee802.org/21/doctree/2006_Meeting_Docs/2006-11_meeting_docs/802.3ah-2004.pdf

Ishikawa, H. (2008). UltrafastAll-Optical Signal Processing Devices. National Institute of Advanced Industrial Science and Technology .

ITU-T G.975. (1996, November). TRANSMISSION SYSTEMS AND MEDIA, DIGITAL SYSTEMS AND NETWORKS.

ITU-T G.984.1. (2008, March). Gigabit-capable passive optical networks (GPON): General characteristics.

ITU-T G.984.2. (2003, March). Gigabit-capable Passive Optical Networks (GPON): Physical Media Dependent (PMD) layer specification.

ITU-T G.984.3. (2008, March). Gigabit-capable Passive Optical Network (GPON): Transmision convergence layer specification.

ITU-T G.984.4. (2008). Gigabit-capable passive optical networks (G-PON): ONT management and control interface specification. .

ITU-T G.987.1. (2010). 10-Gigabit-capable passive optical networks (XG-PON) .

Joergensen, C. (1996). Wavelength Conversion by Optimized Monolithic Integrated Mach-Zehnder Interferometer. IEEE PHOTONICS TECHNOLOGY LETTERS , 8 (4).

Kramer, G. (2005). In Ethernet Passive Optical Network (EPON) (pp. 25-50). McGraw-Hill .

Kramer, G. (2006). How efficient is EPON? Retrieved from http://glenkramer.com/ucdavis/papers/epon_efficiency.pdf.

Kramer, G. (2002, July). Interleaved Polling with Adaptive Cycle Time (IPACT): A Dynamic Bandwidth Distribution Scheme in an Optical Access Network. IEEE Communications Magazine , 40 (2), pp. 74-80.

Kramer, G. (2004). On Configuring Logical Links in EPON.

Lam, C. (2007). Passive Optical Networks . In Principles and Practice. Academic Press.

Leonid G. Kazovsky, N. C.-T.-W. (2011). Broadband optical access networks. Willey.

Li, Z. (2007, June). Ultrafast all-optical signal processing using semiconductor optical amplifiers .

Liu, Y. (2003, January). Wavelength Conversion Using Nonlinear Polarization Rotation in a Single Semiconductor Optical Amplifier . IEEE PHOTONICS TECHNOLOGY LETTERS, VOL. 15, NO. 1 .

Masaki Noda, N. S. (2010, July). Burst-mode Transceiver Technology for 10G-EPON Systems . IEEE Explore .

Matsuura, M. (2011). Broadband Wavelength Conversion with S/C/L-band Flexible Operation Using Cross-Gain-Modulation in a Single Quantum Dot SOA .

McAvoy, D. (2010, March). Network Traffic Distribution- Wireless Technology Strategy Architect. Bell.

Mendonça, C. S. (2010). Requisitos para Redes NG-PON2. MSc. Thesis , 19.

PON, A. v. (2008). – A comparison of two optical access network technologies and the different impact on operations . White Papper, keymile.

Senior, J. M. (2009). Optical Fiber Communications, Principles and Practice third edition.

Silveira, T. G. (2011). All-optical processing systems based on semiconductor optical amplifiers. PHd. Thesis , 49-102.

Soto, H. (1999, August). Cross-Polarization Modulation in Semiconductor Optical Amplifiers. IEEE PHOTONICS TECHNOLOGY LETTERS, VOL. 11, NO. 8 .

Statistics: The Poisson Distribution. (n.d.). Retrieved August 2012, from http://www.umass.edu/wsp/statistics/lessons/poisson/index.html

Sun, J. (2002, May). Relaxation of facet reflection restrictions in XGM wavelength converters . Optics Communications .

Tang, W. W. (2005, September). Optical Pumping of a Semiconductor Optical Amplifier for Wide-Band Noninverting Wavelength Conversion. IEEE PHOTONICS TECHNOLOGY LETTERS, VOL. 17, NO. 9 .

Veerasubramanian, V. (2008). Propagation analysis of an 80-Gb/s wavelength-converted signal utilizing XPM . IEEE Explore .

Weisstein, E. (n.d.). Gamma Distribution. Retrieved August 2012, from http://mathworld.wolfram.com/GammaDistribution.html

YAHAY, E. .. (2007, April). MACH-ZEHNDER INTERFEROMETER. Msc. Thesis , 36-38. (U. o. Malaysa, Ed.)